Novel method for electrically tuning the resonant frequency of Piezoelectric Vibration Energy Harvester (PVEH) by using low power actuation

By

Sreekumari Raghavan

A Dissertation Submitted in Partial Fulfillment of the

Requirements for the Degree of

DOCTOR OF PHILOSOPHY

in the Department of Civil Engineering

Novel method for electrically tuning the resonant frequency of Piezoelectric Vibration Energy Harvester (PVEH) by using low power actuation

By

Sreekumari Raghavan

Supervisory Committee

Dr. Rishi Gupta, Department of Civil Engineering
Supervisor

Dr. Cheng Lin, Department of Civil Engineering
Departmental Member

Dr. Fayez Gebali, Department of Electrical and Computer Engineering
Outside Member

Abstract

Advancements in electronics and MEMS (Micro Electro Mechanical Systems) technology have enabled the deployment of a large number of sensors and signal transmitters on structures at critical locations to extract vital data and avoid catastrophic failures. This approach leads to condition-based maintenance of structures. In this scenario, the critical requirement is an autonomous power source that can power the system. In most cases, wired connections to a central power unit are not feasible, resulting in the use of batteries to power the sensors and transmitters. In recent years a great deal of research has been focused on harvesting from solar, thermal, kinetic, and RF (Radio Frequency) energy available in the environment. Of all these ambient conditions, kinetic energy in the form of vibrations is more prevalent in many structures and machinery. This has resulted in an increased focus on effectively converting vibration energy to electrical energy. Among many methods adopted, the application of piezoelectric materials has led to promising results. A piezoelectric energy harvester in a cantilever design can generate high power output, only at its resonant frequency and much research has been focused on methods of tuning the harvester to match the ambient frequency of vibrations.

This dissertation details an active tuning methodology and design of a device, which has resulted in achieving a net power gain. The concept is to utilize a low power actuation mechanism integrated with the harvester to enable active tuning of the resonant frequency of the device. The approach was to make use of Ionic Polymer Metal Composites (IPMC) for the required actuation. IPMC is a smart material, whose actuation can be altered by varying the input voltage to the device.

The IPMC used here is perfluorinated Nafion films with noble metal coated on both sides as electrodes. When subjected to an applied voltage, the free cations in the membrane, tagged to the water molecules, move to the negative electrode. This phenomenon creates bending of the film. This is the actuation process associated with IPMC.

The actuator unit of two strips of IPMC, attached at the tips was powered by a very low voltage ranging from 1 to 4 V. The various levels of actuation generate corresponding block forces and functions as equivalent to tunable stiffness stoppers. This dissertation provides details of experiments carried out, theoretical analyses, and the applications of this novel device.

Table of Contents

List of figures

List of Tables

Tables **Page no.**

List of abbreviations

Abbreviations

PVEH	Piezoelectric Vibration Energy Harvester
SHM	Structural Health Monitoring
IPMC	Ionic Polymer Metal Composites
PZT	Lead Zirconate Titanate
MFC	Macro Fiber Composite
PVDF	Polyvinylidene Fluoride
MEMS	Micro-Electro Mechanical System
MsM	Magnetostrictive material
RF	Radio Frequency
IoT	Internet of Things
RS	Root Section
EB	Extender Beam
HDPE	High Density Poly Ethylene
AlN	Aluminum Nitride
PDE	Partial Differential Equation

Acknowledgments

First and foremost, I would like to express my sincere gratitude to my supervisor Dr. Rishi Gupta for the continuous support, guidance and encouragement during my research period. I would also like to thank my supervisory committee members; Dr. Fayez Gebali and Dr.Cheng Lin, for their invaluable advice and support during my research work. I gratefully acknowledge the Natural Sciences and Engineering Research Council of Canada (NSERC) for the financial assistance provided for my research.

I would like to extent my gratitude to CAMTEC. I am also grateful to Dr. Mohsen Akbari for his invaluable help. I am extremely thankful to Patrick Chang, Department of Mechanical Engineering for all the support. My sincere thanks to Dr. Sardar Malek, Dr. Loveleen Sharma, Dr. Ashutosh Sharma, Clinton Pereira and all the members of FIMIM.

I also extent my gratitude to Dr. Armando Tura and other members of the Tech support team as well as the admin team of Department of Civil Engineering.

I am immensely thankful to my husband Raghavan, my son Jayant, my brother Balakrishnan and family who supported me throughout my research journey. My thanks are also due to my loving late parents-in-law Mannadiar and Amminiamma and family.

Dedicated to

My ever-loving late parents Narayana Panicker and Kamalakshiamma, who always stood for learning and advancing scientific knowledge.

Chapter 1

Introduction

1.1 Research background and motivation

Remote monitoring of structural health of infrastructure, aircraft, and biological systems gained importance recently since such a system can detect and avoid potential hazardous failures. Advancement in Structural Health Monitoring (SHM) in real- time mode has been enabled by the innovations in electronics and related technologies such as Micro Electro Mechanical Systems (MEMS). The concept of "Trillion Sensor World" [1], where every critical structure can be monitored remotely, demands sustainable autonomous power sources for the sensor nodes. This has led to the focus on research towards realizing methods to convert the ambient energy that is already present in various forms, to usable electrical power. The concept is to deploy a very large number of sensors connected to the internet and have them communicate with each other too. This Internet of Things (IoT) has the potential to collect the relevant data and direct it to the decision-making algorithms. The MEMS sensors utilize very low power, making the above concept feasible. However, the main issue associated with the scheme is the mode of powering the sensors and the transmission electronics. Since wired connections to any central power supply are not a feasible option due to the inaccessibility and hostile conditions of the host structures where the sensors are deployed, batteries are being used in such cases. This leads to the requirement of regular recharging of the batteries, which results in increased down time and cost. In the present goal of "Trillion sensor world", powering the systems in the IoT using conventional batteries is not feasible. Hence researchers are trying to figure out ways to autonomously power the vast number of sensors that are connected to the internet as well as connected to each other, without depending on conventional batteries, by harvesting useful electrical energy from the ambient sources of energy such as electromagnetic, kinetic, and temperature variations.

The schematic diagram of such a system is shown in Fig. 1.1. In a typical SHM system, the sensors and the circuits on the structures are dependent on batteries for the power supply. A microcontroller will be part of a power management unit, to selectively power the sensors as per

requirement, based on the algorithm. The power storage unit can be kept fully charged if a source of power from the ambient conditions can be enabled. The energy harvester will be on the structure itself. The output will be conditioned and fed to the sensors through a power management scheme, such as a Field Programmable Gated Array (FPGA), to minimize power consumption.

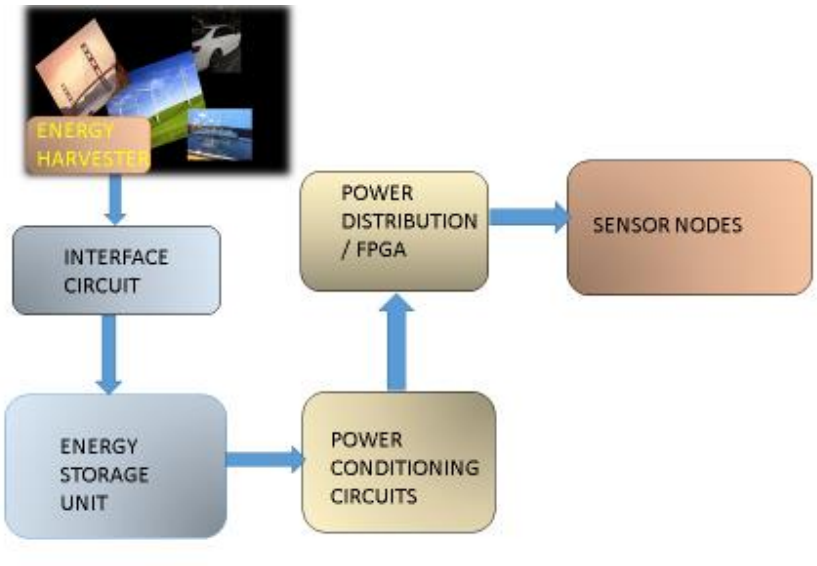

Fig. 1.1 Scheme of a typical energy harvester powering sensor nodes

1.2 Research objective

The main objective of this dissertation is to describe the novel design of PVEH that can be tuned to variation in the ambient frequency using another smart material as a low-power actuator.

The various steps towards this are as noted below:

- Literature study of PVEH
- Literature study of various existing methods for tuning PVEH.
- Literature study of smart materials that can be used as actuators.
- Pilot study to assess the feasibility of using various materials as a fixed actuator.
- Design of PVEH configuration for the device.
- Determine the feasibility of using IPMC as a low-power actuator.

- Study the performance of IPMC under various step voltage input conditions.
- Arrive at a configuration of IPMC that is best suited for the device.
- Integration of IPMC along with the PVEH.
- Study of a shift in the resonant frequency of the device by various experiments.
- Study of the frequency response of the PVEH when IPMC is used as a stopper.
- Formulation of theoretical analysis of the function of the device.

1.3 Original contributions

- This research has put forward a novel method to tune the resonant frequency of a PVEH by integrating an IPMC actuator as a stopper above the cantilever beam
- The novel design generates a net positive power output.
- Detailed experiments were carried out, studying the frequency shift, broadening of frequency bandwidth, etc. It was verified that no similar work has been reported in the literature so far.
- A US Patent application has been filed vide application no. 20210159816.

1.4 Organization of Dissertation

Chapter 1 provides the background and motivation that led to this research. This chapter also gives the research objectives and original contributions.

Chapter 2 presents a summary of energy harvesting methodologies and the Context of this research.

Chapter 3 presents material from a peer-reviewed paper published in the journal, ***Mechanics of Advanced Materials and Structures,*** with permission where appropriate. **It** covers the relevant details of literature, the conceptual design of the device, and the steps taken to realize the design. It also covers various experiments carried out to prove the functioning of the novel device design and theoretical analysis of the results.

Chapter 4 presents material from a journal paper that is to be submitted. It gives details of experiments done to study the frequency-broadening characteristics of the device. The theoretical analysis of the results is also presented.

Chapter 5 presents material from the peer-reviewed paper that has been published in the journal, ***Micromachines*** with permission where appropriate. This paper describes the applications of the device, detailing the experiments carried out, to power a MEMS accelerometer using the harvested power from the device. It is also demonstrated that the device could power a strain gauge bridge to sense the strain in a structure and could power a low-power MEMS accelerometer. Further, it was also demonstrated that it could power a Bluetooth accelerometer sensor and transmitter effectively.

Chapter 6 presents material from a peer-reviewed paper published in the ***Journal of Composite Science***, with permission where appropriate. It gives the details of experiments done as part of the characterization of the device, which was used for filing the patent application.

Chapter 7 Patent publication details of a US patent pending. Publication number: 20210159816

Chapter 8 summarizes the research and gives the conclusions and future scope of work.

Bibliography

Annexures give details of results obtained at various stages of research, specifications and setups of equipment and other relevant information.

Chapter 2

Summary of methodologies for energy harvesting and the context of this research

A brief description of various methodologies for energy harvesting is provided here, to present the essential background of this research. This section also provides the fundamental approach leading to the novel methodology implemented in this research.

There are different forms of energy present in the environment that are normally wasted if not converted to usable electric power. These are solar energy, Radio frequency waves, Thermal energy and Kinetic Energy such as vibrations. If an appropriate transduction is employed, these forms of energy can be converted to electrical energy. However, considering different characteristics of energy forms, the energy conversion systems have to be designed. A brief account of various energy harvesting methods is presented below:

2.1 Solar Energy (Electromagnetic)

Solar energy converters or photo voltaic cells consist of p and n-type of semiconductors, forming a p-n junction as shown in Fig. 2.1. When the p-n junction is formed, an electric field will be generated at the junction, by the movement of electrons to the positive p-side and the holes to the negative n-side of the junction.

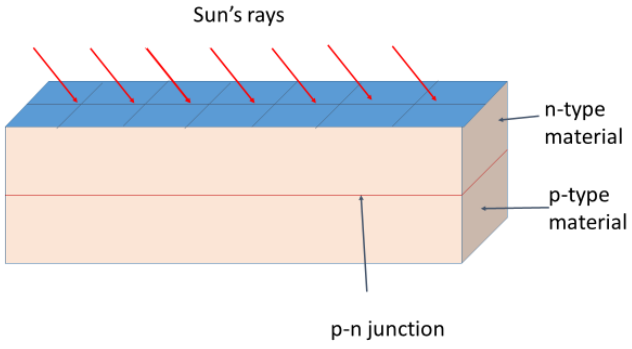

Fig. 2.1 Solar energy conversion by photovoltaic effect (Adapted from [2])

When the sun's rays which are electromagnetic radiations, fall on this, the energy associated with photons will get transferred to the electron of the semiconductor [2]. Due to this transfer of energy, the electrons jump to the conduction band, which is a higher energy state. Due to this

higher energy state, these electrons are free to move in the semi-conducting material, and this movement creates the electric current. This phenomenon is called the photovoltaic effect. The higher weight of the solar panels and dependence on solar energy are the limitations of this method.

2.2 Radio Frequency (RF) energy

The radio frequency energy converter can convert electromagnetic energy in the ambiance into a usable DC voltage [3]. The main components of the RF energy harvester are the antenna and rectifier circuits. Fig.2.2 depicts the schematic diagram of an RF energy harvester.

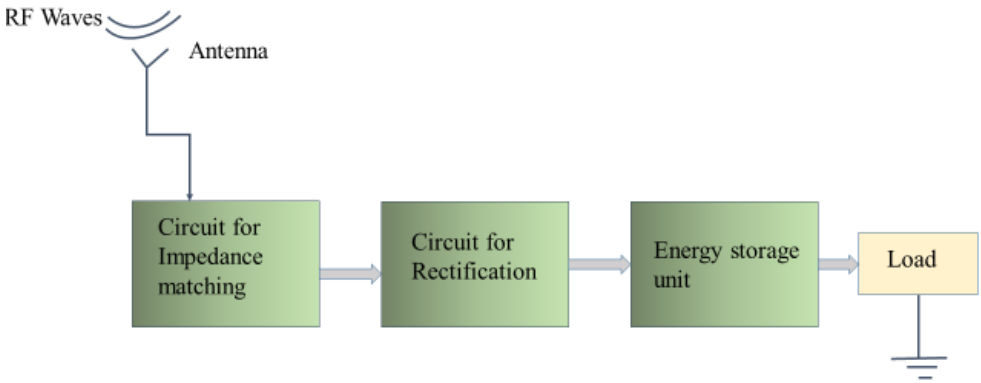

Fig. 2.2 RF energy converter (Adapted from [3])

The power that can be generated is prone to reduction due to atmospheric conditions or obstacles.

2.3 Thermal gradient

Electric voltage develops across the junction of two dissimilar conducting materials when there is a difference in temperature between the two points [4]. The conductors which are in series electrically, are connected thermally in parallel. This phenomenon is known as Seebeck Effect. The heat from machinery or chemical reactors can be converted to electricity. Fig. 2.3 shows a typical connection of conductors for thermal energy harvesting.

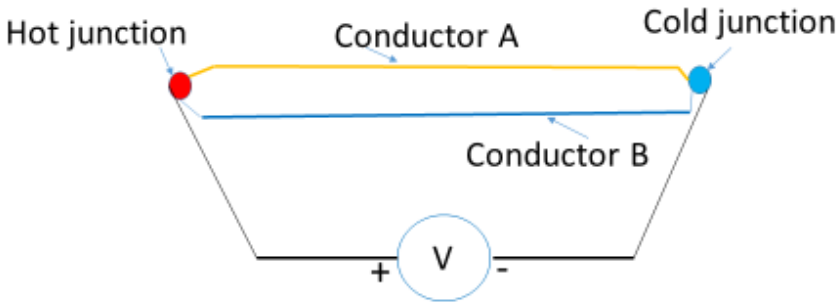

Fig. 2.3 Connection details of a thermoelectric generator (Adapted from [4])

A thermal gradient is not present in most of the structures and hence this method has got limitations.

2.4 Vibrations

Compared to the above-mentioned methods of energy harvesting, vibrations are more ubiquitous and hence the effort toward achieving a more efficient vibration energy harvester is a field of great importance.

Vibrations in ambient conditions can be converted to electrical energy using electrostatic, electromagnetic, magnetostrictive, and piezoelectric transduction. Such a transduction should meet the requirements regarding the power output, output impedance and the ease of fabrication and integration to a sensor system, to be effective in an SHM system.

2.4.1 Electrostatic vibration energy harvesting

The electrostatic energy harvester is based on the principle of varying capacitance leading to energy conversion. The voltage across a variable capacitor increases when the capacitance decreases since the electrical charge in the capacitor gets constrained. When the capacitance decreases, a net current flows through the circuit if the voltage on the capacitor is fixed [5]. An electrostatic energy harvester consists of two conductors separated by a dielectric material, as given in Fig. 2.4. The relative motion between the conductors due to the vibration, generates a variation in the capacitance. The configuration can be easily miniaturized. The requirement of an external power source is the disadvantage of this device.

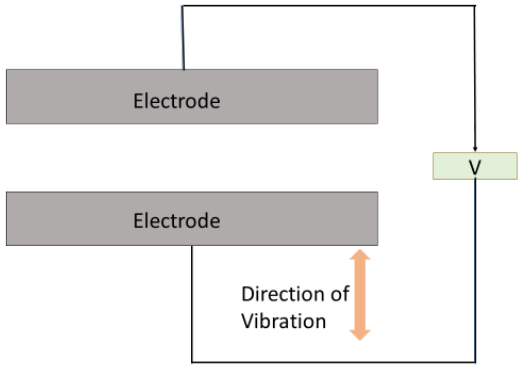

Fig. 2.4 Structure of an electrostatic vibration energy harvester (Adapted from [5])

2.4.2 Electromagnetic vibration energy harvesting

Electromagnetic vibration energy harvesting is based on Faraday's law of electromagnetic induction. If a magnet moves inside a coil, the relative movement induces a change in magnetic field and hence generates current in the coil [6]. An electromagnetic energy harvester consists of a coil, a permanent magnet, and an oscillating spring or cantilever beam. The coil or the magnet will be attached to the vibrating unit. The electromagnetic energy harvester can generate high current output at low voltage, typically less than one volt. Fig. 2.5 depicts the structure of an electromagnetic energy harvester.

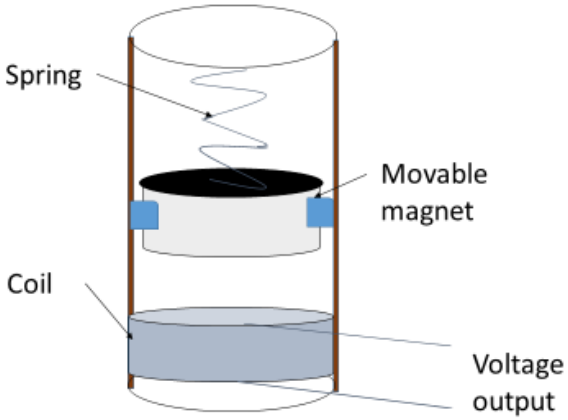

Fig. 2.5 Structure of an Electromagnetic vibration energy harvester (Adapted from [6])

2.4.3 Magnetostrictive vibration energy harvesting

Magnetostrictive materials (MsM) are compounds that deform when exposed to a magnetic field. When subjected to deformation, the magnetic field associated with it changes. This reverse effect is known as the Villari effect.

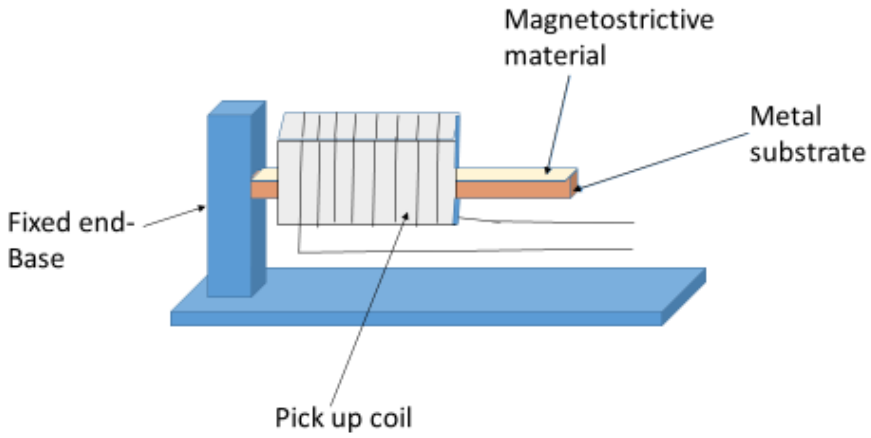

Fig. 2.6 Structure of a magnetostrictive vibration energy harvester (Adapted from [7])

Unlike piezoelectric materials, MsM need not be poled since magnetostriction is an inherent material property [7]. Fig. 2.6 shows the structure of a magnetostrictive vibration energy harvester. When the device is subjected to vibrations, the magnetostriction induces a change in the magnetic field, resulting in a change in the current in the coil around the beam.

2.4.4 Piezoelectric Vibration Energy Harvesting

2.4.4.1 Fundamentals

The piezoelectric effect is the result of the orientation of dipoles in piezoceramic materials. Usually, the dipoles are randomly oriented as shown in Fig. 2.7(a). When an electric field of the order of 1kV/mm is applied, at a temperature just below the Curie point, the randomly oriented dipoles in the piezoceramics will be aligned as shown in Fig. 2.7(b). When the electric field is removed, the dipoles maintain the alignment to a great extent as given in Fig. 2.7(c) and shows strong piezoelectric coupling. The material can be de-poled by subjecting it to a high electric field in the opposite direction to the existing poling direction. Exposure to a temperature higher than the Curie temperature of the material can also result in depolarization [8].

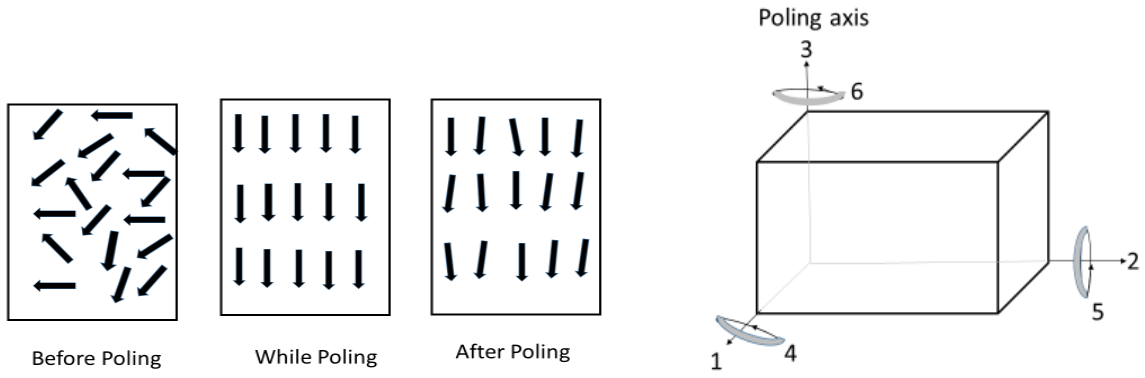

Fig. 2.7 Dipole alignment in a piezo ceramic material and the co-ordinate system

Piezoelectric coefficients are given below:

1. Piezoelectric Charge (Strain) Coefficient

The piezoelectric charge coefficient (d) relates the electric charge generated per unit area with an applied mechanical force and the unit is Coulomb/Newton (C/N) [7, 22].

Two important d constants are: d_{31} and d_{33}

If x, y, and z axes are represented by 1, 2, 3, and shear about these axes are represented by 4, 5, 6, (Fig. 2.7 (d)) then,

d33- Induced polarization in the direction of z axis for unit stress applied along z axis.

d31- Induced polarization in the direction of z axis for unit stress applied along x axis.

d15- Induced polarization in the direction of x axis for unit shear stress applied about y axis.

2. Piezoelectric Voltage Coefficient

The piezoelectric voltage coefficient (g) is the ratio of the electric field produced to the mechanical stress applied and the unit is voltage-meter/Newton (Vm/N).

Depending on the type of relative directions, the g constant can be represented as g_{33}, g_{31}, or g_{15}, corresponding to d_{33}, d_{31}, or d_{15}, respectively.

3. Piezoelectric Coupling Coefficient

The piezoelectric coupling coefficient or the electromechanical coupling coefficient is defined as the ratio of the mechanical energy accumulated in response to an electrical input or vice versa. It also corresponds to the fraction of electrical energy that can be converted into mechanical energy and vice versa.

4. Mechanical Quality Factor

The mechanical Quality factor Q_m is the ratio of the reactance to the resistance in the series equivalent circuit representing the piezoelectric resonator. It indicates the sharpness of the resonance frequency. The mechanical Q_m can be calculated as below:

$$Q_{\mathrm{m}} = \frac{f_{\mathrm{r}}}{f_2 - f_1} \tag{2.1}$$

where fr is the resonance frequency, f_1 and f_2 are frequencies at −3 dB of the maximum admittance.

2.4.4.2 Cymbal type

The cymbal transducer structure consists of piezoelectric material bonded on a metal substrate and hollow steel end caps attached to it [9]. The hollow metal end caps redirect the applied axial compressive load into radial tension on the PZT disc. The PZT disc has end caps on both sides as shown in Fig. 2.8. This configuration generates a higher stress on the PZT, compared to the case when it is directly impacted.

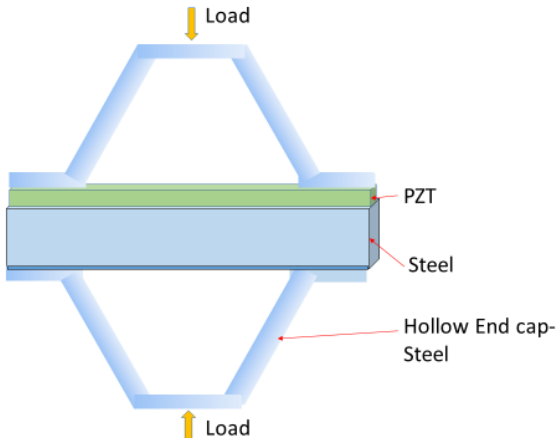

Fig. 2.8 Structure of a cymbal-type piezoelectric energy harvester (Adapted from [9])

2.4.4.3 Stack type

Piezoelectric material in bulk form can be stacked in series or parallel to form a Stack type harvester [9]. Fig. 2.9 shows a series stack type energy harvester. The axis of the stack will be the axis of linear motion. Fabrication involves the preparation of a homogeneous slurry of ceramic powder, dispersant, binder, plasticizers, and solvent. Then Tape casting technique is applied to form ceramic films. These ceramic film layers are stacked and sintered. The electrodes are screen-

printed to the layers before stacking. The piezoelectric stacks in series can generate higher open circuit voltage, whereas stacks in parallel generate higher electric current.

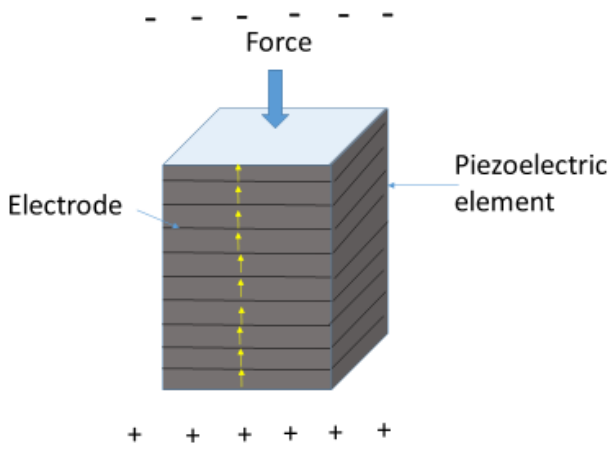

Fig. 2.9 Structure of a stack-type piezoelectric energy harvester (Adapted from [9])

Features of different types of vibration-based energy harvesters [5, 6, 7, and 9] are given in the Table 2.1.

Table 2.1 Features of different types of vibration-based energy harvesters

Vibration energy harvester	Advantages	Disadvantages
Electrostatic	Compatible with MEMS output voltage of 2–10 V	external voltage source required Capacitive
Electromagnetic	No external voltage source is required	Bulky due to magnets and pick-up coils Miniaturization is difficult
Magnetostrictive	High coupling coefficient >0.9 Polarization is not required, hence no depolarization problem High flexibility Can be used for high-frequency vibration	Nonlinear characteristics A pick-up coil is required Bias magnets are required in some cases Difficult to integrate with MEMS
Piezoelectric	No external voltage source required High output voltages in the range of 2–10 V on load Compatible with MEMS High coupling effect in single crystals	High output impedance Depolarization happens with cycling Brittleness in PZT Poor coupling in PVDF

2.4.4.4 Cantilever type PVEH

A cantilever type PVEH is widely used since it has various advantages such as simple design, high output at resonant frequency, and amenable to miniaturization. The device consists of a cantilever beam on which the piezoelectric material is bonded. A proof mass is normally used to get a desired resonant frequency range and also to optimize the power output.

There are many methods explained in the literature for tuning the resonant frequency of a cantilever type PVEH, to match the frequency of ambient vibration. However, there is no reported work on using IPMC for tuning a PVEH. Since the novel device described in this research uses IPMC as a low-power actuator, the basic details of IPMC are added below:

2.5 Ionic Polymer Metal Composites (IPMC) - Salient features as low-power actuators

The salient features of IPMC used for the design of the device in this study are given here. IPMC is made of polymers, such as Nafion, and filled with ionic conductive liquid. The proton

connected to the chemical unit at the end of a polymer chain is replaced with a metal ionic cat-ion (N+, Li+). These cat-ions get dissociated in water, generating a negative charge and free cat-ions in the material. Metal coating is given to a sheet of this material. This is the general fabrication process of IPMC [10]. Platinum or gold is used for the metal coating. Water molecules get tagged onto the free metal cations. When an electric field is applied, cations move to one side pulling the attached water molecules along. This causes an osmotic pressure difference, which will cause the actuation of IPMC. When the polarity of the electric field changes, the direction of actuation also changes.

Paquette et.al. have discussed [15] an electrical equivalent circuit of IPMC as shown in Fig. 2.10.

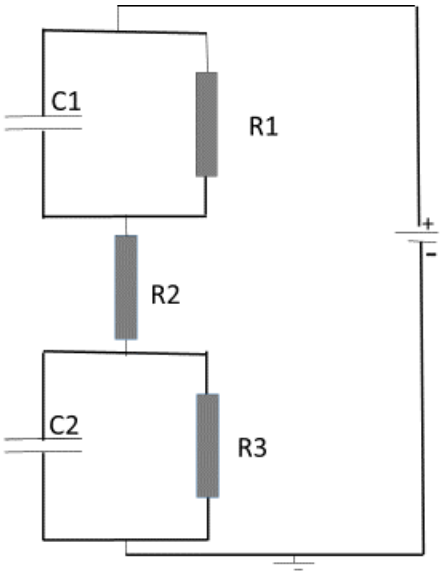

Fig. 2.10 Electrical equivalent circuit of IPMC (Adapted from [15])

It has two resistors (R1 and R3) and two capacitors (C1 and C2), which correspond to the two electrodes. The resistor R2 represents the material between the electrodes. The electric field E is given by the following relation.

$$E = V/h \tag{2.2}$$

where *V* is the voltage applied across the IPMC and *h* is the thickness of the IPMC.

The particle electrodes on the IPMC surface, are capacitive and resistive due to particle separation and density, which leads to a nonlinear response.

It is reported [10] that a square wave modulated with asymmetric impulses can be applied to the IPMC for better performance and to reduce energy consumption. The frequency of the modulating impulses should be much lower than the response time of the IPMC, to get the best response. Another feature is that the modulating impulses have a sharp rising edge and a sloping falling edge. The mechanism of IPMC actuation is dependent on the ionic diffusion when a voltage gradient is applied.

The characteristics of the ionic solution influence the physical properties of the IPMC. By using a parylene coating and an ionic solution with a high electrolysis voltage, the lifetime of the IPMC in dry air can be significantly improved [11].

It is also reported [12] that the driving voltage can be reduced by using silver electrodes, which have low resistance and large ductility, avoiding possible electrolysis. The blocking force of the actuator is dependent on its thickness. Hence a great deal of research has been done to improve the blocking force by introducing thickness-controlled ion exchange membranes. Performance is also enhanced by going for nano-dispersed metal electrodes instead of coated metal electrodes. Thicker membranes are realized by stacking pre-extruded Nafion films. Thickening of the electrode layer by metal deposition will not be a good option for improving the actuation performance of IPMCs, since it makes the IPMCs stiff, leading to lowering strain. Since the characteristics of the IPMC vary with its thickness, the availability of IPMC of different thicknesses is important for many applications. Hence casting method has been developed to fabricate Nafion films of the required thickness.

IPMC films show remarkable displacement under relatively low voltage, using very low power [13]. It has recently been established that by modifying the chemical composition of IPMC, the force capability is greatly improved.

IPMC materials are different from other electroactive polymers [14]. The most unique aspect of IPMCs is that their actuation is based on the active motion of ions and solvent molecules within the membrane under applied voltage or force. It means, the mechanism in IPMC is

anisotropic or directional, whereas other materials exhibit passive and isotropic responses to stimuli. The performance of IPMCs as actuators depends on their surface morphology. The best electrodes for IPMC actuators will be those that involve the largest available surface area and maximum conductivity. Configurations with multilayers are also advantageous to achieve better actuation characteristics [15].

The displacement and force generation of IPMC are dependent on the humidity [16]. The reason for this effect is a decrease in the stiffness as a result of the humidity. The actuators have a reverse motion and a negative force, which can be decreased by decreasing humidity. Increase in water-uptake will lead to an enhanced velocity of the displacement. Humidity near 50-60% gives a better actuator bending performance.

Experimental investigations are reported to study the effects of humidity and actuation time on the electromechanical properties of Ionic Polymer-Metal Composites (IPMC) in both the open atmosphere (uncontrolled environment at room temperature) and inside a controlled environmental chamber under different input voltages of different wave shape, value, and frequency [17]. It is demonstrated that the IPMC's electromechanical properties, namely the deformation capacity and electrical resistance, highly depend on the water content (in the IPMC strip and environment) and the duration of actuation. IPMC deformation capacity decreases with an increase in material electrical resistance. The IPMC material shows a relaxation behavior for a step voltage input, due to the back immigration of the hydrated cations from the anode to the cathode due to higher pressure at the anode side of the IPMC strip.

The electrochemical properties of IPMC indicate that it is possible to use them as compact fractional-order elements (FOEs) [18].

The electromechanical performance of IPMC depends on the electrical stimulus, environment humidity, counterions, and the number of actuation cycles, blocking force, and electric charge storage [19]. The hydration level and the counter ion type have a great impact on IPMC electromechanical properties.

The electrical-chemical-mechanical response of IPMC is dependent on the cations used, the solvent, the amount of solvent uptake, and the morphology of the electrodes [20]. If water is

used as the solvent, the applied electric potential must be less than 1.3 V at room temperature, to avoid electrolysis. Moreover, water evaporation in open air leads to dehydration of the sample. These factors limit the application of IPMCs with water as the solvent. Glycerol has a viscosity of about 1000 times that of water at room temperature and has a greater molecular weight. Like water, it consists of polar molecules and thus can serve as a solvent for IPMCs. IPMCs with glycerol as their solvent have greater solvent uptake and can be subjected to relatively high voltages without leading to electrolysis. They can be actuated in the open air for long periods. They are suited for low-frequency applications.

The displacement of a Nafion-based IPMC is proportional to the total charge imposed [21]. This property is the basis of self-sensing controllers for Nafion-based IPMC bending behavior. Self-sensing controllers are proposed using feedforward, feedback, and two-degree-of-freedom techniques. All three controllers can effectively control the actuation of the Nafion-based IPMC actuator.

It is found that IPMC exhibits hysteresis between its bending curvature and the applied quasi-static voltage [22]. The response of IPMC under a quasi-static voltage is explored to model the IPMC under DC actuation and to develop an open-loop control strategy based on the derived model. Open loop control is preferred in microsystems since additional circuitry is not required.

Water is the most used solvent in IPMC. So during the air operational life of IPMC, it will eventually dry. To produce an air-operable IPMC actuator, a new encapsulation process using a dielectric gel is proposed [23]. The results show that the encapsulated IPMC remained hydrated and its performance did not deteriorate.

IPMC can be used as actuators to carry out delicate surgeries [24]. It is to be noted that it is very similar to biological systems. The design of a single degree of freedom robotic surgical instrument actuated by IPMC is designed with a strain gauge element as a feedback sensor. A controller based on Proportional Integral (PI) was integrated into the system.

Many different methods to improve the IPMC response are being discussed [25]. By applying a large amplitude and short duration pulses, a fast response can be induced, since ion re-distribution will be speeded up. Similarly, isopropanol-assisted technique is useful in developing

better-performing electrodes. It is also reported that sulfur and nitrogen co-doped graphene electrodes improve the conductivity and capacitance of the device.

Research is carried out on IPMC as energy harvesters investigating its main features such as mechano-electric transduction capability, stiffness, impedance etc. [26]. Studies are made based on an electromechanical transducer model. It has been demonstrated that IPMC can be used for energy harvesting at frequencies less than 50 Hz. Experimental results are also reported.

A model for IPMC is proposed where the electromechanical component of the model includes formulation to include the effect of electrolysis current [27]. The mechano-electrical component of the model is analyzed to determine the cause for the delay between induced voltage and applied deflection. It is demonstrated that the volumetric effect of the anion charge plays an important role in mechano-electrical transduction calculations.

Nafion membranes operate as electromechanical actuators and sensors [28]. It is reported, that the use of 1-ethyl-3-methylimidazolium trifluoromethane sulfonate ionic liquid is explored as a solvent for Nafion™ polymer actuators and sensors. Nafion™ transducers with this ionic liquid have improved stability when operated in air as compared to the same materials with water (Figure 10). However, a drawback observed is that ionic liquids lead to a reduction in the speed of response.

IPMCs can be used as soft actuators in various practical areas like robotics, biomedicine and micromanipulation systems [29]. IPMC actuators have many advantages over other actuators such as lightweight, low operating voltage, possibility of miniaturization. However, their properties of back-relaxation, hysteresis, high sensitivity to ambient conditions, etc. lead to difficulty in precise and reliable control. Here various control methods for IPMC actuators are explained.

IPMC has an electromechanical response that is dependent on the driving voltage and method. Here an equivalent electrical circuit model for the IPMC actuator is developed using experimental data [30]. The effect of the waveforms and frequencies of driving inputs on the characteristic features of the IPMC actuator are studied. Various signal forms such as square, triangular, and harmonic waves are applied and studied. It is observed that large consumption of

current during actuation is caused by the high-frequency components of the driving waveforms. This is due to the fact that the IPMC actuator has the characteristics of a damped high pass filter.

Enhanced force by IPMC as an actuator, can be realized by increasing the thickness of the film [31]. To cater to various applications, mechanical characteristics such as stiffness, displacement, and force were measured for the fabricated specimens using cast ion-exchange-polymer films and analyzed.

Improving the force developed by IPMC along with the deflection is a challenge. Normally a non-corrosive material is used as an electrode. In the study reported here, silver, a corrosive metal is used as an IPMC electrode [32]. The reversible redox reaction of the silver electrode results in the material characteristics change of the IPMC, and it results in higher curvature and blocking force. This is an extremely interesting result and it calls for further research.

A Nafion-based IPMC with high-quality metal electrodes study shows large deformation and fast response can be achieved. [33].

Tatbatabaie has proposed many novel designs of IPMC [34]. The various configurations are realized by stacking the IPMC strips in different patterns such as helical, tubular, spherical, strips in series, etc. By attaching strips of IPMC, it can be actuated to get a movement mimicking a snake. The whole structure is an active element.

Another configuration reported is a rolled IPMC [34]. This configuration can be used to effect a rotating motion to a part. The part should be attached to the pre-rolled IPMC. When an input voltage is applied to the IPMC, the part will rotate, as the IPMC unwinds or winds up.

The literature above indicates various research that is going on, to address the basic issues associated with IPMC actuators such as improving the blocking force, reducing the electrolysis and dehydration when water is used as a solvent, lowering the power consumption, and improving the stability. The use of different electrode materials is a promising approach to enhance the actuation characteristics. Another important finding as reported above is the possibility of realizing different actuation modes by different patterns of IPMC that will be useful in new device designs. It is interesting to note that since it is a Nanocomposite, many of its characteristics can be tailored.

Chapter 3

A Novel tunable PVEH

Note: This chapter is adapted from a peer-reviewed paper that has been published in ***Mechanics of Advanced Materials and Structures*** with permission where appropriate. This chapter highlights the relevant literature survey, the conceptualization of the device, fabrication, and experiments conducted to characterize the device. The theoretical analysis of the results is also covered here.

The article citation is:

Raghavan, S., Sharma, A., & Gupta, R. (2023). Resonant frequency tuning of a novel piezoelectric vibration energy harvester (PVEH). Mechanics of Advanced Materials and Structures, 1-16.

Article link: https://www.tandfonline.com/doi/abs/10.1080/15376494.2023.2209078

Abstract

It is imperative to provide autonomous power supplies for the sensor nodes in Structural Health Monitoring. Piezoelectric Vibration Energy Harvesters (PVEH) can generate power to meet this. Here, studies on a novel PVEH design integrating Ionic Polymer Metal Composites (IPMC), for electrical tuning of resonant frequency of the harvester have been discussed. The device for which a patent is pending has two sections. Macro Fiber Composite (MFC) is bonded on the root section and the extension beam is impacted by IPMC. Net power output was achieved with varying conditions. This paper also discusses the theoretical analysis of results and next-generation devices.

3.1 Introduction

Health monitoring of structures has become a key factor in developing an effective strategy for maintenance and retrofitting. This has benefited from the fast-paced development of different types of sensors with low power requirements. However, there have been issues associated with powering the deployed sensors that are generally inaccessible such as the ones used in nuclear power reactors, remote bridge structures, aircraft, human bodies, etc. [36, 37]. In the last decade, the focus on automated Structural Health Monitoring (SHM) to reduce human intervention and related costs has led researchers to look for alternative sources of power [38, 39]. Harvesting energy from the ambient sources of vibration (Fig. 3.1) including the thermal gradients, mechanical vibrations, solar, fluid flow, human-driven sources, etc. is a potential alternative source of energy [40–45]. This can potentially replace the traditional power sources with limited life and storage capacity such as batteries, thereby significantly reducing the required maintenance and subsequent costs [36, 46].

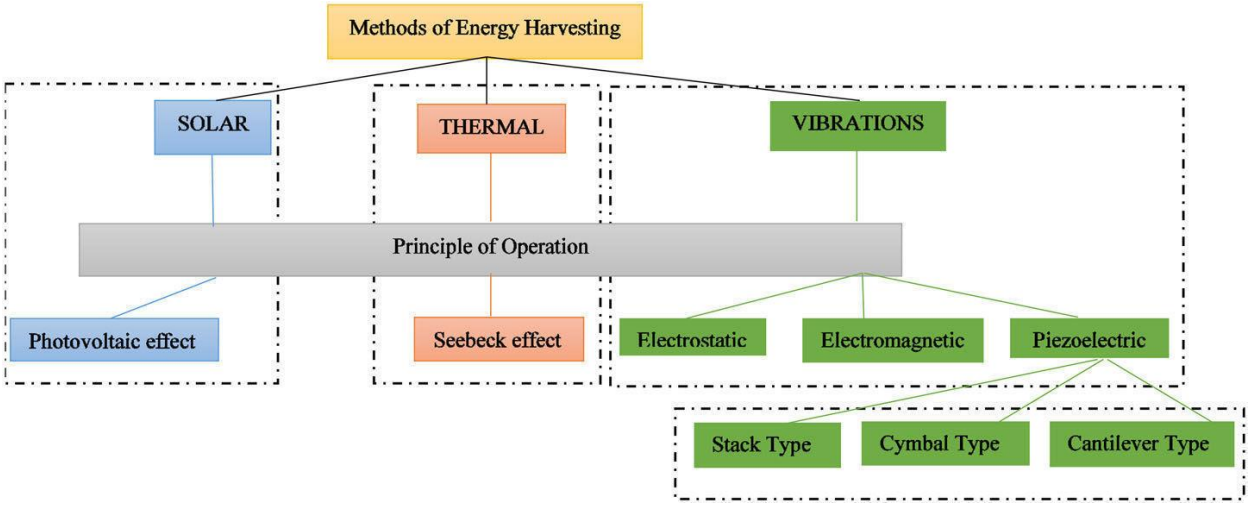

Fig. 3.1 Methods of Energy Harvesting

Thermal energy harvesters utilize the Seebeck effect that correlates the conversion of heat into electricity but their power output dependence on the temperature gradient significantly limits their scope [47]. More effective new methods are developed, by using thermal energy to switch thermomagnetic materials between magnetic and nonmagnetic states, which enable the conversion of thermal energy to electrical energy [41]. Solar energy harvesters are used to achieve the highest power output but are limited by outdoor applications and the availability of a source of power [48].

Another way of energy harvesting is by tapping the mechanical ambient energy that can be found through vibrations, fluid flows, pressure fluctuations, etc. [49]. Vibrations being most immanently available in the environment, provide a more robust source for harvesting energy for applications which are shown in Table 3.1.

Table 3.1 Ambient sources of vibration

Source of Vibration	Frequency of vibration (Hz)
Car hood	12
Bridge	2.1-2.3
Aircraft	26
Helicopter	5 -gives peak power
Ship	5-20
Satellite Launchpad	5-200
Offshore wind turbine systems	0.5-1.5

Vibration-based energy harvesting has numerous applications such as in the case of dynamic structures including automobiles, helicopters, fixed-wing aircraft, and many land-based structures such as buildings, bridges, and satellite launch pads [50–52]. Energy harvesting from such sources of vibration is based on the transduction principles of kinetic energy and is usually classified as 1) Electrostatic; 2) Electromagnetic; 3) Magnetostrictive; and 4) Piezoelectric [53–57]. Depending upon the source and the transduction mechanism, the generated output power can vary widely. While energy harvesting is possible even at a larger scale, with other amounts of power, in micro and mini systems, power will be from μW to mW [56]. Energy harvesting using electrostatic transduction involves the conversion of vibration energy into electrical charges based on the principles of a variable capacitor as the change in capacitance will induce an increase in voltage in the harvesting system [37, 39, 58]. Several factors such as the requirement of an external power source, the presence of low capacitance, the high impact of parasitic capacitance, etc. limit their applicability. Electromagnetic transduction involves the movement of the armature inside a coil with reference to a vibrating source [59]. In a typical device, the armature will be connected to a source of vibration hence enabling a movement along with the ambient vibratory movement. This movement will generate a voltage in the coil surrounding it due to electromagnetic induction [37]. The applicability of such devices is limited by factors such as the size of the device, generated

low level of voltage, extremely low efficiency in low frequencies, and small sizes. Magnetostrictive material can produce electric energy from the mechanical vibrations in a two-step process. When the magnetostrictive material is subjected to mechanical vibrations, a corresponding magnetic field is produced in it. When this magnetostrictive material is introduced as a core of a coil, this resulting change in the magnetic field induces an electric field in the coil. Since the device is quite bulky and of low output, these devices are not considered very efficient [60].

Many researchers have experimented using IPMC for energy harvesting. Farinholt et al. [61] have compared two types of vibration energy harvesters, one using piezoelectric polymer polyvinylidene fluoride and another using IPMC. The harvesters operated at resonance frequencies of 138Hz. and 70 Hz. The generated power in the case of the harvester using IPMC was two orders of magnitude less. Jamshidi et al. [62] have worked on energy harvesting using large strain characteristics of IPMC from the oscillation of rectangular cantilever plates having a low aspect ratio. About 1.75 mW of power could be generated with a flow velocity of 60 meters per second. Martin [63] has worked on energy harvesting from vibrations using IPMC. Further, he has demonstrated that they have an inherent capacity to store electrical energy akin to a capacitor when mechanically deformed. Soh et al. [64] have discussed the research by many researchers on IPMC. IPMCs are capable of converting mechanical energy to electrical energy and vice versa. Hence they are ideally suited to function as sensors and as actuators. They need an aqueous environment to function and this makes them very suitable for converting aqueous flows to electrical energy. Due to their similarity in function with human muscles, they have applications in robotics and biomedical fields. They can be miniaturized in any shape and dimension and fabricated as MEMS.

3.1.1 Piezoelectric vibration energy harvesting

The advancements in sensor technology have led to the realization of sensors that can function with very low power consumption. Hence, the low output power generated by the energy harvesters can be utilized in providing autonomous power sources for these MEMS-based sensors [65-67]. Here energy harvesting using piezoelectric transduction overcomes most of the limitations associated with other methods [37]. This method is based on the piezoelectric effect of certain materials that involves the generation of voltage when subjected to mechanical stress [55].

Piezoelectric materials such as PZT (Lead zirconate titanate), barium titanate, lithium niobate, etc. undergo a reorientation of the electric dipoles, resulting in the formation of electric charges that can be harvested [54].

The constitutive equations for piezoelectric material (IEEE Std. 176 (1978)) are the basis to derive the governing equations of electromechanical modeling for PVEH systems and owing to the higher Young's modulus of piezo ceramics, larger strains have been reported to be obtained by using different configurations of PVEH including 1) Stack; 2) Cymbal- type; 3) Cantilever type. Larger strains are advantageous since they lead to higher voltage output from the harvester.

These cymbal-type devices don't generate fairly good output at low frequencies which are normally present in ambient conditions. The stack-type is considered effective only for higher load applications and does not give a reasonable output in the normal ambient vibration conditions.

Cantilever PVEH configuration is a simple yet effective design to generate higher strain under moderate values of excitation from a vibration source and has been tried by many researchers [49, 51]. A cantilever PVEH can be designed as a unimorph (with one active piezoelectric layer on a substrate) or a bimorph (with two active piezoelectric layers). Researchers have been trying different configurations in order to increase the power output of cantilever- type PVEH. Aladwani et al. [104] have reported a method to increase the power output of PVEH by enhancing the strain with a spring and mass system between the fixed end of the harvester and the vibrating structure. This spring and mass system can improve the bandwidth of the harvester also. Raju et al. [105] have worked on structural design-based methods for increasing the harvester output. They have proposed a rectangular section ending with a tapered section and a tapered section ending with a rectangular section. They have also studied the effect of introducing a cavity in the cantilever. Askari et al. [106] worked on another structural approach, where the advantage of a multi-beam harvester is made use of. The device was designed for frequencies less than 100Hz. Panda et al. [107] have analyzed a laminated composite beam energy harvester for optimum performance. Specifically, a multilayer carbon epoxy composite beam was used for the studies. Meng et al. [108also studied a composite material used in the harvester. They have analyzed a 3D braided composite material as the cantilever beam. The material properties of the 3D braided composite beam could be tailored during the design phase. Chand et al. [109] worked on an energy harvester with a cantilever beam having a parabolic tapering width structure. The harvester could generate a higher output and had a low natural frequency.

While a cantilever configuration can generate much higher output at lower ambient vibration levels, it has an inherent disadvantage of generating peak output voltage only at its resonant frequency. As the ambient frequencies can vary around the resonant frequency of PVEH, this results in the loss of a substantial amount of output power. Hence, many researchers have looked into methods to overcome this characteristic of a cantilever-type PVEH [60, 68].

3.1.1.1 Passive methods for tuning the resonant frequency of PVEH

In general, passive and active methods have been explored by researchers to tune the resonant frequency of PVEH following variations in the frequency of the ambient vibrations. Passive methods require human intervention since it does not have an autonomous system to change the frequency. The passive methods include i) changing stiffness by axial preload[69-71], ii) spring-loaded cantilevers [68, 73, 74], iii) magnetic stoppers [75, 76], iv) multiple elements of piezoelectric materials[77], v) multiple interlinked cantilever beams [45, 77] vi) changing the shape and cross-section of cantilever beam [78], vii) moving tip mass [79, 80]. Leland et.al. [69] have worked on tuning the harvester by applying axial pre-load. Another passive method of utilizing multiple cantilever beam structures has been widely explored for optimal energy harvesting [77]. Fan et al. [110] worked on a Nano energy harvester, where porous piezoelectric material was used. It was demonstrated that the solid-fluid coupling dielectric coefficient modifies the peak power output and the resonant frequency during the fabrication phase.

3.1.1.2 Discussion on Active Methods for Tuning the Resonant Frequency of PVEH

Active methods involve elements that constantly work on changing the resonant frequency of the PVEH following the change in the ambient vibration frequency [56]. In general, the active method involves some form of actuation which will lead to the requirement of actuators that can be integrated with the device. The actuator has to be "on" always. However, realizing an actuator that consumes very low power compared to the harvested power is a challenge. In this regard, Roundy et.al. [38] have reported the feasibility of active tuning using actuators, and the potential of tuning stiffness, mass, and damping was evaluated theoretically and experimentally. It was reported that the power required for tuning always exceeded the resulting increase in power. In another research reported by Roundy et.al. [82], a PVEH that has wideband tunability utilizing a stiffness-altering adjustment is discussed. The same report gives the details of an active tuning method based on the stiffness change of the piezoelectric material. They have used piezoelectric

benders as cantilever beams of the generators. Two electrodes are integrated on the surface of the beam, one of them is used for harvesting the energy and the other for tuning. This is based on the fact that the stiffness of a piezoelectric material depends on its elastic constant as well as the electric field across the material. Hence the method used is to control the electric field applied to the tuning electrodes, which will change the natural frequency of the PVEH. However, it was reported that it did not result in an effective tuning since the power required for tuning was high and could not achieve net positive power output from the PVEH. It was indicated that a low-power actuator should be explored to control the stiffness of a PVEH.

From the literature review, it can be seen that while passive techniques provide different methods for obtaining the tunability of PVEH, their dependence on human intervention limits their scope in several real-time applications. On the other hand, active techniques do indicate a potential to overcome the above-mentioned limitation by realizing an autonomous system configuration that makes use of self-actuation. However, there is limited literature available exploring possible active techniques for achieving efficient tunability of PVEH.

3.2 Research significance

The various literature shows, that there have been many issues in designing a cantilever-based PVEH for functioning at different ambient frequencies without much reduction in its power output. Many researchers have been working on resolving these issues. However, finding a mechanism to tune the PVEH that uses less power so that net power output doesn't suffer, is still a challenge. Our research is to arrive at a method of design of PVEH, which can be tuned while maintaining the net power output to a great extent. This task involves identifying a suitable concept for changing the stiffness, identifying a suitable device to realize that, studying the effectiveness experimentally, and correlating it with a theoretical analysis.

The proposed design of the device uses IPMC as a stopper to shift the resonant frequency of the PVEH. An earlier paper by us on the subject [83] indicates limited tests on a device using different materials for PVEH to demonstrate this approach is possible. Here aluminum was used for the root section and the extension beam. The harvester was studied varying the gap between the IPMC tip and the surface of the cantilever beam. The results of this present research bring out in greater detail, with additional experiments on a device using different materials, the feasibility of using a very low power actuation that can be introduced in the design, to tune the resonant

frequency of the PVEH. This is of importance since there had been no other literature on this novel approach of utilizing a very low-power actuation as a stopper in the design.

The salient features that highlight the significance of this research are as given below:

- The concept of integrating IPMC into the PVEH design is not reported by any other authors.
- The power required for the IPMC to shift the resonant frequency of the PVEH is low enough to be provided by the harvested energy, still gaining net power output.
- The IPMC is a nanocomposite, which can be easily miniaturized into MEMS form [84] in the PVEH MEMS design.
- The range of frequency through which the PVEH can be tuned depends on the blocking force that can be developed by the IPMC, with the low-power input. The IPMC fabrication technology is constantly evolving to generate higher blocking forces for the same low power input [85, 32]. Hence the frequency range through which resonance can be tuned, will significantly be improved by using the higher force IPMCs.
- The IPMC actuator in the design can be kept active and the necessary steps of DC voltage can be given to shift the resonance. This method significantly reduces the power consumed by the IPMC to a still lower value [10].

The above-mentioned features of this novel design will be further explained in this paper at different stages. Based on this concept, a full US patent has also been filed [86].

3.3 Materials and Methods

3.3.1 Initial Study

In order to develop the final design of the device, a series of preliminary experiments were conducted on PVEH, applying various methods such as shifting mass along a cantilever beam and different fixity conditions. All these methods require manual intervention to achieve a change in the resonant frequency.

3.3.2 Frequency tuning of PVEH

The limitations of passive tuning techniques can be overcome by using active tuning methods that rely on varying the mechanical stiffness of PVEH using piezoelectric actuators [87]. However, piezoelectric actuators do not work on the very low input voltage (1-10 V) and power. Hence these tuning methods still consume a considerable amount of power. This proposed

design of the device using IPMC as the actuator overcomes all the above-stated limitations and provides a low-power solution for electrical tuning.

We will now discuss the proposed novel design. The device consists of the cantilever beam, MFC patch bonded on it and IPMC actuator. The experimental setup includes an exciter, amplifier, signal conditioner, rectifier circuit, oscilloscope, etc. The details are covered under the relevant headings.

3.3.2.1 Piezoelectric Cantilever Set-up

Based on the initial study by the authors, the conventional PVEH cantilever beam design was modified by including an extension beam with the focus of developing a tunable PVEH device. Table 3 entails the details of the different types of PVEH cantilever beams that were used for the experiments. Fig. 3.2 represents the schematic diagram of the finally proposed PVEH cantilever design (also shown in "Fig. a" in Table 3.3).

Initially, the selection of the substrate was done using pre-existing literature of PVEH [37, 55, 56] wherein the device included only one section (as root section). During the initial design process, it was found that the range of force associated with IPMC actuation was not large enough to effectively change the resonant frequency of the root section. Therefore, it was hypothesized that a thinner beam might better respond to the impact of IPMC actuation. However, it was subsequently found that thinner sections of the substrates (as root section) are unable to transfer sufficient stress to generate a substantial output from the MFC. Hence, a PVEH cantilever design that includes a root section (RS) and an extension beam (EB) of thickness 1.25 mm and 0.3 mm respectively was taken up for experiments. These values of thickness were considered as a typical case that satisfies the above mentioned criteria of realizing an effective transfer of load from the IPMC. Lightweight glass fiber (FR4) was used for the RS of the beam. A thin section of aluminum was chosen for the EB portion of the beam to effectively transfer the load from IPMC to the RS of the cantilever. Table 3.2 details the material properties of RS and EB. The EB was bonded to RS using 3M465 film tape**.** Furthermore, a tip mass weighing 6.06 gm was mounted on the tip of the RS. This was done to obtain the desired range of resonant frequency for the basic PVEH cantilever beam.

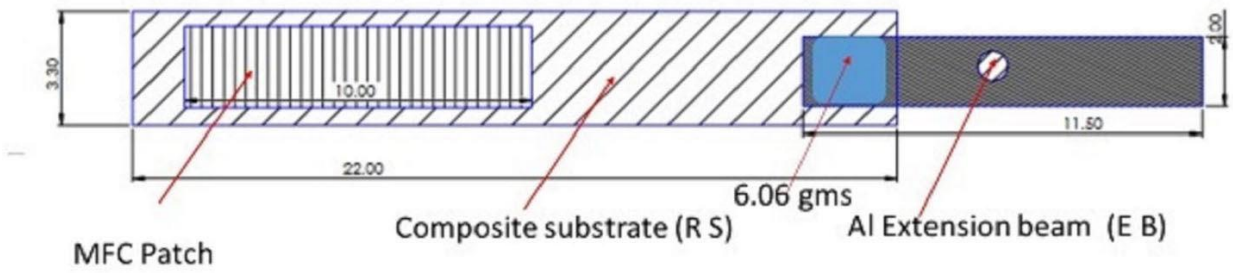

Fig. 3.2 Piezoelectric Cantilever set-up (Dimensions in cm)

Table 3.2 Properties of materials used as root section and extension beam of the PVEH

Properties	**Composite**	**Aluminum**
Thickness mm	1.25	0.3
Young's Modulus, E (in GPa)	21	69
Length cm	22	11.5
Width cm	3.3	2
Density g/cm^3	1.850	2.7

The Macro Fiber Composites, originally developed by NASA's Langley Research Center are PZT (Lead (Pb) Zirconate Titanate) based piezoelectric patches with great flexibility which can be bonded on structural elements that undergo higher deflections [88]. The interdigitated electrodes of MFC make the transfer of signals more efficient. Given these features of MFC, it was decided to use MFC in the proposed device design. Many researchers have reported work on MFC patches for various applications such as energy harvesting and vibration control [89-92]. Fig. 3.3(a) and 3.3(b) represent the structure of the MFC patch and the typical MFC patch used in the study. MFC is made of piezoelectric fibers of a square cross-section bonded together with epoxy to form a sheet. This sheet is sandwiched between polyimide films and electrodes. Piezoelectric materials can be in two configurations, depending on the direction of force applied with reference to the poling direction. When the direction of force is in the same direction as the poling direction, it is called d_{33} mode and when it is perpendicular to the poling direction, it is called d_{31} mode (Fig. 3.4).

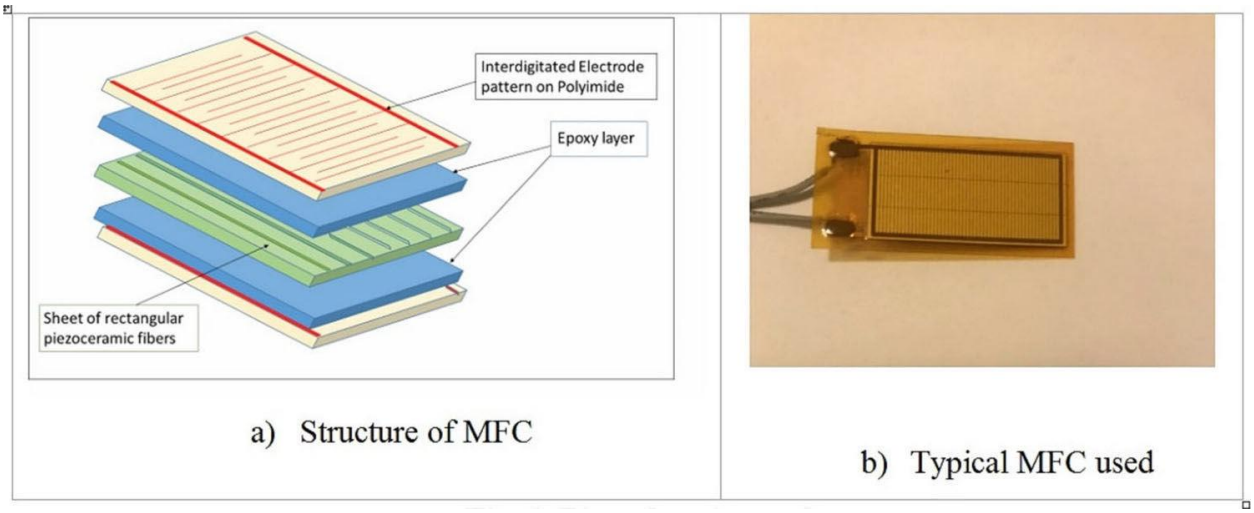

Fig. 3.3 (a) Structure of MFC **Fig. 3.3 (b) Typical MFC**

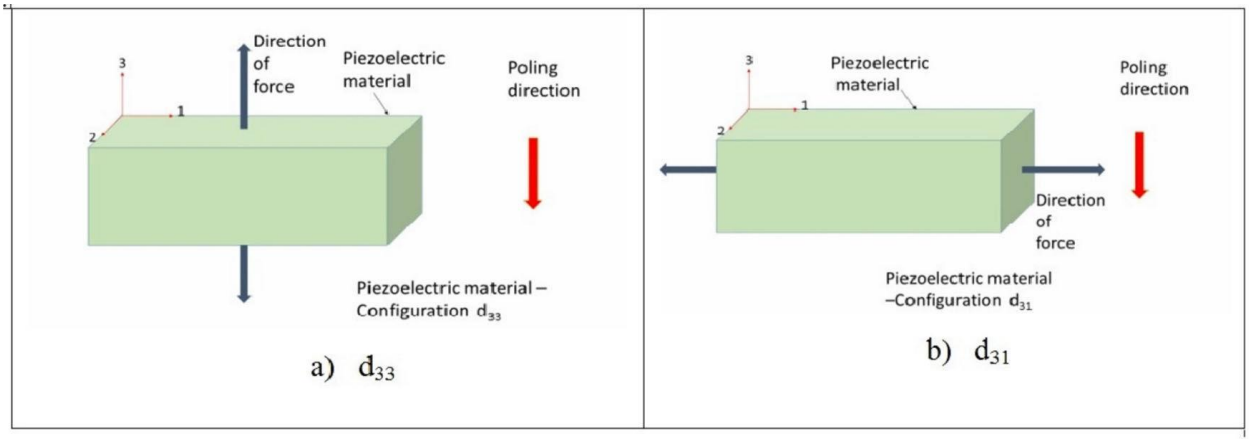

Fig. 3.4 (a) d_{31} type piezoelectric material **Fig. 3.4 (b) d_{33} type piezoelectric material**

Different types of MFCs have been reported in existing research [37–41] for various applications. However, in this study, P2 type MFCs obtained from Smart Material Corporation, USA [93] have been used. This is because P2 type MFC responds best for energy harvesting applications due to its higher capacitance. P2 type MFCs function based on the d_{31} effect for actuation. Table 3.3 gives the details of the different types of MFCs used in the study. It should be noted that the novel design of the device can be realized on any of the P2 type MFCs and therefore, there is no specific reason behind the choice of MFC for a particular experimental work.

Table 3.3 Details of the different types of Specimens used for experiments

Specimen with MFC	Type & substrate dimension	MFC Type	MFC Specifications (by the manufacturer)						
			A_L mm	A_W mm	O_L mm	O_W mm	C_{nF} ±20 %	F_{strain} ppm ±10 %	B_F (N) ±10 %
Fig.a 	RS:Composite (22cm, 3.3 cm) EB:Aluminum (11.5cm, 2cm)	M2814-P2	28	14	37	18	43	-630	-76
Fig.b 	RS: composite (22cm, 3.3 cm)	M2814-P2	28	14	37	18	43	-630	-76
Fig.c 	RS:HDPE (18cm, 4.5cm) EB:HDPE (9cm, 2cm)	M5628-P2	56	28	67	31	175	-740	-175
Fig.d 	RS:Aluminum (17cm,3.5cm)	M8503-P2	85	3	94	7	15.5	-430	-11
Fig.e 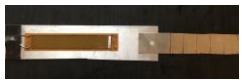	RS: Aluminum (17cm,3.5cm) EB: Aluminum (10cm, 2cm)	M8514-P2	85	14	100	18	127	-630	-76
Fig.f 	RS:Composite (22cm,3.3cm) EB:HDPE (9.5cm,2cm)	M8528-P2	85	28	103	31	258	-740	-180

Note: A_L- Active Length, A_W- Active Width; O_L-Overall Length O_W – Overall Width; C_{nF} – Capacitance in nano Farad; F_{strain}- Free Strain; B_F – Blocking force HDPE

HDPE- High-Density Polyethylene

In Table 3.3, the indicated active length and active width are the dimensions corresponding to the active fiber sheet of the MFC whereas the overall length and width correspond to the physical dimensions of the MFC. The capacitance and the free strain are important parameters in the function of a piezoelectric device. The blocking force is the force that the piezoelectric element can develop with zero deflection, in the actuation mode.

A limited analysis to get confidence that our samples did not change their characteristics and the output was stable during our experiments was done as detailed below:

A test was developed and carried out on 4 MFC patches in cantilever configuration for 1 million cycles of operation at the resonant frequency of each device. The output voltage was monitored at fixed intervals of 10,000 cycles and the results are plotted in Fig. 5**.** The output voltages were stable at the peak value and no change in values was observed, indicating no deterioration. These experiments were carried out on M2814P2, M8528P2, M8514P2, and M5628P2. Further, test was carried out at 12 Hz for 3 MFC patches, M5628P2, M8503P2, and M8514P2 for additional 4.5 million cycles to explore if there are any variations in the behavior for an extended period. After the test, each of the MFCs was tested at its resonant frequency and still no deterioration in the performance was recorded.

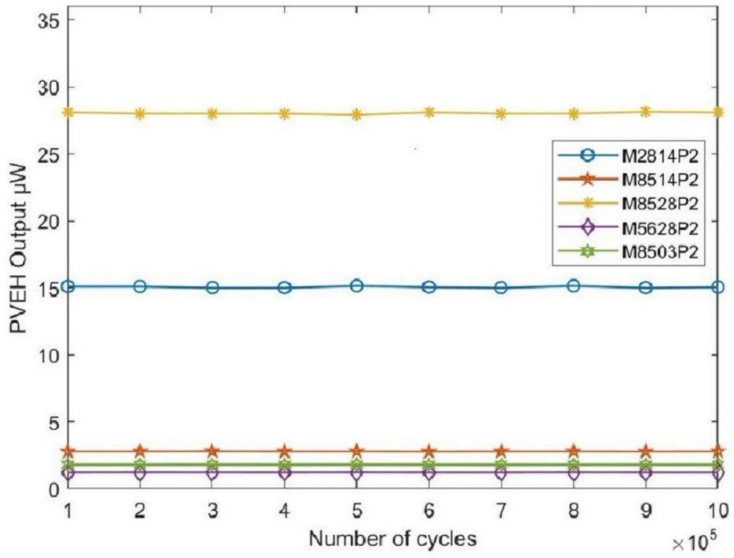

Fig. 3.5 Response of MFC

The higher value of output voltage seen in the above plot is due to the choice of the cantilever, in addition to the MFC properties.

3.3.2.2 IPMC

IPMC materials are porous fluorinated polymers that are filled with an ionic liquid, which is conductive. During fabrication, cations replace the protons attached to the terminal group. These cations will dissociate in water, and terminal groups will have a negative charge. This process will lead to an excess of free cations in the material. This material sheet will be given a coating of a noble metal. This device is an ionic polymer-metal composite (IPMC) where dipoles can orient themselves when subjected to the electromagnetic field. They get attached to the free metal cat-ions. When an electric field is applied, this configuration leads to an electric current and cat-ions move to one side of the material. This process results in the actuation, by bending of the IPMC strip in a pattern defined by the electrode configuration [22, 94-97].

Blocking force of IPMC is the force it can withstand with zero displacement, and is defined by the following equation.

$$F = C_1 \times \frac{wt^2}{L} \lfloor gf \rfloor \qquad (3.1)\ [95]$$

F is in gram force (gf), C_1 is a constant; *w*, *t*, and *L* are the width, the thickness, and the length of IPMC in mm respectively.

A long IPMC can create a large displacement, but it cannot produce a high tip force. A thick IPMC can generate a high tip force. When the applied voltage is increased, tip displacement and tip force are also increased. Another factor that contributes to a better displacement and force is the low surface resistance of platinum electrodes in an IPMC.

The generated force shows an almost increasing trend with the voltage. This is due to the movement of cations along with the water molecules driven by the voltage applied across the sides of IPMC. The capacitance of IPMC also increases as the thickness increases in a non-linear pattern. As the applied voltage increases, both bending displacement and the tip force increase. The bending displacement and tip force exhibit a more linear pattern with an increase in voltage, when thickness reduces. The uniformity of the electrodes is better when the thickness of the actuator is reduced.

Governing PDE for charge distribution in an IPMC is as given below in [98],

$$E = \frac{D}{K_e} = -\nabla\Phi \qquad (3.2)$$

D, E, φ, and ρ denote the electric displacement, the electric field, the electric potential, and the charge density, respectively. K_e is the effective dielectric constant of the polymer.

$$\nabla . D = \rho = F(C^+ - C^-) \qquad (3.3)$$

F is Faraday's constant, and C^+ and C^- are the cation and anion concentrations, respectively.
The response of IPMC [98] is a function of the structure of the backbone ionic polymer, the conductivity of the metal electrodes, the properties of the cations, and the extent of hydration. The speed and magnitude of the actuation also depend on the type of solvent. Hence the operation time is a parameter that depends on the type of solvent. The loss of solvent can be due to evaporation or electrolysis. If a higher voltage is applied to the IPMC, electrolysis can take place leading to loss of solvent. However, recent research leads to new encapsulation techniques using a dielectric gel, which will be important in applications involving long-term operation. Since the IPMC strip can be cut into units of very small sizes, they can be easily considered for MEMS-based actuation applications. It can also be operated with an open-loop control system. The advantage of open-loop control over feedback control is that external sensing devices and circuitry are not needed, which can be very important in microsystem design.

Commercially available Nafion-based IPMC is considered for this study. For the design, IPMC of length 30mm, width 5mm, and thickness 2 mm from Environmental robots, USA was used. This IPMC can function as an actuator if a low voltage in the range of 1 to 4 V is applied. On application of a voltage, the IPMC actuates, generating a blocking force.

With different blocking forces, the IPMC in contact with the cantilever beam behaves like an impact with elements of different reaction forces. These above details of IPMC characteristics clearly state the reason for using IPMC in this design. Fig. 3.6 (a) depicts the structure of a typical IPMC. Fig. 3.6 (b) shows the photograph of the IPMC used for the experiments. In Fig. 3.6 (b), b_1 depicts a single IPMC and b_2 depicts a configuration of two IPMC strips joined together. Since the Nafion-based IPMC selected for the study utilizes water as the ionic solvent, proper hydration of the IPMC is critical in ensuring effective actuation. Hence, IPMC strips were immersed in water for 16 hours. Then the samples were checked for moisture loss by measuring the mass in a precision balance, until the mass reached a stable value. This is required to make sure that IPMC is used with its stable saturated water content.

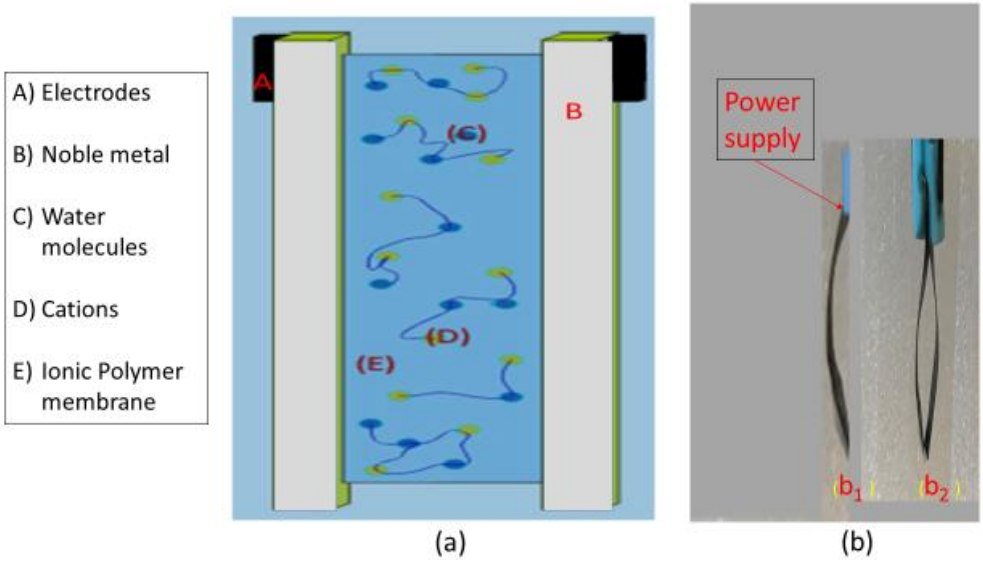

Fig. 3.6 The structure of IPMC (a) and the IPMC used in the experiment (b)

Fig. 3.7 shows the graph plotted between the time lapsed and the mass of IPMC. It can be seen that after 1 hour, the IPMC has reached saturated stage, and no mass loss takes place subsequently. To make sure the actuation is consistent, care was taken to maintain its hydration level during the experimentation.

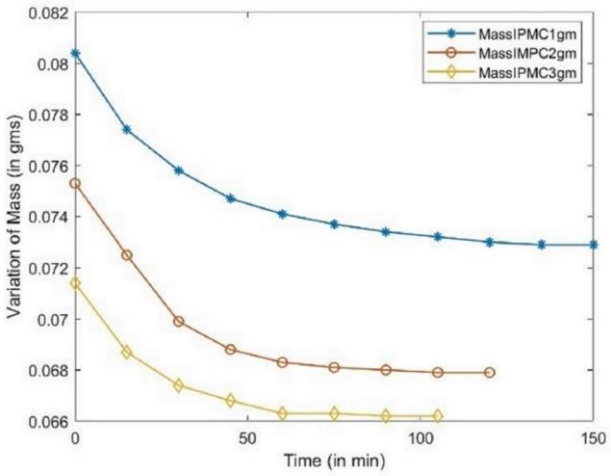

Fig. 3.7 Moisture content study of IPMC

3.3.2.3 Rectifier Circuit

The output of the PVEH will be an alternating voltage corresponding to the varying stress values resulting from the sinusoidal nature of the input vibrations. Hence a full-wave rectifier was to be designed and interfaced with the PVEH, to acquire the output in DC form. It is desirable to

use a passive circuit since no power will be required for that. The rectifier circuit used in the study consisted of 4 diodes (IN 4001) and a capacitor (220μF). The diodes form a Wheatstone bridge and the output of the PVEH is connected to the terminals across the bridge as shown in Fig. 3.8.

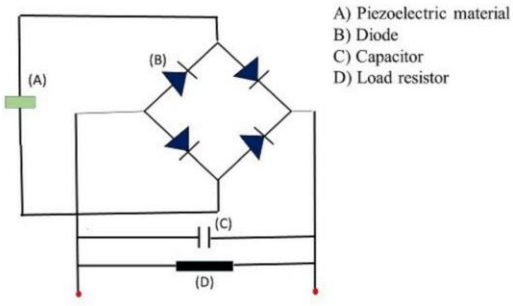

Fig. 3.8 Rectifier circuit

The output of the bridge is taken across the other two terminals of the Wheatstone bridge and connected across a capacitor. A load resistor (1MΩ) was connected across the capacitor and the voltage across the resistor was monitored. Since the piezo element has a high output impedance, the load resistor had to be selected to match the high impedance, so that usable power can be acquired. Even though, a passive circuit is used, there will be a small amount of power loss due to leakage current, which is ignored.

3.3.2.4 Integration of the Design setup of Energy Harvester

The design utilizes the integration of another smart material (IPMC) in the cantilever beam configuration to induce a stiffness change by virtue of contact mechanics. IPMC works as an actuator with a low input voltage in the range of (1-4 V DC). The blocking force (load that IPMC can withstand with zero deflection) of the IPMC changes with variation of the input voltage. This property is utilized to provide an impact response in the extension beam of the PVEH. As a result, a change in the stiffness of PVEH will be induced, changing the resonant frequency. Hence, a shift of the resonant frequency can be achieved by varying the input voltage to the IPMC. In general, power output very near to the peak power output of the PVEH corresponding to its resonant frequency can be achieved even if ambient frequency drifts from the basic natural frequency of the harvester [86].

From the initial study, it was found that when a single IPMC was used, the results were inconsistent due to the lack of a stable contact point. This led to the use of stacking of two IPMCs to improve the efficacy of the design. The two IPMCs were powered at the same point on one end

and the other end was joined and was touching the beam. This was found to be a stable configuration. Fig. 3.9 represents the integrated setup used for the experimental analysis of the novel device and Fig. 3.10 shows the photograph of a typical setup used. Care was taken to make sure the IPMC setup was consistently stable throughout the experiment. The set-up includes a signal generator (GW Instek GFG8250 A make), oscilloscope (HP 54603 B make), exciter (Miniature shaker K2007E01-Modal shop make), multimeter (Agilent make), and wireless accelerometer unit (Pasco make).

The resonant frequency of a PVEH is a function of the type of constraint that it is subjected to. A fixed-free cantilever behaves differently from one that is fixed-quasi-free. The proposed novel design primarily utilizes this concept to enable a tunable PVEH system. If the cantilever beam is subjected to an impact with an element, the energy associated with it changes and goes to a higher resonant frequency. If the impact element is of different stiffness, this change in energy varies and so does the resonant frequency. As mentioned earlier, the IPMC functions as an actuator where the actuation is a function of input voltage of the range 1-4 V. On actuation, the blocking force of IPMC changes. Hence, an IPMC under actuation is an impact element to the cantilever beam, the change in energy of the cantilever beam will be the function of the level of actuation of the IPMC. In the proposed design, the integration of an IPMC as an impact element located above the cantilever beam is considered to be the novel aspect of the tunable harvester design. A study on the electrical characteristics of IPMC shows, it requires very low power to operate, which is ideal for achieving net power gain from the PVEH. The IPMC was also powered separately during detailed experimentation to ensure no other extraneous factors added error to the results.

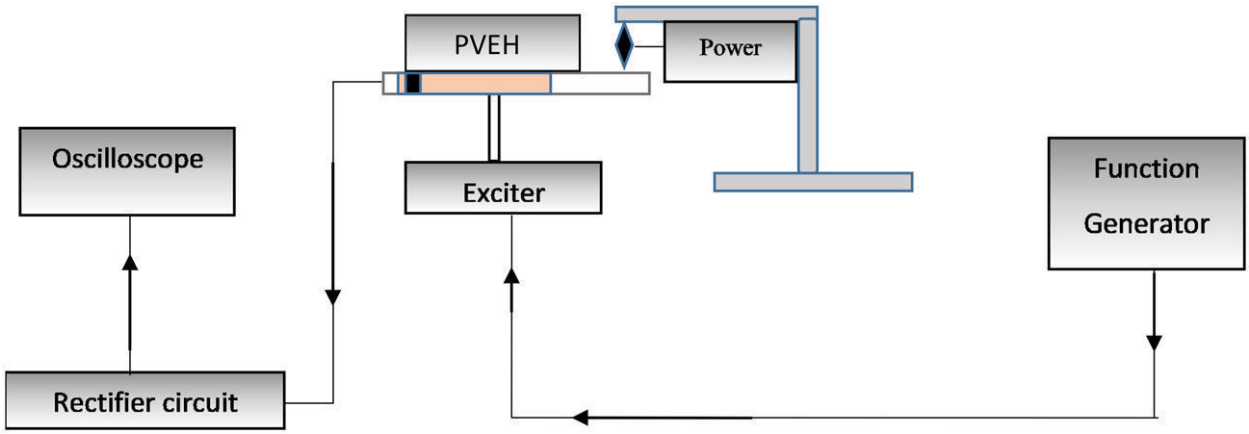

Fig. 3.9 Schematic Set-up for PVEH test

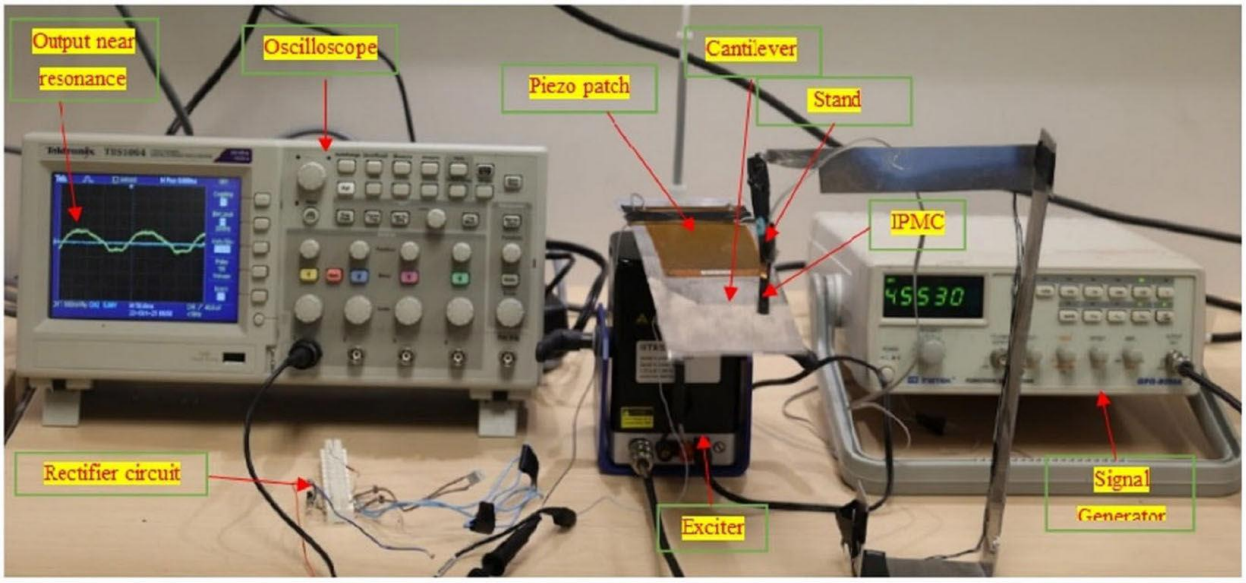

Fig. 3.10 Experimental Set-up

3.4 Theoretical analysis of the Tunable PVEH design

The theoretical analysis of the novel design is based on the Euler Bernoulli beam theory and the basic theoretical formulation of IPMC, the brief of which is given below. Euler-Bernoulli beam theory is based on the following assumptions: (1) The beam section is infinitely rigid in its plane. Hence, there will not be any deformation in the plane of the cross-section. (2)The cross-section of the beam remains plane to the deformed axis of the beam. (3) The cross-section of the beam remains normal to the deformed axis of the beam. The novel design meets the above requirements while the device generates power from the ambient energy.

The resonant frequency of a mechanical energy harvester is the function of the stiffness of the system K and the effective mass of the system m. Hence, controlling or modifying these two parameters can effectively lead to frequency tuning of a vibration energy harvester [99]. For an energy harvester, the mode of vibration of interest is the first Eigen frequency. In the case of the present novel design, the stiffness value can be changed by, the gap between the IPMC tip and the cantilever, the distance of the IPMC contact point from the free end of the cantilever, and by the input voltage to the IPMC. In the new design, the resonant frequency is tuned by impacting the cantilever with the IPMC actuator that functions as a stopper. The literature indicates that impact

effect is a function of the blocking force of IPMC which in turn is a function of the cation concentration, the electrode properties, the thickness of IPMC, and the input voltage [100, 101].
The maximum blocking force can be given as below in equation: (3.4)

$$F = b_0 + b_1 U + b_2 U^2 + b_3 U^3 + b_4 U^4 \quad (3.4)$$

Where b_i (i = 0, 1, 2, 3, 4) is a constant and U is the applied voltage [100]
The resonant frequency of the PVEH can be derived as given below [99].

$$f_r = \frac{\nu_n'^2}{2\pi}\frac{1}{L^2}\sqrt{\frac{K}{m_e+\Delta m}} \quad (3.5)$$

$\nu_n'^2\ represents\ \nu_n^2\sqrt{X}$.
v_n = 1.875 is the eigenvalue for the fundamental vibration mode, K represents the effect due to the cantilever, m_e= 0.236 mwL is the effective mass of the beam where m is the mass per unit length of the cantilever beam, X =0.236/3, L is the length of the beam, and Δm is the proof mass. In the present design, we have used an extended beam attached to the root section and IPMC as an actuator contacting the extension beam. Hence the effective K will be different.
The shift in the resonant frequency is

$$\delta f_r = f(s, d) \quad (3.6)$$

where *s* is the gap between the IPMC tip and the cantilever, and *d* is the distance of contact point on the extension beam from the tip of the extension beam.
The parameters that can be controlled for achieving the desired frequency shift are the response parameter of the stopper, the location of the impact of the stopper on the cantilever, and the gap between the stopper and the cantilever beam. Larger gaps will reduce the event of an impact (which means the beam may not get in contact with the stopper), leaving the harvester in the linear region.

3.5 Results and Discussion

The functionality of the proposed design of the device was evaluated for performance under different conditions. The experiments were carried out in three stages (Stages A, B & C).
Stage A: To study the Voltage vs Frequency response of the PVEH with root section and the extension beam

Voltage output vs frequency of vibration was plotted for the PVEH with extension beam as shown in Fig. 2 with a mass of 6.06 gm at the junction of the root section and the extension beam. The response is shown in Fig. 11.

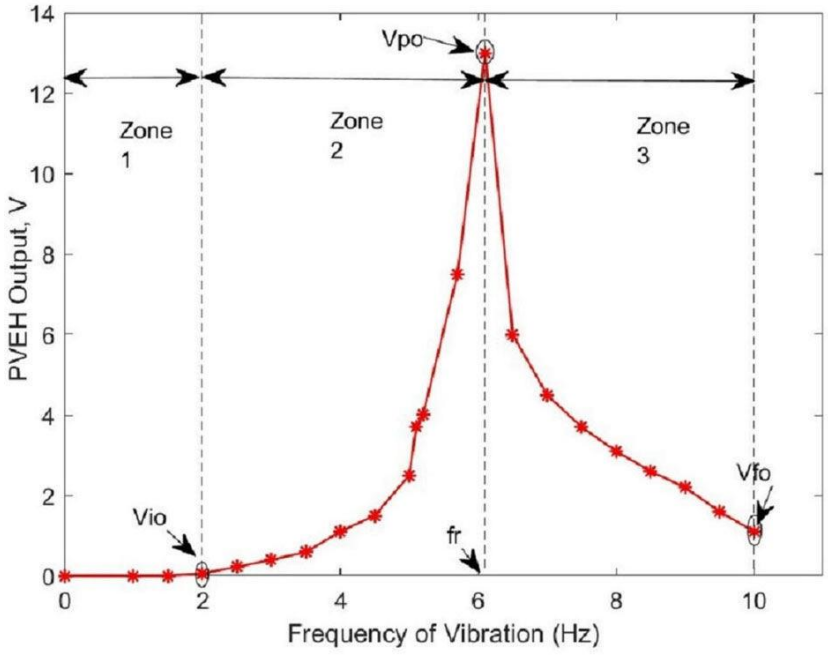

Fig. 3.11 Frequency of vibration vs PVEH output

Stage B: To evaluate the electrical tunability of the PVEH maintaining a net power gain.

Two experiments were conducted in Stage B. In the first experiment, the resonant frequency of only the root section (along with the mass of 6.06 gm) with IPMC actuation at different locations was studied.

In the second experiment, the effect of IPMC on the resonant frequency of PVEH, with root section along with the extension beam and the mass of 6.06 gm as in Fig. 2 was studied for different IPMC locations.

This was done to study: 1) the importance of the extension beam of the device; 2) the importance of the inclusion of IPMC as an impact element; 3) the feasibility of tuning the resonant frequency of PVEH electrically.

Stage C: To study the performance of the harvester with extension beam and IPMC as stopper under various acceleration conditions

Experiments were conducted by varying the acceleration values of vibration and the performance of tuning was studied.

Stage A: To study the Voltage vs Frequency response of the PVEH with the root section and the extension beam

Fig. 2 shows the PVEH that was used for the experiment. It has a composite material as substrate with MFC type M2814-P2 bonded on it (from Smart Material corporation [93]). The dimensions and material properties of the above are given in Table 2. An extension beam was attached to it and a mass of 6.06 gm was introduced at the junction of the root section and the extension beam. The exciter was driven by a sinusoidal signal from the signal generator and a power amplifier which in turn induced vibrations in the PVEH. The corresponding frequency was monitored. The output of the PVEH was connected to a full-wave rectifier to acquire a DC output signal. This output was monitored on the oscilloscope. The input frequency given to the exciter was continuously increased from 0 and the corresponding voltage from PVEH was monitored until resonant frequency for the PVEH was found. The experiment was carried out to study the PVEH by subjecting it to vibrations with frequencies ranging from 0 to 10 Hz. Fig. 11 shows the plot between the frequency of vibration and the output voltage. This is divided into three zones.

Zone 1:

In a cantilever mode, a piezoelectric energy harvester produces a substantial output only when it gets closer to the resonant frequency [71, 82]. The harvester output in the initial frequency zone much before the resonance will be very low. This is seen in the Fig. 3.11.

Zone 2:

From Fig. 11, it can be noted that from the point V_{io} (V-Voltage, i-initial, o-output), there is a sudden acclivity in the gradient of recorded PVEH output voltage until reaching V_{PO} (V-voltage, p-peak, o-output). It should be noted that the region of increasing voltage output varies from V_{io} at 4 Hz to V_{PO} at 6 Hz (resonant frequency).

Zone 3:

From Fig. 3.11, it can be seen that the output voltage of PVEH undergoes declivity with the further increase in input frequency

Stage B: To evaluate the electrical tunability of the PVEH maintaining a net power gain

the above phase of research was succeeded by the introduction of IPMC in the test set-up for the PVEH with only the root section, to evaluate the tunability of the PVEH. This was done by using IPMC as an impact element for the cantilever beam at six different locations, A, B, C, D, E, and

F. The distance from the free end of the cantilever to point A is 1cm, B is 2cm, C is 4cm, D is 5cm, E is 7cm and F is 8cm. At each location, the voltage input to IPMC was varied from 0-4 V DC in steps and the corresponding effect on the resonant frequency was recorded. Fig. 12 shows the plot between the input voltage given to IPMC (at A, B, C, D, E, and F) and the corresponding resonant frequency of the PVEH. From the figure, it can be seen that there is only a small variation in the recorded resonant frequency of the PVEH with the actuation of the IPMC at different voltages for this configuration.

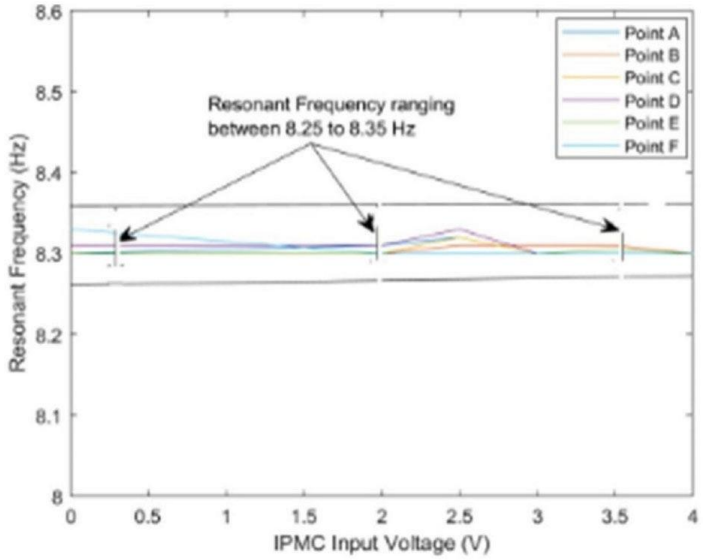

Fig. 3.12 IPMC input vs Resonant frequency for the PVEH without the Extension Beam [EB]

This is because the range of force generated by this commercially available IPMC cannot make a significant change in frequency as the effect of impact is less on a thicker root section of PVEH. The output from PVEH in terms of voltage and current was also recorded. Based on the recorded values of voltage and current, total power generated was calculated using the formula, $P_O = V * I$ *(*where *P*= Power generated, *V*= voltage from PVEH, *I*= Current obtained from PVEH*).* Further, the net power (P_N) was calculated by subtracting the power supplied to IPMC from P_O.

The second experiment was done on the proposed design of the PVEH device that includes an extension beam and a tip mass placed at the junction where the extension beam joins the root section. As discussed earlier, Fig. 3.2 represents the harvester that was used for this phase of

research. This PVEH device was impacted using IPMC (input voltage varying from 0 – 4 V DC) at six different locations along the extension beam only. Corresponding to the input voltage given to IPMC at a specific point, the resonant frequency was recorded. Fig. 3.13 shows the variation of the recorded resonant frequency of the PVEH for the increasing voltage input of the IPMC. The graph shows that the variation in the resonant frequency is the largest at point A and it decreases as we move from point A to point F. This is basically due to the moment effect as the maximum bending moment in the case of the cantilever is near the free end. As a result, the impact effect of IPMC at this point induces a greater change in the response of the cantilever beam. Hence, a change in the response of the cantilever causes a change in the resonant frequency of the beam. This also explains the reason for the reduction in recorded resonant frequency as we move away from point A to point F. Furthermore, at points A and B, an increase in the resonant frequency was also seen as the input voltage given to IPMC was increased from 0 to 4 V DC. This is due to the increase in the blocking force induced with the increase in input voltage to IPMC. The reaction of the IPMC closely emulates the reaction of a material with different stiffness. As a result, the integrated device behaves like a tunable system.

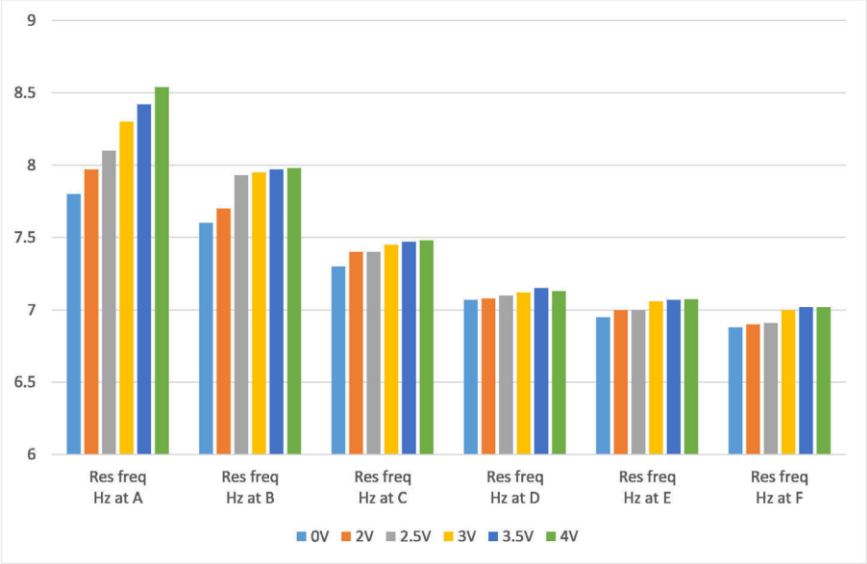

Fig. 3.13 Variation of Resonant Frequency w.r.t IPMC Input Voltage

Table 3.4 Calculated Net power gain from the novel PVEH device

			A		B		C		D		E		F	
IPMC Input (V)	Current, *I (μA)*	Input power (P_I= *I*V*)	P_O	P_N (Po-P_I)	P_O	P_N (Po-P_I)	P_O	P_N (Po-P_I)	P_O	P_N (Po-P_I)	P_O	P_N (Po-P_I)	P_O	P_N (Po-P_I)
0	0	0	123	123.21	121	121	121	121	123.21	123.21	121	121	121	121
2	20	40	110.25	70.25	102.21	62.01	106.99	66.09	108.16	68.16	106.09	66.09	102.01	62.01
2.5	20.5	51.25	108.16	56.91	110.25	59	106.09	54.84	106.09	54.84	104.04	52.79	104.04	52.79
3	21	63	116.64	53.64	108.16	45.16	108.16	45.16	106.09	43.09	104.04	41.04	102.01	39.01
3.5	21.25	74.375	114.49	40.12	108.16	33.79	106.09	31.72	110.25	35.88	102.01	27.64	102.01	27.64
4	22	88	116.64	28.64	110.25	22.25	106.09	18.07	108.16	20.16	104.04	16.04	104.04	16.04

Table 3.4 shows the net power gain from the novel PVEH at different input voltages. All values of power are given in μW. As explained in Fig. 3.16, the resonant frequency could be shifted with input voltage to the IPMC. As a result, the power output from the PVEH could be enhanced at a range of frequency values above the resonant frequency. Further, the net power obtained at A is the highest and it decreases as we move from A to F. Additionally, it can be observed that with the increase in input voltage to IPMC, there is a reduction in the net power output, which is expected. This is due to the comparatively higher power consumption of the IPMC.

Stage C: Performance of the device at different vibration acceleration conditions

In general, there is characteristic frequency and acceleration associated with vibrations present in any structure or machinery. A PVEH is expected to be able to generate power in varying frequencies and acceleration conditions. The performance of the proposed novel device with a variation of frequency around the resonant frequency has already been discussed in the previous section. In this section, the main focus of the study is to assess the behavior of the proposed novel PVEH in different conditions of acceleration of vibration.

In order to study this behavior, the proposed device as shown in Fig. 3.2 was subjected to varying accelerations of vibration. As the study is focused on low frequency and low acceleration levels of vibration, different values of acceleration within that range such as 1g, 1.25g, 1.5g, and 1.75g were used. Using the signal generator, a sinusoidal signal with an input amplitude of 4V was applied to the exciter through a power amplifier. Then the frequency of vibration was varied from zero continuously and the corresponding output was recorded. PVEH was subjected to different input amplitudes, and the resulting acceleration on the PVEH was measured using PASCO wireless accelerometer unit. The PASCO unit was mounted on the PVEH (as shown in Fig.3.14) to capture the acceleration experienced by the PVEH. The resonant frequency was identified by observing the frequency at which the PVEH output voltage reached a peak.

A correlation between the input amplitude and the recorded acceleration of PVEH was developed as given below: X: = 0.25 A, where X: = acceleration of PVEH, A, Amplitude of the signal given to exciter. Using this correlation, the acceleration values of 1g, 1.25g, 1.5g, 1.75g were selected and the corresponding voltage amplitude was given to the exciter. For each value of input acceleration, different input voltages (0V, 2V, 3V, 4 V DC) were supplied to IPMC. The

corresponding resonant frequency was recorded, and the output power was calculated as explained in the previous section.

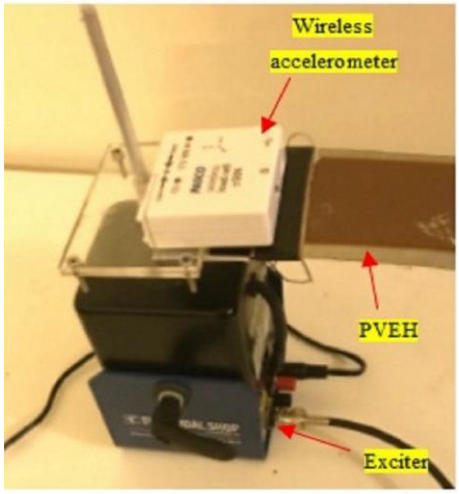

Fig. 3.14 PASCO acceleration measurement unit on the exciter

Fig. 3.15 represents the plot between the recorded resonant frequency for 1g, 1.25g, 1.5g, and 1.75g corresponding to the input to IPMC. From the figure, it can be seen that with the increase in the input to IPMC, there is an increase in the recorded resonant frequency for each input acceleration. This is because the resonant frequency of the PVEH varies when the EB gets impacted by the IPMC of different blocking forces as noted in stage A of the experiment.

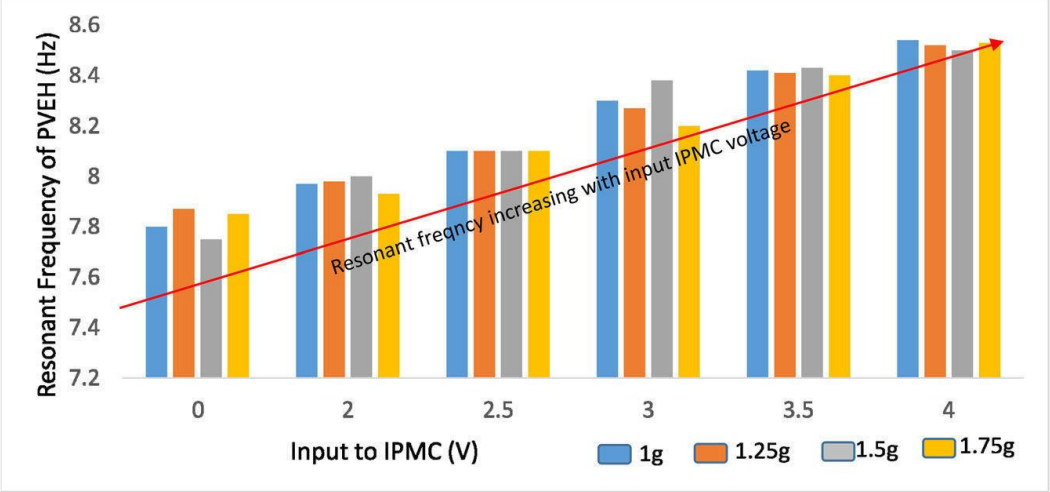

Fig. 3.15 Resonant frequency of PVEH corresponding to the input voltage to IPMC at different g values

Fig. 3.16 represents the plot of the calculated output power for each input acceleration corresponding to the input given to IPMC. From the figure, it can be seen that with the increased

input acceleration to the PVEH, there is a significant increase in the output power. This is because, with an increase in acceleration, MFC undergoes higher stresses resulting in higher output.

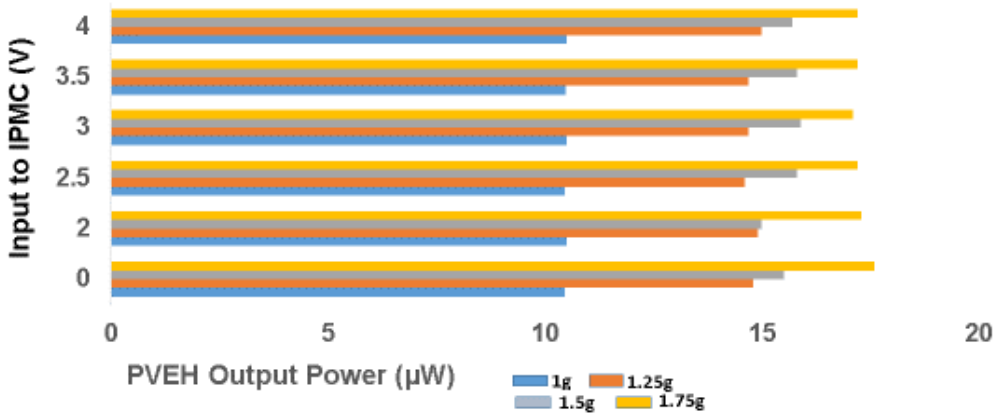

Fig. 3.16 PVEH output power corresponding to the input voltage to IPMC at different g values

Further, it should be noted that power output from PVEH exhibited negligible variation with the change in the input provided to IPMC. This is because, for different values of voltage supplied to the IPMC, this PVEH can achieve resonance at frequencies beyond its basic resonant frequency. The frequency range of tuning achieved in the study is based on the blocking force of the commercially available IPMC.

3.6 Concluding remarks

This experimental study clearly demonstrates a novel low-power solution using IPMC as a stopper to tune the resonant frequency of a cantilever type PVEH as given below:

1. IPMC can be used as a stopper/actuator on the PVEH, generating a shift in resonant frequency.
2. The impact effect of the stopper can be changed by applying different voltages to IPMC.
3. The proposed device scheme maintains the characteristics of a standard PVEH in generating higher power in higher acceleration conditions. The power output was found to be stable under the varying acceleration conditions.
4. The proposed novel device with IPMC tuning still generates a net positive power output.
5. Here commercially available IPMC was used. If the IPMC is fabricated with the specifications required for this application, a larger tuning range can be achieved. With the advancement in

the fabrication technology of IPMC, a higher blocking force can be achieved which will lead to a higher tuning range.

Chapter 4

Frequency broadening characteristics and Theoretical Analysis of the novel PVEH

Sreekumari Raghavan[1*], Rishi Gupta[1], Sardar Malek[1], Loveleen Sharma[1]

[1]*Department of Civil Engineering, University of Victoria, Victoria, British Columbia Canada*

This chapter presents material from a journal paper that is to be submitted. A novel device was described in Chapter 3. This paper gives details of experiments done to study the frequency-broadening characteristics of the device. The theoretical analysis of the results is also presented.

4.1 Introduction

The frequency response of PVEH in cantilever configuration can be shifted and broadened by introducing nonlinearity in the system, and researchers have found many novel ways to do this. These have been referred to and summarized in sections 1.1 onwards. However, in many of these cases manual intervention is required. In many other cases electrical methods for intervention are made use of. Nevertheless, such interventions require a separate power source to power the electrical circuit. Nowhere methods to introduce nonlinearity using a low-power device, which can be powered from the harvester is mentioned. The method followed here is to use a low-power smart material IPMC to actuate a PVEH in a sensitive cantilever configuration. The idea is novel and there are no published models or experimental results to show the feasibility. No such configuration using two smart materials is also available. After a detailed study, a device was designed and fabricated to introduce tuning. Experimental results have indicated that the idea is feasible with commercially available PVEH and IPMC. Since the commercially available IPMC suitable for our design was limited, it was not possible to generate experimental data with multiple specimens for designing a model to predict experimental results. The device also generated net power after utilizing a small portion to activate an IPMC actuator. The details are covered in our

earlier paper [146]. Here we cover experiments to study the broadband response of the device. Analysis of the results has drawn reference to papers, where stoppers with different materials were used. A full patent application for a novel device was filed in Nov.2020 [86]. In the device design, IPMC is used as a low-power actuator in a cantilever PVEH configuration.

4.1.1 Basic configuration of PVEH

Piezoelectric cantilever is an inertia device that can generate a substantial amount of electric power when it resonates at the ambient frequency (Fig. 4.1). A typical PVEH has a cantilever beam, where the piezoelectric material is bonded to its fixed end. A proof mass may be attached to the free end to get a lower resonant frequency. The value of this mass is optimized to generate a higher power at the desired frequency. The PVEH will be fixed at one end such that the direction of vibration is perpendicular to the axis of the beam, as shown in Fig. 4.1.

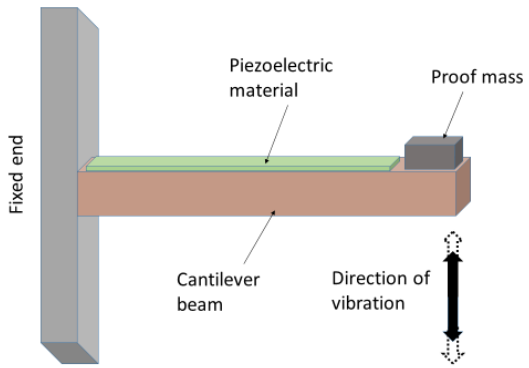

Fig. 4.1 A typical cantilever-type PVEH

Researchers have proposed various methods to design piezoelectric cantilevers.

Liao et al. [111] developed a method to formulate the maximum power equation that integrates the physical phenomena into a simple model. This equation can be used in the design and analysis of piezoelectric vibration energy harvesters. The design equation can be applied to different interface circuit types. It was reported that under the same level of excitation, there is an optimal thickness of the piezoelectric material, namely, PZT (Lead Zirconate Titanate) for generating maximum power.

Noel et al. [112] carried out a set of experiments, adapting optimized results from a previously developed coupled electromechanical model. The experiments covered various design conditions and performance was compared with the models. The authors have generated a large amount of

data, which is useful in testing of other theoretical models. When many models are formulated as independent approaches regarding the mechanical and electrical function of the PVEH, some have come out with an integrated approach. Yang et al. [113] worked on an equivalent circuit model of a piezoelectric energy harvester, considering the mechanical and electrical interactions, and applying Simulation Program with Integrated Circuit Emphasis (SPICE). This process integrates both structural modeling and electrical simulation, leading to a more comprehensive approach. Cheng et al. [114] proposed a system level coupled model for vibration energy harvester so that the system as a whole can be optimized to improve its efficiency. Their approach involves integrating the equivalent circuit model of the mechanical structure with the interface circuit and integrating the equivalent electrical impedance of the interface circuit with the finite element model of the structure. Similar studies on compression-based systems are also reported where an axial compression is present on the beam. Jiang et. al. [115] theoretically studied a compression-based piezoelectric energy harvester in a multilayer stack configuration. This is suitable for applications with large compressive loads. Analytical and numerical modeling of the design under axial compressive loading was carried out based on the linear theory of piezoelectricity. The harvested electrical power under an external electrical load was calculated, considering mechanical and electrical aspects. Studies on a test prototype were carried out and the results were reported to be in agreement with the calculations.

4.1.2 Configurations for altering structural stiffness of PVEH

A significant amount of research has been carried out to explore the possibilities of improving the performance of PVEH by altering its structural stiffness by various means.

Berdy et. al. [116] designed a laser-machined meandering PZT bimorph and carried out finite element analysis to optimize various parameters such as dimensions of the beam and tip mass. Their design demonstrated that a low resonant frequency can be achieved by maintaining a form factor required for sensor nodes. Using this method, energy can be harvested from vibration sources that produce frequencies less than 100 Hz. Stiffness can also be changed by changing the angle between the different beams in the integrated PVEH design. Zhao et al. [117] made use of this approach and proposed a novel V-shaped vibration energy harvester in the conventional piezoelectric bimorph cantilevered design to achieve a broad frequency range of operation. The performance of V-shaped harvester was studied under different design parameters including changing the angle between two piezoelectric bimorph beams. Another approach was to apply an

axial preload to the cantilever beam by Hu et al. [70], and it was demonstrated that the harvester can be driven into resonance by adjusting the axial load. As a result, the output power density can be increased.

A key parameter that determines the structural stiffness of the cantilever beam is the position at which the beam is supported. Yun Wang et al. [118] proposed a method to tune the resonant frequency of harvesters by adjusting the supporting position of the vibrator. Liu et al. [119] employed beams with different stiffness values to cover a range of stiffness and to increase the power output; they designed an array of harvesters, matching various frequencies in Micro Electro Mechanical Systems (MEMS) configuration. The prototype was fabricated and experiments were carried out to study the natural frequency, output voltage, and rectification properties. A novel design was proposed by Berdy et al. [120], where a meandering structure was realized by cutting bimorph material using a pulsed laser. Due to a series of curves, positive and negative strains were present in a piezoelectric layer. To avoid the resulting voltage cancellation, the electrodes were cut and connections were made accordingly. This new design could reduce the resonant frequency by 70% compared to a straight cantilever design of similar size, due to the distributed inertial mass in the configuration.

In order to increase the bandwidth, Koven et al. [121] designed a base- mounted piezoelectric (BMP) harvester with a piezoelectric transducer mounted below the base of a cantilevered beam resonator. A prototype was made by using a polyurethane cantilever beam of dimensions 1.6 mm × 4.9 mm × 20.0 mm as the cantilever beam and a PZT-5H piezoelectric material as the transducer. A tip mass of 8.36 gm was also employed. The harvester functioned as a damped mass-spring system. Various designs for mechanically tuning the harvester's resonant frequency were studied and analyzed by Eichhorn et al. [122] by applying a compressive pre-load. This study has brought out the relationship between the applied compressive preload and the corresponding resonant frequency. A piezo-polymer cantilever beam with two additional thin arms was used to apply an axial compressive preload to the tip of the beam. Using this method, the resonant frequency could be shifted from 380 Hz to 292 Hz and from 440 Hz to 460 Hz. The stiffness of a beam can be modified by applying a stretching force. Based on this concept, Hajati et al. [123] achieved a wider bandwidth by making use of the stretching stiffness of a doubly clamped beam. The power estimated from the measured open circuit voltage of the device was 45 μW.

A method of shifting gravity center by a moving mass for tuning the resonant frequency of the harvester was examined by Xiaoming Wu et al. [124]. An FEM model was developed for the design of the system. Experiments were carried out on a prototype and the results indicated a possible adjustment from 130 Hz to 180 Hz. A theoretical model was used to explain the effects of preload on the harvester to shift the natural frequency.

Studies by Leland et al. [69] have proven that axially compressing a piezoelectric bimorph lowers its resonant frequency. An axial preload can shift the resonant frequency of a simply supported bimorph to 24% below its unloaded resonant frequency. Four parylene-C beam structures with an inertia silicon proof-mass were designed along with a PVDF piezoelectric layer by Huang et al. [125]. The beams were doubly clamped to introduce the stretching strain instead of bending, to achieve a higher bandwidth. For an acceleration of 0.5 g, a maximum open-circuit voltage of 368 mV was achieved. The maximum output power was 0.288 μW.

In addition to the above methods, stiffness change of the harvester can be achieved by applying a magnetic field or chaotification [126-130]. The effect of a magnetic field acting on the tip mass of the harvester is to change the deflection pattern, resulting a in non-linear response.

4.1.3 Configurations for introducing nonlinearity in the PVEH

In order to improve the performance of the harvester, many researchers have come up with designs utilizing the introduction of nonlinearity in the system.

Liu. et al. [131] designed an energy harvester, consisting of an outer main beam and an auxiliary inner beam to realize two close resonant frequencies. A stopper was added to the end of each beam to generate nonlinearity resulting from impact. This resulted in increased bandwidth of the harvester. A flexible element can introduce a degree of nonlinearity to a structure. Consequently, Li et al. [132] put forward a vibration energy harvester in which a flexible beam-based interdigital structure was utilized. The design consisted of a series of cantilever beams fixed to a rectangular flexible frame. It was reported that the frequency response of the designed device exhibits a significant increase in bandwidth below 80Hz. Non-smooth response can be achieved based on the contact mechanics of a cantilever beam impacting a stopper. Rodrigo et al. [133] worked on a broadband energy harvester design based upon this non-smooth nonlinearities, by introducing mechanical end stop. This integrated design enhances the bandwidth. However, a reduction in energy was reported and studies are on, to investigate various end-stop stiffness values.

Other approaches have multi-beam structures with different piezoelectric materials or with springs that interconnect the beams. Therefore, Meruane et al. [134] presented a design involving an array of piezoelectric cantilevered beams connected by springs to achieve a broad-band energy harvester. The results were compared with those of an array of beams with no springs. The results indicated that connecting the beams with springs can increase the bandwidth as well as the power output.

Another design by Halim et al. [135] incorporated a mass-loaded polymer beam (primary spring-mass system) that works as a dynamic magnifier for another mass-loaded piezoelectric beam (secondary spring-mass system) clamped on primary mass. The piezoelectric beam was clamped with 2 degrees of freedom. The polymer beam responds well to low frequencies. When excited, the dynamic magnifier gives a mechanical impact on the base stopper, resulting in an impulsive force on the energy harvester. Beams connected with a spring can provide an additional moment.

Aryanpur et al. [136] studied two bimorph designs with a hinge, consisting of two pieces of machined aluminum (Al). A dowel and a torsion spring were used to make the connections. The spring gives a wider frequency range due to its additional moment.

A polyethylene terephthalate (PET) based flexible vibrational energy harvesting system using ZnO as piezoelectric material, was designed and studied by Pan et. al. [137] for enhanced frequency bandwidth. This broad bandwidth harvesting system has been modeled to arrive at the optimum thickness of the PET substrate. However, the conversion efficiency of ZnO is less than that of PZT. Similarly, Hasan et al. [138] designed a harvester with elastomer pillars, standing on a piezoelectric polymer layer. The elastomer pillars function as oscillators and as an energy sink. They demonstrated that a system with 10 mm diameter and aspect ratio of 3 with an active area of 39 mm^2 and thickness of 28 μm generated a voltage of 4.5 V. An output power of 58.4 μW was achieved for an input acceleration of 3 g at 62 Hz with optimized load resistance.

Another approach is to design a spiral-shaped cantilever, as it will lower the frequency due to its increased length as shown by Liu et al. [139]. The device consists of a spiral shaped PVDF (polyvinylidene fluoride) cantilever with copper (Cu) and silicon (Si) proof masses. Due to the flexibility, it can harvest energy from even weak vibration energy sources. The device operates from 15 to 50 Hz and can give an output of 1.8 V with an acceleration of 0.2 g. Rezaeisaray et al. [140] made use of the lower resonant frequency of a polymer structure due to its lower stiffness.

The authors fabricated aluminum nitride (AlN) pads on an SU8 membrane and introduced a proof mass of silicon. Microfabrication process was also proposed. However, as reported, the Aluminum nitride may have to be replaced with PZT to increase the output power.

H-HanHuang et al. [141] proposed a method for introducing non-linearity by designing a harvester expending polymer piezoelectric materials. A beating mechanism was also introduced that creates an impact force through the low-frequency vibratory motion. This excited the system's natural frequency. The details of the design of the mechanism and the results were discussed. Friswell et al. [142] worked on a new design consisting of a cantilever beam with a tip mass mounted vertically and excited in the transverse direction at its base. The design introduced two wells for large tip masses when the beam gets buckled, and hence introduced a high nonlinearity. However, it was restricted by a few frequencies, which can be covered by the design of the wells and locations.

Mechanical coupling between two beams can be used to increase the output power in a harvester. Li et al. [143] designed a bi-resonant structure consisting of two cantilevers with different resonant frequencies to generate mechanical coupling between the two systems. At high vibration amplitudes, due to a resulting collision, a strong mechanical coupling happens and an output power of 0.35 W could be realized. Considering the nature of low-power output of piezo-based systems, this was a good development. As it is known, improving both power output and the frequency bandwidth simultaneously is a challenging task. The authors used piezoelectric PVDF (Polyvinylidene fluoride) film energy harvester (PPEH) to achieve this. A bi-resonant structure is capable of generating higher power output compared to that of the sum of the two separate units from low-frequency vibration. Frequency-up conversion is another method for low-frequency vibration energy harvesting. Using this concept, Dauksevicius et al. [144] demonstrated a nonlinear frequency up-converting vibration energy harvester, which works on vibro-impact interaction between two high-frequency piezoelectric generators and two low-frequency resonators. The finite element model also was developed and analyzed. This design increased the frequency bandwidth due to the nonlinearity of the harvester.

The above literature has focused on describing various designs of PVEH and electro-mechanical models for the different configurations of PVEH. Many models have been put forward for various types of design approaches and improving the performance of PVEH. However, there is no literature on designing a composite device structure, utilizing two distinct materials, such as

piezoelectric material and IPMC, or modeling such configuration. As will be demonstrated in this paper, this configuration can be advantageous in realizing low-power actuation for tuning the resonant frequency of a harvester. Some researchers have assumed that a stopper action is similar to that of a trilinear spring, where the force produced by the spring is proportional to the cube of its displacement for soft materials like rubber, and indicated experimentally this holds good for a portion of the response before it drops steeply. This has been referred in the analysis of this contribution. However, there is no literature on designing a composite device structure, utilizing two distinct materials, such as piezoelectric material and IPMC, or modeling such configuration. We considered this as a novel idea since IPMC is a low-power device that can be powered from the generated power without the need for an external power source. The use of a second smart material IPMC that consumes little power to change the frequency response of PVEH and the fact it can do so without an external power source makes it novel. Much research is underway to enhance the IPMC blocking force. The device described can also be miniaturized in MEMS form. As will be demonstrated in this paper, this configuration can be advantageous in realizing low-power actuation for tuning and broadening the resonant frequency of a harvester.

4.2 Methodology

The device used and some of the experiments done are described in our earlier paper [146]. We now discuss additional experiments that were carried out.

To study the frequency response of the device using low-power IPMC actuator, the following experiments were done:

a) Frequency response of the device without IPMC actuation is compared with the response when IPMC is present and not powered. Para 3.1.1 Fig. 4.5.
b) Frequency response of the device without IPMC actuation is compared with the response when IPMC is present and powered at 2.5V. Para 3.1.1 Fig. 4.6.
c) Frequency response of the device without IPMC actuation is compared with the response when IPMC is present and powered at 3.5V. Para 3.1.1 Fig. 4.7.
d) Experiment to study the force needed to compress the IPMC actuator for different displacements. Fig. 4.12 and Fig. 4.14.
e) Force exerted by the IPMC actuator when it is powered at different voltages. Fig. 4.14).

The experiments were also repeated to verify results were stable. Care was taken to see the IPMC actuator was stable during operation ensuring repeatability. During experiments, the IPMC was

powered separately from a stable source to ensure measurement accuracy. The device is shown in para 4.2.1, Fig. 4.2.

The experimental results indicate that it is possible to shift the resonant frequency and broaden the frequency response by powering the IPMC as required, from the device itself, as it consumes very low power. Analysis of experimental results indicates conformance to the basic theory of PVEH in a cantilever configuration and IPMC actuation. While analyzing our results, published papers by other authors where different stopper materials and configurations are used, are referred to. The basic physics of impact to achieve nonlinearity remains the same even though the mechanisms for impact widely vary as well as models used for verification. The differences noticed are also highlighted where applicable and reasons attributable to specific response of IPMC are mentioned. IPMC displacement for varying blocking forces and blocking forces generated by IPMC for varying input voltages have been measured and their response curves plotted to aid analyses.

4.2.1 Device

A typical design of the novel tunable PVEH [83, 86] has two sections in the cantilever beam as shown in Fig. 4.2. The main root section (RS) is fixed at one end and bonded with a Macro Fibre Composite (MFC) patch. An extension beam (EB) of a thinner cross-section is bonded to the main beam with an overlap section (Fig. 4.2). The external impact load on the beam is achieved by actuating the IPMC with a low voltage input. The IPMC is integrated above the EB with a variable gap (*s)* from the EB and functions as a stopper with variable blocking force.

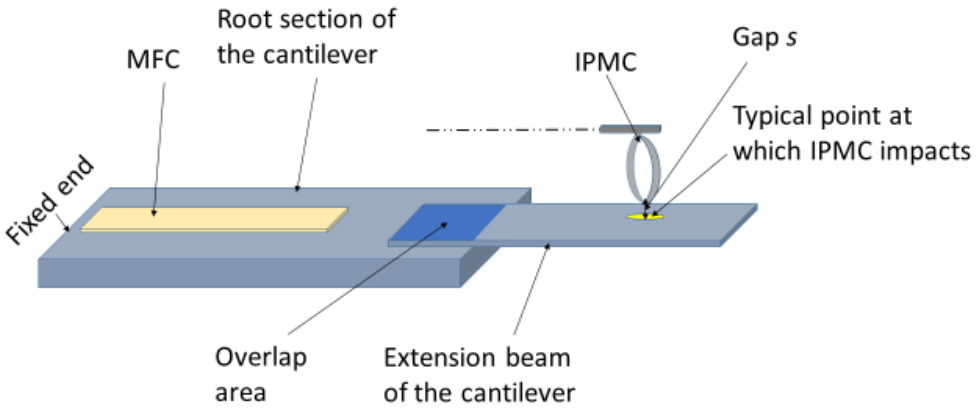

Fig. 4.2 Tunable PVEH with root section and extension beam of cantilever

The thinner beam provides a sensitive loading point, at which a very small force can generate a significant shift in the resonant frequency. The device can incorporate the suitable design of IPMC, from the point of requirement of the range of frequency band width. Since the power required for the IPMC is very low, it can be tapped from the harvester itself. Two IPMC strips are joined at the ends and powered at a common point.

The IPMC loading is applied by varying the input voltage to IPMC in the range of 1V to 4V. The resonant frequency shifts to higher values with each step. For the experiments, P2 type MFC (PZT (Lead Zirconate Titanate) designed for energy harvesting) from Smart Material Corporation, USA [93] and IPMC strips of dimension 30mm x 5mm x 0.2mm from Environmental Robots, USA [145] were used.

4.2.2 Characteristics of IPMC as a Tunable Stopper

4.2.2.1 Structure of IPMC

IPMC material consists of a per-fluorinated ion exchange membrane sandwiched between two electrodes. Nafion membranes are widely used in IPMC. The chemical structure of Nafion is shown in Fig. 4.3(a).

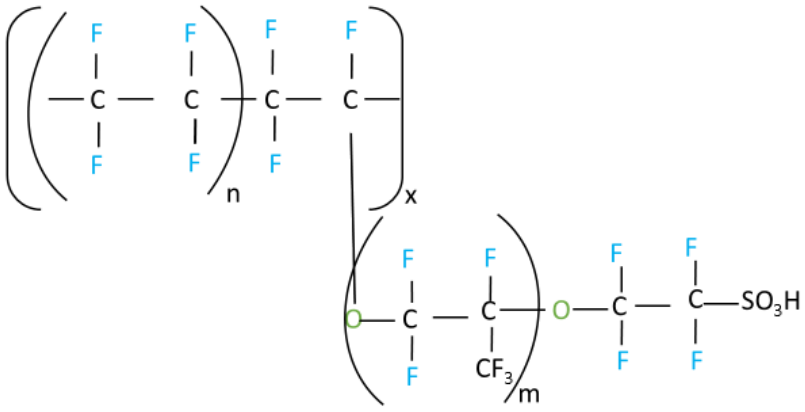

Fig. 4.3 (a) Chemical structure of Nafion

The anions are fixed in the polymer. Cations will become mobile when hydrated and will move towards negative polarity when subjected to an electric field.

The water molecules tagged with the cations will be dragged along with the cations. This leads to an osmotic pressure change and the IPMC bends by an expansion of polymer near the cathode and a shrinkage near the anode [34]. This shifting of cations and water molecules is across the thickness of the film. This is the basic phenomenon associated with the IPMC actuation and is depicted in Fig. 4.3 (b).

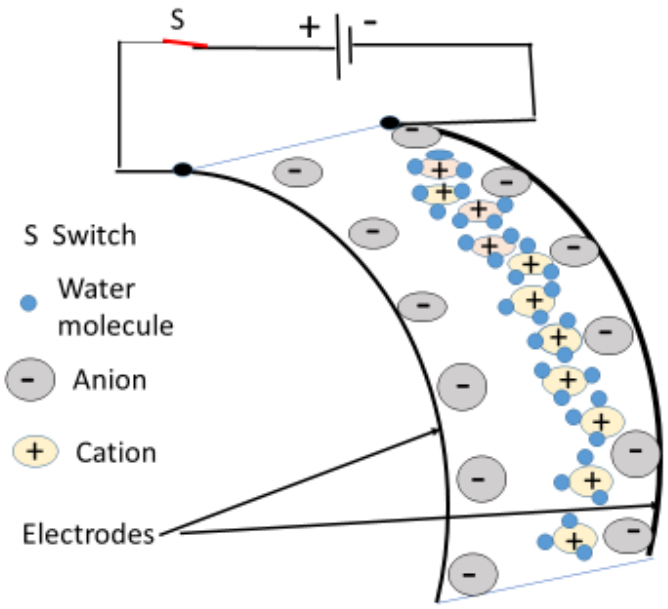

Fig. 4.3 (b) Internal configuration of IPMC after actuation

4.2.2.2 Modeling approach for IPMC

There are different approaches reported in the literature for modeling IPMC based on its basic physical features [110, 34, 98, 147, and 148]. There is a blocking force associated with any actuation, which is of interest in this analysis [110]. The IPMC is considered to be divided into many small segments, where cation is taken as the unit element. The distribution of these units is uniform. The unit force of IPMC is the unit force of a single cation. Maximum deformation is proportional to the unit deformation and blocking force is a function of the applied voltage as depicted in Eqn. (4.1) and (4.2):

$$S = a_0 + a_1 U + a_2 U^2 + a_3 U^3 + a_4 U^4 \quad (4.1)$$

where a_i (i= 0, 1, 2, 3, 4) is a constant and U is the applied voltage to IPMC and S is the deformation.

$$F = b_0 + b_1 U + b_2 U^2 + b_3 U^3 + b_4 U^4 \quad (4.2)$$

where b_i (i = 0, 1, 2, 3, 4) is a constant and U is the applied voltage to IPMC and F is the blocking force. In view of this, when the input voltage to IPMC increases, its deformation increases resulting in an increased blocking force of the actuator. This in turn results in a change in the effective stiffness of the cantilever beam leading to a change in its resonant frequency.

If D, E, ϕ, and ρ denote the electric displacement, the electric field, the electric potential, and the charge density, respectively, the following equations hold:

$$\mathrm{E} = \frac{\mathrm{D}}{\kappa_e} = -\nabla\phi \tag{4.3}$$

$$\nabla \cdot \mathrm{D} = \rho = F(C^+ - C^-) \tag{4.4}$$

where κ_e is the effective dielectric constant of the polymer, F is Faraday's constant, and C^+ and C^- are the cation and anion concentrations, respectively [98].

The ion flux consists of diffusion, migration, and convection terms [98]. Hence solvent transport is a contributing factor to the actuation and the water content of the IPMC is a factor to be considered

4.2.2.3 PVEH cantilever beam

The PVEH cantilever beam, is modeled as an Euler-Bernoulli beam since the width is much less than the length.

The resonant frequency of a simply supported Euler-Bernoulli cantilever beam is described by the following equation:

$$f_r = \frac{\nu_n^2}{2\pi}\frac{1}{L^2}\sqrt{\frac{EI}{mw}} \tag{4.5}$$

E is Young's modulus, ν_n = 1.875 is the eigenvalue for the fundamental vibration mode, I is the moment of inertia, L is the length, w is the width of the cantilever, and m is the mass per unit length of the cantilever beam [99]. A proof mass attached to the free end of the cantilever beam can further decrease the resonant frequency and the corresponding equation can be written as in Eqn. (4.6).

$$f_r = \frac{\nu_n'^2}{2\pi}\frac{1}{L^2}\sqrt{\frac{K}{m_e+\Delta m}} \tag{4.6}$$

where, $\nu_n'^2$ is $\nu_n^2\sqrt{X}$, X =0.236/3. m_e = 0.236 mwL, the effective mass of the cantilever and Δm is the proof mass.

In our case, the effective K of the system (K *(effective)*) will change as we have used an extended beam impacted by IPMC as a tunable stopper.

From the above equations, it is obvious that the resonant frequency of a mechanical energy harvester is the function of the stiffness of the system K and the effective mass of the system m_e.

Hence, controlling or modifying these two parameters can effectively lead to frequency tuning of a vibration energy harvester [66, 149]. For an energy harvester, the mode of vibration of interest is the first eigen frequency. The above relation can also be written in general as below:

$$f_r = f\,(E, I, M_c, M_p) \tag{4.7}$$

where E is the Young's modulus, I is the moment of Inertia, M_C is the mass of the cantilever and M_p is the proof mass [59].

4.2.2.4 Effect of IPMC impact on cantilever beam

When a fixed free cantilever beam is impacted with a contact material of stiffness k, the resonant frequency of the beam shifts to a higher value [152]. In the device, the extended portion also adds nonlinearity to the system. In the case of IPMC, the blocking force defines the response while in contact. The blocking force B_f of IPMC is a function of the cation concentration C_n, the electrode properties E_p, the thickness of IPMC t, and the input voltage V.

$$B_f = \left(C_n, E_{p,} t, V\right) \tag{4.8}$$

IPMC is both resistive and capacitive. Its electrodes can be considered as an RC circuit and the IPMC material as a capacitor [34, 150]. The capacitance value of IPMC is a function of the density and penetration depth of the particles in the polymer. The blocking force is a function of capacitance and thickness. It increases with capacitance. It is also a function of the R and C values of the electrodes. The blocking force also increases with the input voltage to the IPMC. From Eqn. (4.7) and Eqn. (4.2), it is obvious that for a given IPMC, the $C_{n,}$ $E_{p,}$ and t are fixed. Hence the blocking force can be changed by changing the input voltage.

The electric field E is given by

$$E = \frac{V}{t} \tag{4.9}$$

where, V is the voltage applied and t is the thickness of the IPMC membrane. The cation concentration in the polymer matrix defines the actuation characteristics since it leads to different ionic currents. The response of IPMC, defined by different block forces is equivalent to the response of different stiffness of materials. Hence Eqn. (4.6) can be rewritten as below.

$$f_r = \frac{\nu_n'^2}{2\pi}\frac{1}{L^2}\sqrt{\frac{K\,(effective)}{m_e+\Delta m}} \tag{4.10}$$

K (effective) is the effective stiffness of the PVEH, which depends on B_f (the blocking force of the IPMC) as given in Eqn. (7) and (2).

4.2.2.5 Effect of gap and distance of contact point (IPMC contact) from the fixed end of cantilever

The shifted resonant frequency f_{rs} is also a function of the gap between the cantilever and the contact tip as well as the distance of the contact point on the extension beam from the free end of the extension beam [152, 154].

$$f_{rs} = f(s, d) \tag{11}$$

where f_{rs} is the shifted resonant frequency, *s* is the gap between the IPMC tip and the cantilever, and d is the distance of contact point on the extension beam from the tip of the extension beam. f_{rs} increases with a decrease in *s* and with a decrease in *d*. These characteristics have been confirmed by experiments as well as modeling by the authors in the above-referred paper [154]. This reference also indicates the broadening of the frequency response and its confirmation through modeling and experiments. In the model, the impact force exerted by the stopper material is taken as proportional to the cube of the displacement it undergoes, when it gets in contact with the beam. Literature [154] indicates that in a PVEH cantilever configuration where different stopper materials like aluminum, steel, etc. were used, the frequency response broadened and the resonant frequency increased with a decrease in *s* and with a decrease in *d*. The same paper also indicates that when the impact force is modeled as akin to the force exerted by a trilinear spring, where the force exerted by the spring is proportional to the cube of its displacement, there was a partial agreement for a stopper of soft material like rubber.

It can be inferred from Eqn. (4.10) and (4.11), that the stiffness of the PVEH system can be tuned by varying the blocking force of the IPMC actuator that is integrated with the device.

4.2.2.6 Resonant frequency change and broadening response due to stopper (IPMC)

When a mechanical stopper is introduced that restricts the movement of the beam, quasi-periodic oscillations of the beam will be converted to periodic vibrations, every time the base frequency happens to be away from resonance. This leads to a sudden increase in effective stiffness [151]. This resultant multiple stiffness values generate an extension of the resonant frequency to a wider and higher range of frequencies [99]. When there is no contact with the stopper, the cantilever vibrates in the first mode shape, where all stresses appear at the fixed point. When the cantilever gets in contact with the IPMC, its dynamic behavior changes as its movement is

restricted and becomes highly nonlinear. This results in a slight power reduction due to less stresses at the fixed point due to restricted movement. The generated high-frequency movements due to the contact with the stopper are different from the steady-state dynamics response of the PVEH when there is no stopper. In the steady state response, the PVEH oscillates between maxima and minima displacement around a central mean. The cantilever with the stopper will oscillate at a higher resonant frequency, which is a function of the reaction level of the stopper. The parameters that can be controlled for achieving the desired frequency shift are the response parameter of a stopper, the impact location of the stopper on the cantilever, and the gap between the stopper and the cantilever beam (see Fig. 4.2). Larger gaps will reduce the possibility of the event of an impact (means, impact may not happen) leaving the harvester in the linear region.

The effective stiffness *K (effective)* is also a function of the cation concentration in the IPMC. The cation concentration in the IPMC can be controlled during its fabrication. This will enable control over shifts in resonant frequency.

4.3 Results and analysis

4.3.1 Results based on experiments

4.3.1.1 Frequency response of the device without and with IPMC contact and Comparison with IPMC powered at different voltages

Schematic diagram of the experimental setup [146] is given in Fig. 4.4

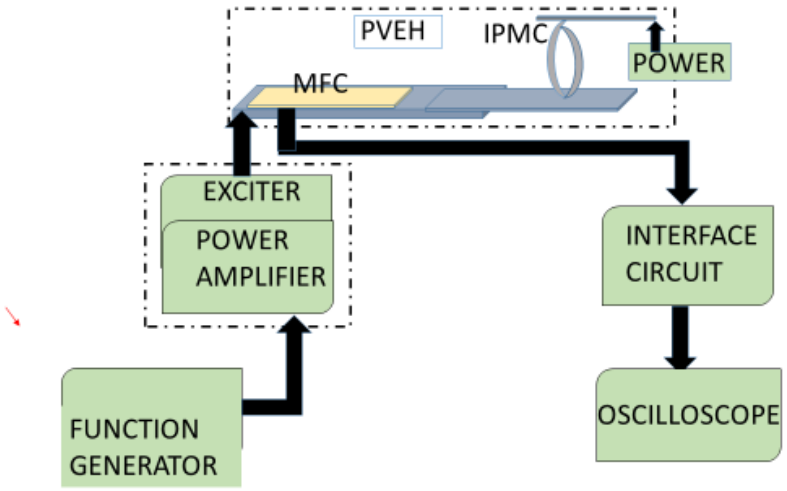

Fig. 4.4 Schematic diagram of the experimental setup for PVEH tests

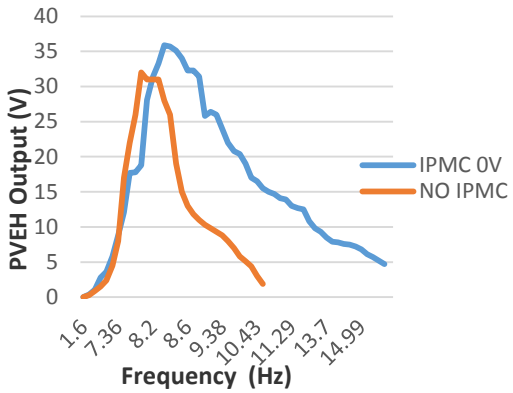

Fig. 4.5 Frequency response with IPMC at 0V

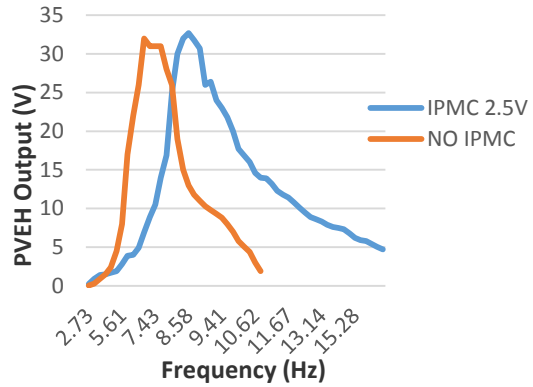

Fig. 4.6 Frequency response with IPMC at 2.5V

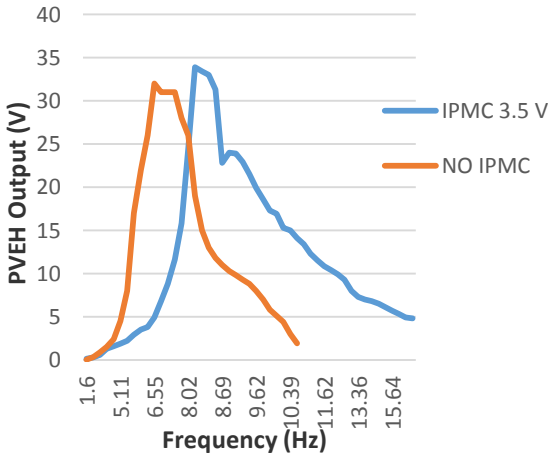

Fig. 4.7 Frequency response with IPMC at 3.5V

Fig. 4.5 compares the response of the device when there is no IPMC actuation with the response when IPMC actuator is not powered. Fig. 4.6 and Fig. 4.7 give a similar comparison when the IPMC actuator is powered at 2.5V and 3.5V respectively. Three separate graphs are drawn to give clarity as the x-axis data points are different for the three curves.

The graphs indicate the following:

Without IPMC actuation the response is steep prior to resonance indicating the device generates output only at resonance. The response after resonance is not that steep as there is some non-linearity in the cantilever arrangement due to the extended thin cantilever.

With IPMC actuation, the response continues to be steep prior to resonance but broadens substantially after resonance. Further, the response falls gradually till the end. This response is different from that observed when materials like steel, aluminum etc. were used to introduce nonlinearity [152], where response broadens after resonance but falls steeply thereafter.

Further observations from the graphs are given below:

If we analyze the device frequency response at different IPMC actuator input voltages, it can be noted that the curves are more or less similar when IPMC actuator input voltage is changed, but for a small lateral shift of the response curve due to a shift in resonant frequency (Fig. 4.8, Fig. 4.9, and Fig. 4.10).

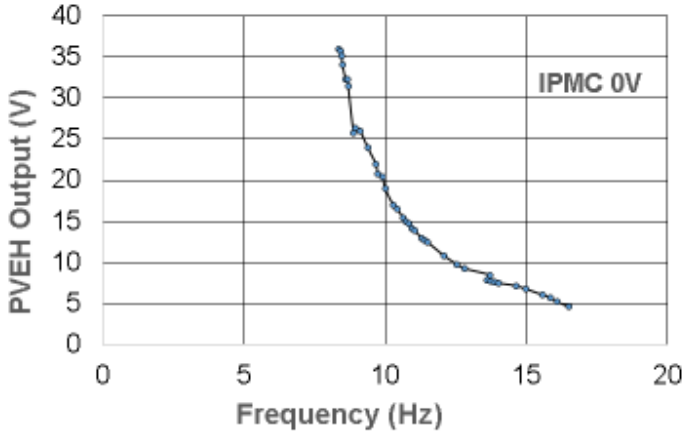

Fig. 4.8 Section of Frequency response curve for IPMC input 0 V

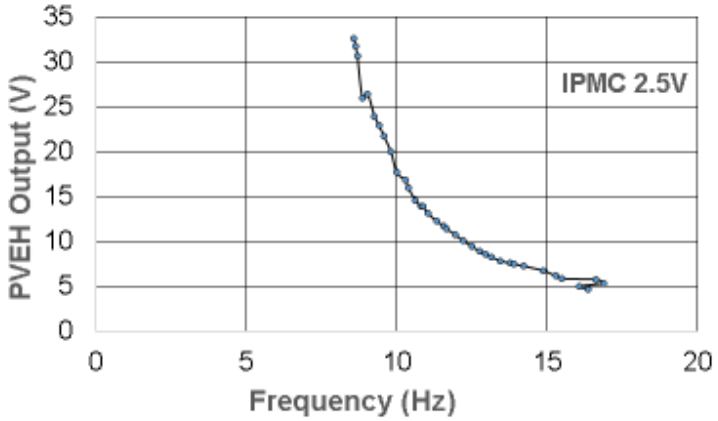

Fig. 4.9 Section of Frequency response curve for IPMC input 2.5 V

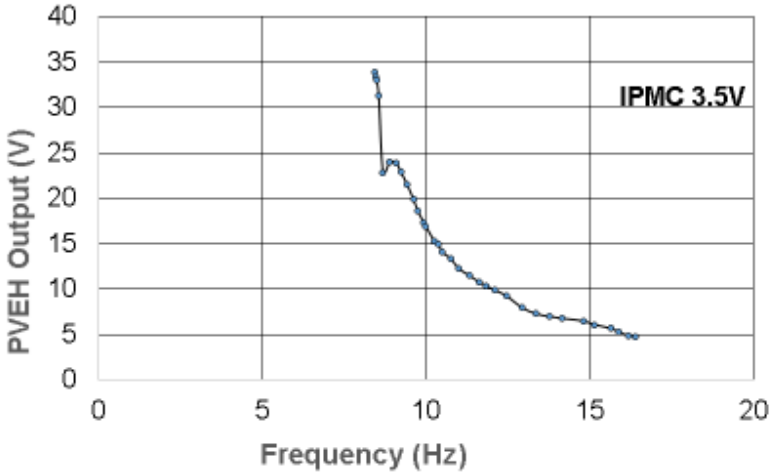

Fig. 4.10 Section of Frequency response curve for IPMC input 3.5 V

We can analyze the broadening effect from the horizontal lines in the response curves in Fig. 4.5, Fig. 4.6, and Fig. 4.7, when PVEH output is at 5V, 10V, 15V, and 20V. If we look at Fig. 4.5 response curve, when IPMC input is at 0V, we see that the harvester maintains an output of more than 20V, when the harvester vibrates in the range of around 8Hz to 9.9Hz (1.9Hz spread). The harvester maintains an output greater than 15V when the harvester vibrates in the range of 7.92 Hz to 10.75Hz (2.83Hz spread). When output is greater than 10V, the range obtained is 12.55Hz to 7.67Hz (4.88Hz spread). These spread values have been computed for the response curves obtained for different IPMC input voltages and is summarised in Table 4.1.

Table 4.1. Frequency spread for different PVEH output voltage

PVEH Output	5V	10V	15V	20V
IPMC 0V	9.3 Hz	4.88 Hz	2.83 Hz	1.9Hz
IPMC 2.5V	9.5 Hz	4.83 Hz	2.94 Hz	1.68 Hz
IPMC 3.5V	10	5	2.5	1

To study the behavior of IPMC that results in a gradual broadening without steep fall, additional experiments were done as detailed below:

4.3.1.2 Force exerted by IPMC actuator at different displacements

The setup to study the force needed to compress the IPMC actuator for different displacements is shown in Fig. 4.11.

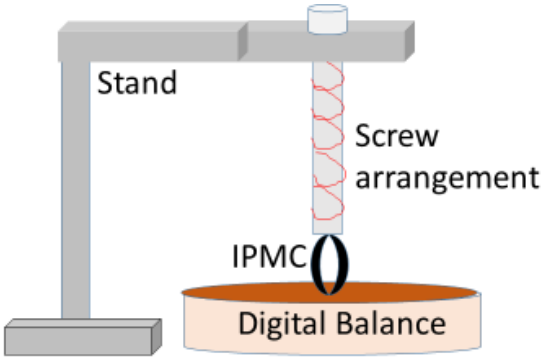

Fig. 4.11 Setup to study force exerted by IPMC actuator when compressed

To study the impact force exerted by IPMC for various displacements, experiments were conducted by placing the IPMC in contact with a sensitive weighing balance and then increasing the displacement in fine steps with IPMC fitted to a threaded screw nut arrangement. The results are given in Fig. 4.12. Care was taken to see the IPMC actuator did not slip on the weighing balance during the test. In the graph, the force exerted is in mg-force (1 mg-force equals 9.80665micro newton) and the displacement is in mm.

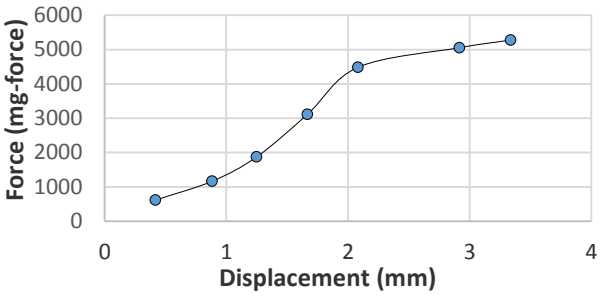

Fig. 4.12 Force exerted by IPMC actuator when compressed

4.3.1.3 Force exerted by IPMC actuator when it is powered at different input voltages

An experiment was done to study the force exerted by IPMC when it is powered at different voltages to analyze its effect on the frequency response of the device. The setup used is in Fig. 4.13 and the results are in Fig. 4.14.

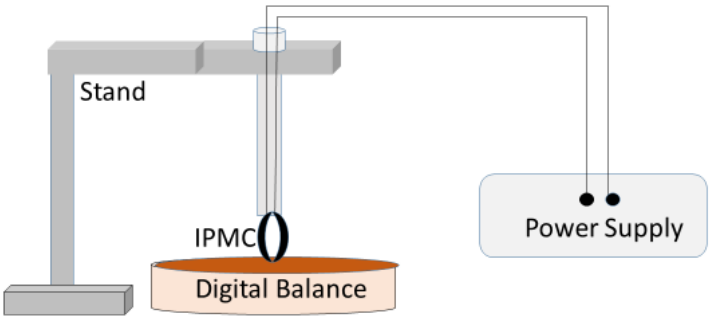

Fig. 4.13 Setup to study force exerted by IPMC actuator when powered at different voltages

Here, the force exerted was measured using a sensitive weighing balance. In the graph, the force exerted is in mg-force (1 mg-force equals 9.80665micro newton) and the displacement is in mm. In the experiments, the force was measured using the sensitive balance in mg-force. Hence the graphs were plotted using the same units.

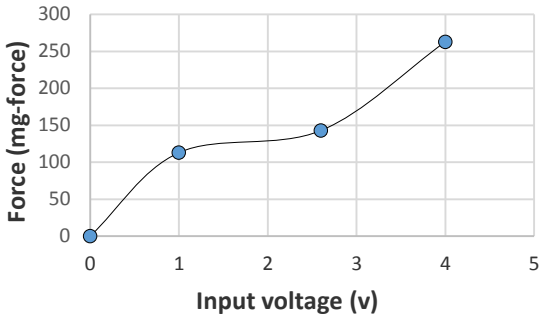

Fig. 4.14 Force exerted by IPMC actuator when powered at different voltages

In our earlier paper [146], the following aspects of the device are covered in detail.

- The novelty of the Device
- Device design considerations
- Device design
- Detailed experiments to study how resonance and power output of the novel device is affected by the varying point of contact
- Detailed experiments to study how resonance and power output of novel device is affected by varying the gap between IPMC actuator tip and beam
- Detailed experiments to study how resonance and power output of the novel device is affected by varying IPMC input voltage

4.3.2 The theoretical analyses of the experimental results discussed above are detailed below:

4.3.2.1 Theoretical Analyses of frequency shift and broadening of PVEH when IPMC is used as a stopper

When the vibrating cantilever makes contact with a stopper, it is subjected to an impact force. Zhou and others [152, 154] have modeled the impact force of the stopper as similar to that exerted by a trilinear spring where the impact force is proportional to the cube of its displacement. The paper indicates that for rubber as a stopper, there is a close agreement with experimental results and also indicates there is a broadening of the frequency response curve. Similarly, broadening was also observed when steel and aluminum materials were used as stopper materials. In all these cases, the response initially broadens and thereafter falls steeply.

Results of the experiments carried out on the IPMC actuator indicate that there is a linear relationship between impact force and the cube of the tip displacement, as shown in Fig.4.15. It is divided into two regions, namely Region A and Region B. This indicates the linearity of the initial curve. Region B is a flattening of the curve beyond the cube of displacement value of approximately 10 mm^3.

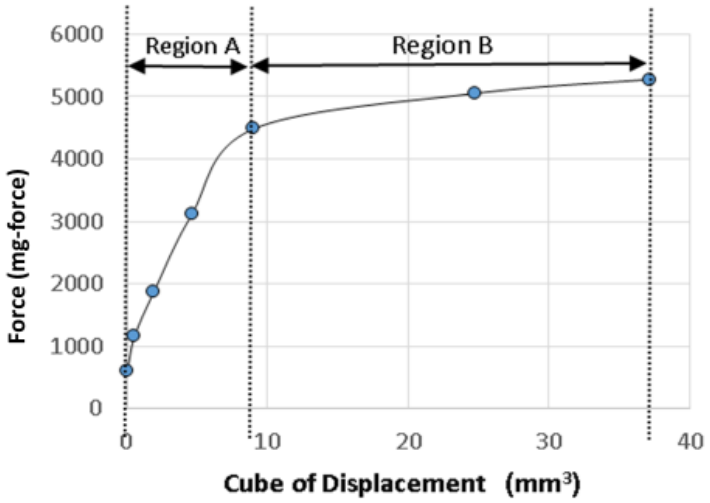

Fig. 4.15 Plot of force by IPMC vs. cube of displacement

From the above, it will be seen that IPMC as a stopper behaves like a trilinear spring (Fig 4.15). There is an initial linear portion (Region A) and a flat linear region (Region B), as shown in Fig. 4.16. When the amplitude of vibration is high, the harvester will be generating higher output. In this situation, the IPMC operates in both regions A and B. When the amplitude of vibration decreases, the PVEH output reduces and the impact of IPMC will be based on the initial region A only. For other stopper materials, the spring constant increases exponentially beyond a certain displacement, and the response after initial broadening falls steeply. In the case of IPMC, this is more gradual and we see the broadening effect continue as the harvester output falls. This is desirable as output is maintained over a larger frequency range.

The above analyses of experimental results are summarized below:

1. The harvester frequency response broadens when a low-power IPMC actuator is used.

2. The broadening of response observed is gradual and no steep fall is observed. Other researchers who have experimented with different stopper materials like rubber, aluminum, etc. have observed a steep fall after initial broadening.
3. Researchers have modeled stopper action as similar to the action of a trilinear spring where the force exerted by the spring is proportional to the cube of its displacement. This results in a broadening of the response. IPMC action is similar to the action of two trilinear springs acting together when displacement is high and acting as one spring for small displacements.
4. Our device was made using commercially available IPMC. When IPMC with higher blocking forces become available commercially, more data can be generated to propose a model.
5. Our earlier paper discusses in detail the device used and experiments done using the device. These experiments were done to see the resonance frequency shift under various conditions of IPMC impact. It was also observed that the net power generated after utilizing a portion for the IPMC actuator is sufficient to power commercially available low-power devices.

To complete our theoretical analyses, two graphs depicting observations from experiments referred in our earlier paper [146] are given below. The results are in conformance with the theory (Fig. 4.16 and Fig. 4.17).

The resonant frequency increases as the distance between the tip of the IPMC and the cantilever beam (*s*) is reduced. This is in conformance with Equation (4.11) (Fig. 4.16).

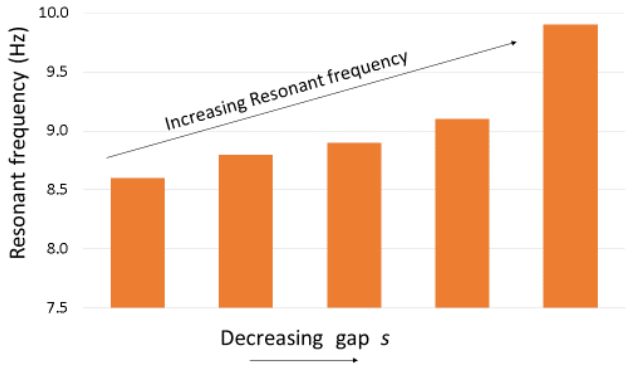

Fig. 4.16 Resonant frequency for different gap values between IPMC tip and cantilever surface

Resonant frequency is reduced with increasing the distance (*d*) of the contact point on the beam from the free end of the extension beam. This is in conformance with equation (4.11) (Fig. 4.17).

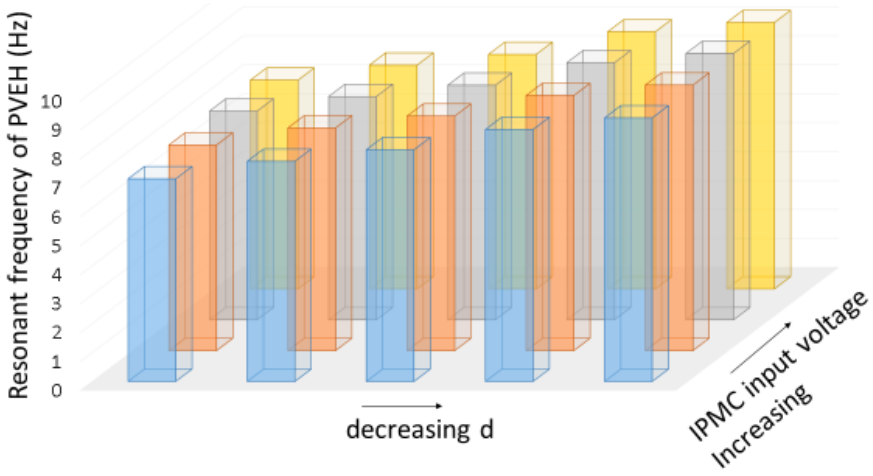

Fig. 4.17 Plot of Resonant frequency of PVEH vs distance of the impact point from the free end of the cantilever for different values of IPMC input voltage

4.4 Concluding remarks

The theoretical analysis and experimental results given in this paper describe the parameters that can be controlled to change the resonant frequency of PVEH using IPMC actuation. The broadening of the frequency response observed with IPMC as a stopper is also explained.

- Compared to the conventional PVEH, the device presented here has the additional feature of an extension beam. The effect of the IPMC unit on the extension beam is to shift the resonant frequency of the beam. The two-section beam enables a high sensitivity for the impact of IPMC. The effect of tuning is to shift the resonant peak to higher values.
- The shift in resonant frequency is based on the:
  -input voltage to the IPMC.
  -gap between the cantilever beam and the tip of IPMC.
  -distance of the impact point of IPMC on the cantilever beam from the free end.
- Based on the advances in the design and manufacturing of IPMCs with higher blocking force, the next-generation tunable PVEH can be realized.

Chapter 5
Applications of the novel PVEH

Note: This chapter is adapted from the peer-reviewed paper that has been published in the journal, ***Micromachines*** with permission where appropriate.

It gives the applications of the device, detailing the experiments carried out, to power a MEMS accelerometer using the harvested power from the device. It is also demonstrated that the device could power a strain gauge bridge to sense the strain in a structure and could power a low-power MEMS accelerometer. Further, it was also demonstrated that it could power a Bluetooth accelerometer sensor and transmitter effectively.

The article citation is:
Raghavan, S., Gupta, R., & Sharma, L. (2023). Applications of a Novel Tunable Piezoelectric Vibration Energy Harvester. Micromachines, 14(9), 1782.

Article link: https://www.mdpi.com/2072-666X/14/9/1782

5.1 Introduction

In recent years, there has been a radical change in the concept of monitoring the health of systems and structures. The concept is to deploy a very large number of sensors connected to the internet and have them communicate with each other. This Internet of Things (IoT) has revolutionized the process by which systems across the world are monitored and controlled. The sensors in microscale, Micro Electro Mechanical Systems (MEMS) utilize very low power, making the above concept feasible. However, the main issue associated with the scheme is the mode of powering the sensors. Batteries or wired connections to a central power supply are not a feasible option in all cases. Further sensors will need to be deployed under inaccessible and hostile conditions where host structures are deployed. In order to overcome these issues, generating useful power from the ambient conditions and its application in diverse areas have been explored by many researchers. Some of the research reported, are detailed below.

Alla et al. [155] discussed piezoelectric vibration energy harvesting for powering the sensors embedded for monitoring tire pressure in automobiles. Hosseinkhani et al. [156] have

provided a comprehensive review of using sound and vibration energy harvesting in railways by providing different methods, their advantages, and drawbacks. Esmaeeli et al. [157] reported their study on a rainbow-shaped piezoelectric vibration energy harvester mounted on the tire to power the sensors deployed for the structural health monitoring of tires. Goel et al. [158] have come out with the application of piezoelectric vibration energy harvesters in space vehicles, as the main source of power in a space vehicle are solar panels that are large in size and heavy. The author proposes the use of vibration energy harvesters which are lighter and cost effective for space applications. Beeby et al. [159] have reported the implementation of vibration energy harvesters in rail and industrial applications. It is reported that the miniaturization of piezoelectric harvesters was realized using the screen printing method for printing the device entirely. Khan et al. [160] have worked on applications for converting bridge vibrations into useful power-adapting PVEH configurations. Bridge vibrations are in the low-frequency range with low acceleration levels. Electromagnetic harvesters which are bulky have also been developed and implemented as space is not a constraint here. Ali et al. [161] in their review covered the recent advances in Piezoelectric Vibration Energy Harvesters and the medical devices that can be powered by them. The application is important since implantable medical devices are being used for managing critical human health conditions, which require continuous power sources for functioning. The kinetic energy generated by muscle relaxation, blood flow, cardiac movements, lung movement, etc. can be harvested using vibration energy harvesters. Hwang et al. [162] described flexible thin film piezoelectric energy harvesters and nano-sensors for biomedical applications. Inorganic bio-compatible piezoelectric materials are being used for implantable devices. Panda et al. [163] described the various applications of piezoelectric vibration energy harvesters in biomedical applications such as cell stimulation, stimulation of the brain, and tissue engineering. The article also details piezoelectric biomaterials. Han et al. [164] demonstrated a 3D piezoelectric microsystem which can be used in sensing mechanical properties and in energy conversion. The article also details the applications in realizing multi-functional sensors for robotic prosthetic interfaces. Mhetre et al. [165] have reviewed various methods in the literature for energy harvesting and have discussed the need for improving the power output. This is even more relevant in the case of human energy conversion which is needed for powering implantable devices. Zheng et al. [166] describe the various structural designs of energy harvesters in order to harvest energy from biomechanical movements to power devices internally. It is emphasized that future work should be focused on flexible,

stretchable, and biodegradable systems that are autonomously powered. Ding et al. [167] have described the need for kinetic energy harvesting for biomedical implants due to the presence of various forms of kinetic energy available in the human body. Kinetic energy harvesting can be very useful in powering micro or nano devices. Townsend et al. [168] worked on a piezoelectric vibration energy harvester to power the sensors on an aircraft. Aircraft systems generate localized vibrations for various frequencies. The work reported here is to generate considerable charge from different conditions. Park et al. [169] have discussed the SHM modules in a typical health monitoring system and the different types of energy harvesters that can be used. The author has analyzed the power requirement of various sensors to study the suitability of energy harvesters to power them. Maruccio et.al. [170] conducted a case study in which health monitoring of a cable-stayed bridge located in Italy was carried out using the harvested power from ambient vibrations. The vibration energy harvester that was deployed, was made of arrays of electro-spun piezoelectric nanofibers.

The low-power sensors developed in recent decades enable us to effectively integrate them into structures. Aspects to be considered are power requirement, the characteristics of structures on which they have to be deployed and the operating conditions. It can be seen that most of the machinery, structures, and moving systems undergo some sort of vibrations during its life cycle. Tapping this vibration energy an autonomous power source for powering the sensors on it can be realized. Here the authors have used a novel tunable piezoelectric vibration energy harvester to power commercially available sensors.

5.2 Materials and Methods

The novel device consists of a two-segment cantilever beam consisting of a root section and an extension beam attached to it. The extension beam is thinner compared to the root section and is sensitive to even small impact loads by a stopper. An actuator arrangement made of two IPMC (Ionic Polymer Metal Composite) strips attached at the tips, is used as a stopper to generate an impact force on the cantilever beam. IPMC acting as a stopper enables a broader frequency response due to its nonlinear response. The IPMC response can be changed by powering it from the same harvester as it consumes very little power. This is akin to changing the properties of the stopper material. The piezoelectric material used is MFC (Macro Fiber Composites) from Smart Material Corporation [171] and IPMC is from Environmental Robots USA [145]. The device has

a patent pending [86]. The device novelty, design details, and detailed experimental results are covered in earlier papers [83, 146].

In this paper, three applications for the novel PVEH are demonstrated with experimental results.

Application 1:

Strain gauges are small and sensitive devices. The resistance of a strain gauge changes when a force is applied to them. Strain gauges are used to measure changes in pressure, force, or tension. They are widely used in monitoring the strain experienced by structures such as bridges, buildings, aircraft, wind turbine blades, ships, and so on. Strain values of a structure can indicate various types of failure and the life left for a safe operation. Hence, monitoring the strain experienced at critical locations of a structure is important. Stress experienced at various locations on bridges, buildings, and other concrete structures can be monitored by embedding strain gauges at these locations. In aerospace applications strain gauges are bonded to load-bearing components such as wings and rotor blades. This helps to ensure flight safety. In railway applications strain gauges are bonded to railway lines to monitor the stress experienced. In automobiles they are bonded onto wheels to measure pressure. This helps to ensure safety and timely maintenance.

It is important to ensure a reliable power source for the strain gauges. A conventional wired system is not practical in many cases where the structure is inaccessible or located in hostile conditions. Hence, there is a need for an autonomous power supply that harvests energy from the environment.

A study to power a strain gauge using the novel tunable PVEH which harvests power from the vibrations present in the environment is detailed below. Fig. 5.1 shows the circuit used for the above study. The setup has 4 sections, a) the tunable PVEH, b) the rectifier circuit, c) the interface circuit for the strain gauge bridge, and d) the strain gauge bonded on the structure.

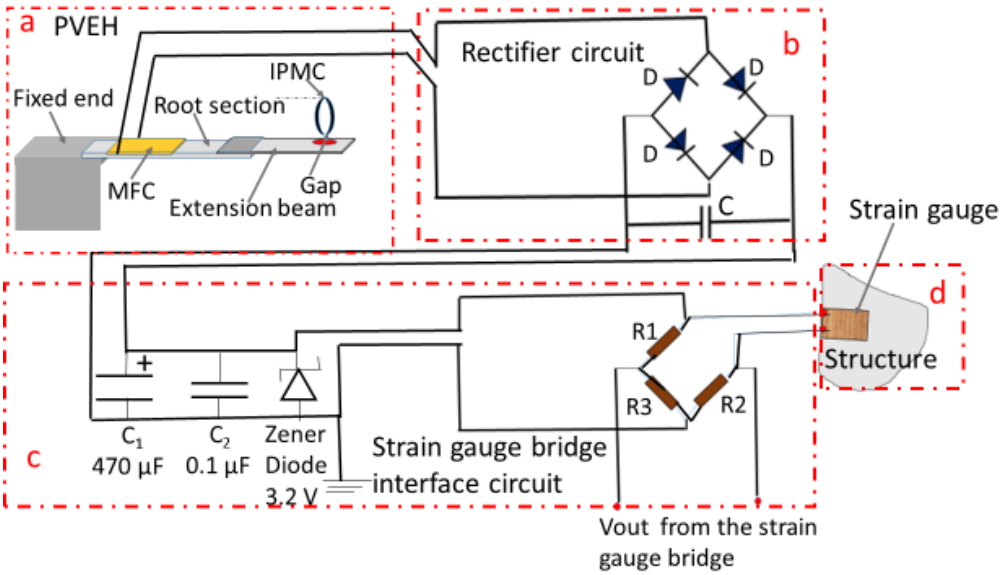

Fig. 5.1 Circuit for powering a strain gauge bridge using the PVEH output

The strain gauge can be wired in different configurations namely Quarter Bridge, Half Bridge or Full Bridge configuration. In the present study, the strain gauge is wired in a Quarter Bridge configuration, where it forms one arm of a Wheatstone bridge. To reduce the power consumption of the strain gauges, high resistance strain gauges (of the order of kΩ) and balancing resisters of high value can be used. Here, however available strain gauge with 120Ω resistance and balancing resistors of 120Ω for R_2 and 1200 Ω for R_1 and R_3 are used.

A typical application for this vibration energy harvester is to effectively monitor the strain developed in a remote structure. In the real scenario, structures will be subjected to strain at different locations, when they undergo loading during their operational cycles. The corresponding strain on the structures has to be monitored to ensure that no catastrophic failure happens. In order to simulate a similar condition in the laboratory, a steel beam of length 11.5 cm and width 1cm with a strain gauge (Micro Measurements) bonded on it, was used for the experiment. The photograph of the beam is given in Fig. 5.2. The beam was fixed at one end as in Fig. 5.3 and loaded at the free end in steps to generate a bending of the beam. This bending generates a strain on the surface to physically extend the strain gauge. This extension of the strain gauge changes its resistance value. When this strain gauge is connected as one of the arms of a Wheatstone bridge, the output of the circuit gives a voltage corresponding to the changed strain value. The tunable

PVEH was subjected to vibrations and operated at the resonant frequency. The output of the strain gauge Wheatstone bridge was monitored.

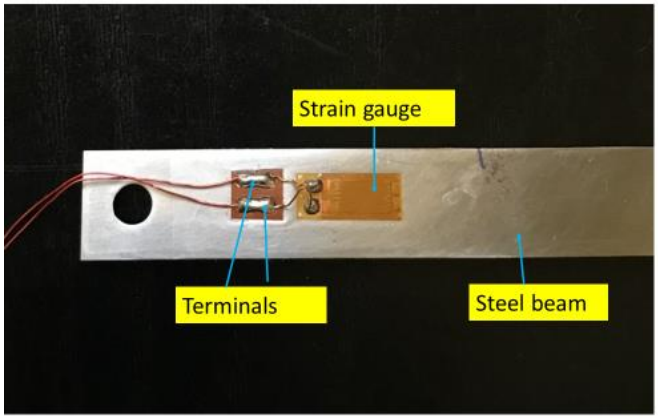

Fig. 5.2 Steel beam with strain gauge bonded on it

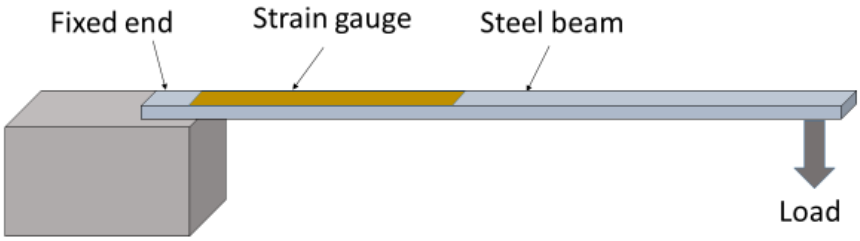

Fig. 5.3 Experimental setup of the strain-gauged beam

Using this novel configuration of PVEH, it is observed that the output of the bridge is maintained even when the ambient frequency drifts slightly away from the resonant frequency due to the nonlinear response of IPMC. Since the power generated is continuously stored, this acts as a stable source of power.

Application 2:

As a second application, a triaxial MEMS accelerometer was selected for the experiments. ADX L335 works on 2 to 3.3 V and draws a current of 300 µA. The Fig. 5.4 depicts the ADX L335 accelerometer and circuit used.

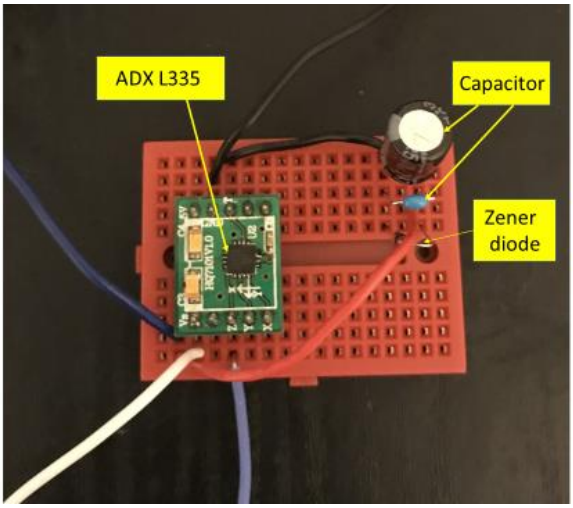

Fig. 5.4 ADX L335 MEMS Accelerometer and circuit

A tri-axial accelerometer is used for motion detection in various applications of surveillance and security. In most of such applications, the accelerometer will have to be deployed in inaccessible locations, which makes wired power using a conventional power supply impossible. Hence, such a scenario calls for an autonomous power source for the sensor.

Fig. 5.5 shows the connection diagram of the interface circuit with the PVEH output. The PVEH output was connected to a full wave rectifier and the output of the rectifier was connected across an electrolytic capacitor C_1 of 470 µF, another capacitor C_2 of 0.1 µF, and a Zener diode of 3.2V. C_1 was used to store the charge developed and C_2 was used to smoothen the signal. The Zener diode was used to regulate the voltage given to the accelerometer, so that it does not exceed the rated 3.3 V.

The analog output of the ADX L335 can be monitored in the X, Y, and Z directions when there is a motion in the X, Y, and Z directions respectively. The output of the Zener diode was also connected to the IPMC. The PVEH was operated on an electromagnetic exciter, which was driven by a function generator and a power amplifier. It was found that the power generated by the PVEH could power both the accelerometer and the IPMC.

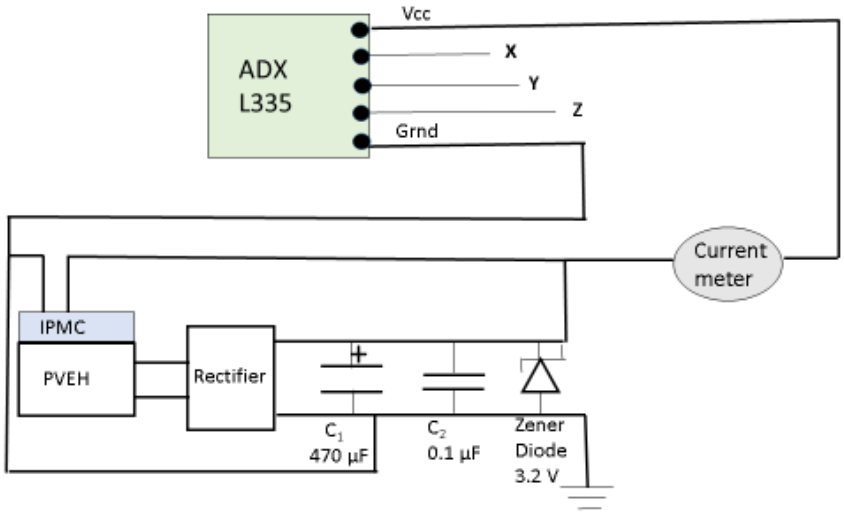

Fig. 5.5 Circuit for powering the MEMS accelerometer and IPMC using PVEH output

Application 3:

In a third application, the PVEH was used to power a Bluetooth PASCO accelerometer along with its transmitter. The vibration signature of a structure is an important input for the diagnosis and prognosis of structural health. Many structures that vibrate are not static, such as rotating gears and rotor blades. In such structures, monitoring the vibration signature with time is a challenge because wired powering of sensors is not feasible. Here an autonomous power source such as a PVEH has great applications. In this application, the sensor output has to be transmitted to a remote station. Hence, both the sensor and the transmitter have to be powered using the PVEH.

In this case, the charge generated from the PVEH was stored in a supercapacitor and interfaced with the Bluetooth device.

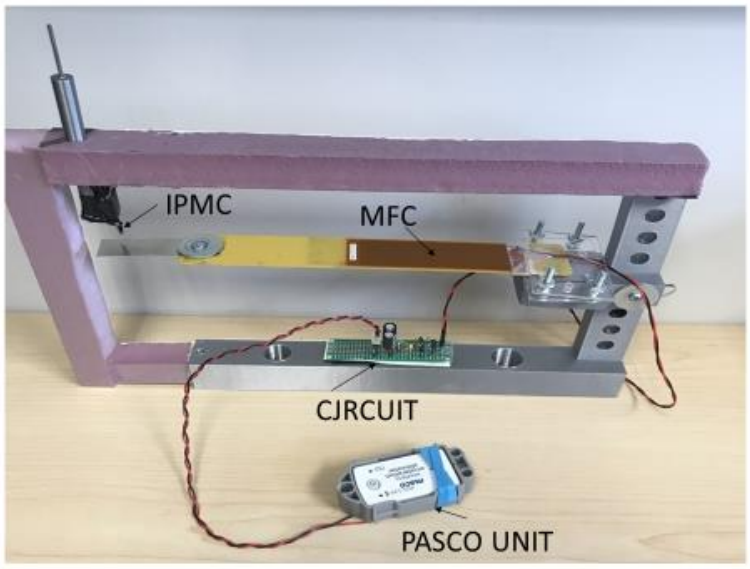

Fig. 5.6 Setup of the PVEH powering PASCO Bluetooth device

PS 3223 accelerometer/ transmitter was used for this application. This is a Bluetooth unit that can transmit data to a remote receiver with the corresponding software. Fig. 5.7 shows the setup for powering the PASCO unit.

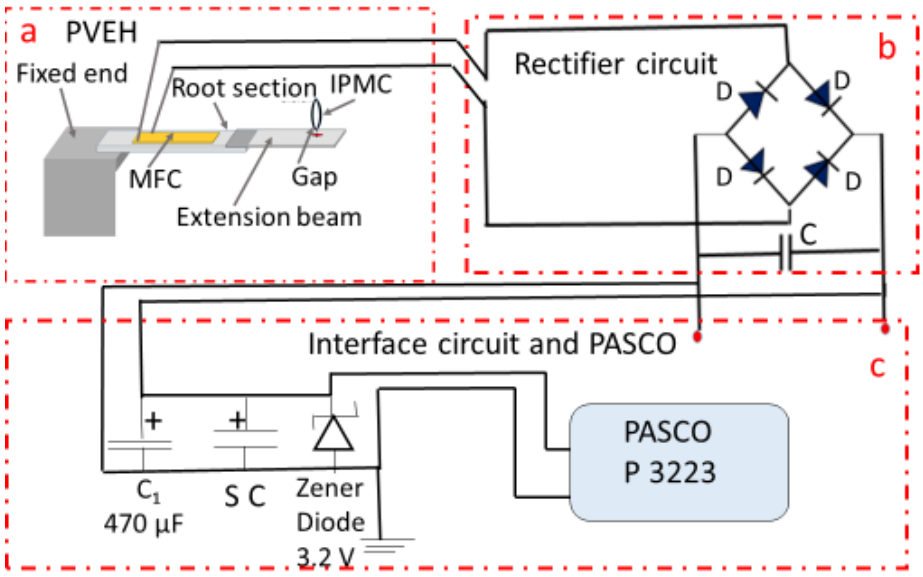

Fig 5.7 Circuit of the setup for powering the PASCO accelerometer/transmitter unit

Fig. 5.7 gives the circuit diagram of the experiment. In the circuit, *SC* is the supercapacitor, rated for 5.5 V.

5.3 Results and Discussion

In the first application, the strain gauge bridge circuit gave an output that increased with an increase in the load applied (between 20 g and 35 g) to the strain gauged beam. The Fig. 5.8 depicts this response and it can be seen that it has a linear response. The stable output of the strain gauge at different loading conditions indicates the presence of constant power source that is enabled by the PVEH with the interface circuit.

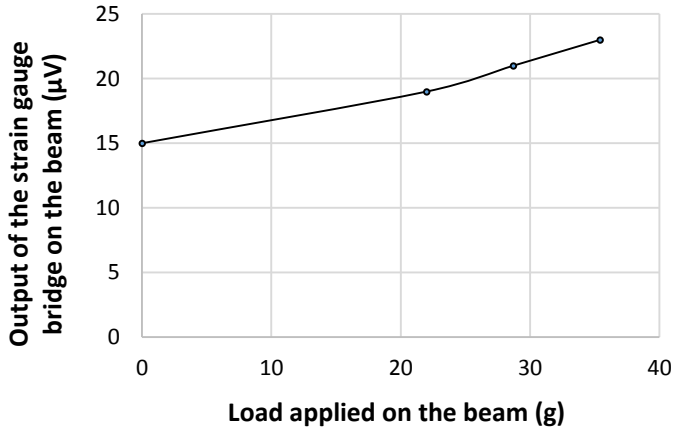

Fig. 5.8 Response of strain gauge bridge powered by the harvester

The stable output across the storage capacitor and the Zener diode that is connected to the Wheatstone bridge makes it possible to obtain a consistent output from the strain gauge, which is important in the measurement.

The second application of powering the accelerometer proves that the harvester could generate output sufficient to power the accelerometer along with the IPMC. The PVEH was in resonance at 8.8 Hz and generated 2.03 V across the Zener diode. The total current drawn was 250 μA. The accelerometer gave an output voltage varying from 1.5 V to 2.7 V depending on the position as it moves along the X, Y or Z direction. The accelerometer and the IPMC could be powered by the harvested power.

In the third application, the CR 2032 3V cell of the PASCO unit was replaced with the output from the harvester. By this, the PASCO unit could be powered successfully to transmit signals. The transmitted signals were acquired remotely using the data acquisition software

SPARKvue. When the PVEH is subjected to vibration, it keeps charging the supercapacitor. The Zener diode of the selected rating enables the required constant power supply to the sensor.

As it is shown above, this system can be adapted to monitor the strain developed or the vibrations on a bridge during its life cycle which will provide the vital data required for its Structural Health Monitoring. Similarly, the strain and vibration values on rotary blades of a helicopter are also critical parameters that can be monitored by adapting the above device setup.

The proposed PVEH can be designed in MEMS configuration since the basic cantilever configuration and the IPMC actuator can be miniaturized effectively. A tri-axial accelerometer that takes just 23 μW can also be integrated for sensing the ambient frequency to enable self-tuning.

5.4 Concluding remarks

The novel tunable PVEH can continuously provide power to low-power devices such as sensors and transmitters.

2. The device generates power at the adjacent frequencies to the basic resonant frequency also, due to the stopper action of IPMC.

3. The proposed PVEH fabricated in MEMS form, can be integrated with other low-power sensors, transmitters, and microcontrollers as required for different applications.

4. The MEMS version of the novel device can be easily integrated with sensor arrays.

Chapter 6

Initial Experiments and Test results of the novel PVEH

Note: This chapter is adapted from the peer-reviewed paper that has been published in the ***Journal of Composite Science*** with permission where appropriate.
It gives the details of initial experiments done as part of the characterization of the device, which was used for filing the patent application.

The article citation is:
Raghavan, S., & Gupta, R. (2020). A novel design and performance results of an electrically tunable piezoelectric vibration energy harvester (TPVEH). Journal of Composites Science, 4(2), 39.
Article link: https://www.mdpi.com/2504-477X/4/2/39

6.1. Introduction

Due to the developments in microsystems [179], very low-power MEMS (Micro Electro Mechanical Systems) based sensors are already realized. Deployment of a large number of sensors on structures enables more comprehensive and interactive Structural Health Monitoring (SHM) for diagnosis and prognosis in the case of critical structures. In this present scenario of low-power sensors and the resulting Internet of Things (IoT) and SHM, enabling autonomous power sources for the sensors by energy harvesting from ambient conditions is of great research interest. This will avoid the need for deploying batteries and the associated issues of recharging procedures. Of the different forms of ambient energy, vibrations of different frequencies are present on many systems and structures, during their operating life cycle. Hence a great deal of research has gone into vibration-based energy harvesting, especially when utilizing piezoelectric materials [180]. Vibration-based energy harvesters using piezoelectric materials have demonstrated good conversion efficiency. However, such harvesters have poor response at all the frequencies of vibration other than their resonant frequency. One method to overcome this limitation is to get a broader bandwidth by enabling tuning of the resonant frequency of the harvester closer to the

ambient vibration frequency. The resonant frequency of a system can be changed only by two methods, by changing the mass or by changing the stiffness [181]. Some of the relevant literature on this is presented below.

A reported method for mechanically tuning the harvester's resonance frequency includes the introduction of notches [122] that bring out the relation between the applied compressive preload and the corresponding resonance frequency. The structure consists of two additional thin arms to apply an axial preload to the tip of the beam. Similarly, studies by Leland et.al. [69] have proven that axially compressing a piezoelectric bimorph lowers its resonance frequency. It is reported that if an axial preload is given, the resonance frequency of a simply supported bimorph can be shifted to 24% below its resonance frequency. Shaofan Qi et.al. [182] have designed a clamped-clamped piezoelectric harvester, having cantilevers mounted on the sides. Different masses added to these cantilevers make their resonant frequencies different, resulting in a wider bandwidth. However, this method can address a limited number of frequencies by this passive approach. S Leadenham and A Erturk [183] have designed an M-shaped harvester to overcome the requirement of having high excitation levels in a nonlinear harvester. The device is made of spring steel on which piezoelectric laminates are bonded. Researchers have also worked with configurations where stretching strain is introduced by doubly clamped structures [184, 123]. It should however be noted that the harvester is not in the conventional cantilever configuration.

Huang H et.al. [141] have used polymer piezoelectric materials, with a beating mechanism. The impact force created through the low-frequency vibratory motion by the beating mechanism excites the system's natural frequency. A method of shifting of gravity center by a moving mass for tuning the resonance frequency of the harvester has been reported by Xiaoming et.al. [124]. Experiments are carried out on a prototype and could achieve adjustment from 130 Hz to 180 Hz. A base-mounted piezoelectric (BMP) harvester is designed by Koven et.al. [121] with a piezoelectric transducer mounted below the base of a cantilevered beam resonator. The harvester behaves like a damped mass-spring system. Zhou et.al. [185] have developed a design by introducing springs in between adjacent harvester beams. The time-varying relative displacement between two adjacent harvesters leads to broadening the bandwidth. Thus the authors could achieve nonlinearity, without introducing magnets, which is very important and relevant in some applications. Researchers have also worked on using magnets in the design in different configurations, to increase the bandwidth by the effect of attractive force on the cantilever [186,

187, and 188]. However, all of the above designs suffer from the limitations of the tunable frequency range. In this paper, the authors present an innovative design that overcomes these reported shortcomings.

6.2 Design of a novel tunable Piezoelectric Vibration Energy Harvester (PVEH) and experimental work

Resonant frequency-based cantilever design of a piezoelectric vibration energy harvester gives better output at its resonant frequency, compared to the impact- type device [189]. Hence, methods to tune its natural frequency to different values matching with the ambient frequency open up a wide range of applications. Several methods that are discussed in the literature so far, are either passive or require a higher power input [190]. This limitation led to the current work presented by the authors.

6.2.1. Materials utilized and Design concept of the device

Materials:

The work presented below focuses on the design of PVEH targeted for low frequencies, which can be tuned to different ambient frequencies. The basic hypothesis is that the power spent on tuning the system should be much lower than the PVEH power output. The proposed design of PVEH integrates two smart materials, piezoelectric material and Ionic Polymer Metal Composite (IPMC), to achieve tuning over a wider frequency range. The discovery by the authors of the right type of IPMC for PVEH tuning was preceded by the thought process described below.

Active tuning requires a smart element that can be electrically controlled. Research into the range of smart materials available revealed that piezoelectric material actuators or shape memory alloy actuators do not meet the requirement of low power consumption. Magnetic shape memory alloys also require higher power than we can expend in this application. Based on this work, it was found that IPMC meets all the essential requirements of power, size, and weight.

The piezoelectric material used in this study is Macro Fiber Composites (MFC) sourced from Smart Material Corporation, USA. [191]. It has advantages over other piezoelectric elements, since it is flexible to a great extent, making it effective in high deflection scenarios. It can also be bonded to any surface effectively. MFC is also effective at energy conversion at its resonant frequency when used in cantilever mode.

The design proposed by the authors involves the application of the actuation properties of IPMC to introduce load on the cantilever beam. IPMC is composed of an ionic polymer like Nafion,

whose surfaces are coated with platinum or gold as conductors. When the IPMC is subjected to a low electric field (1 to 4 V), positively charged hydrated cations in the membrane network get repelled by the anode and they migrate to the negative electrode. Hence, the water molecules also get shifted within the membrane. This leads to an osmotic pressure gradient, which results in the bending of the IPMC strip. Hence, it functions as an actuator with a low driving voltage as reported by Shahninpoor and Kim [192]. The actuation force associated with an IPMC can be utilized for applying a pre-defined force on the cantilever of the energy harvester. The force applied is a function of its mass and the applied voltage.

Assuming the mass remains the same, we can control the force by controlling the input voltage. Since the actuation mechanism is dependent on the water molecules in the polymer film, the hydration of the IPMC is of importance to achieve the correct load values.

Governing Equations:

IPMCs can be characterized using the governing Partial Differential Equations (PDE) is given below: [192]

$$E = D\,\kappa e = -\nabla\varphi \tag{6.1}$$

$$\nabla \cdot D = \rho = F(C^{+} - C^{-}) \tag{6.2}$$

Where D, E, φ, and ρ denote the electric displacement, the electric field, the electric potential, and the charge density, respectively. κe is the effective dielectric constant of the polymer, F is Faraday's constant, and C+ and C− are the cation and anion concentrations, respectively. The corresponding continuity equation is given by

$$\nabla \cdot J = -\partial C^{+} / \partial t \tag{6.3}$$

where J is the ion flux vector.

Design concept:

In this investigation, as an initial step, the characteristics of IPMC were studied by applying several different steps of voltages, ranging from 0.5 V to 4V. It should be noted that different actuation characteristics of IPMC can be selected by choosing the right thickness of the Nafion film.

The IPMC strips can be easily miniaturized to introduce into the harvester design. It is bio-compatible, in case of applications in biological systems. The additional advantage of using IPMC is that its driving current is also very low. Hence the power required can be tapped from the generated power from the harvester itself. The MFC used in this study is made of piezoelectric fibers of square cross-section, bonded together to form a piezoelectric sheet. This piezoelectric

sheet is placed in between layers of adhesive, electrodes and a polyimide film. The interdigitated pattern of electrodes enables better contact with the fibers and in-plane poling/actuation. This pattern also leads to a very low voltage drop at the interface. The electrical and mechanical properties of MFC used in this study are given in the manufacturer's datasheet [191]. P2 and P3 type MFCs work on the d_{31} effect for actuation and are mostly used for energy harvesting [191]. The novel tunable PVEH consists of a cantilever beam on which MFC is bonded in unimorph configuration, and an IPMC actuator integrated in the system. The IPMC specimens from Environmental Robots, USA were used to actuate during the experiment. The properties of IPMC are provided by the manufacturer in their datasheet [145]. The force applied by the IPMC on the cantilever generates a compressive load component, which contributes to the stiffness change of the device.

In this study, the authors chose an aluminum cantilever beam that consists of two sections, 0.64 mm thick root section of 15cm x 3.5 cm and 0.37 mm thick extension of 10.5 cm x 2 cm, with an overlap of 3 cm. (Fig. 6.1). For these specimens, the thickness of the beam were intentionally kept low so as to allow effective control in the frequency shift using the applied load by IPMC.

The dynamics of the cantilever beam can be described by the Euler -Bernoulli Beam equation as given below in equation (6.4)

$$\frac{d^2}{dx^2}\left[EI\frac{d^2w}{dx^2}\right]=p \tag{6.4}$$

where w is the out of plane displacement of the beam, p is the force per unit length acting in the direction y (and w), E is Young's modulus of the beam, and I represents the moment of inertia of the cross-section of the beam. The present case of a cantilever beam of two sections can be represented by the change in I.

Configuration 1 consisted of an MFC M 8514 P2 that was bonded on the thicker cantilever section in unimorph configuration (having a single active layer of piezoelectric material), as shown in Fig. 6.1.

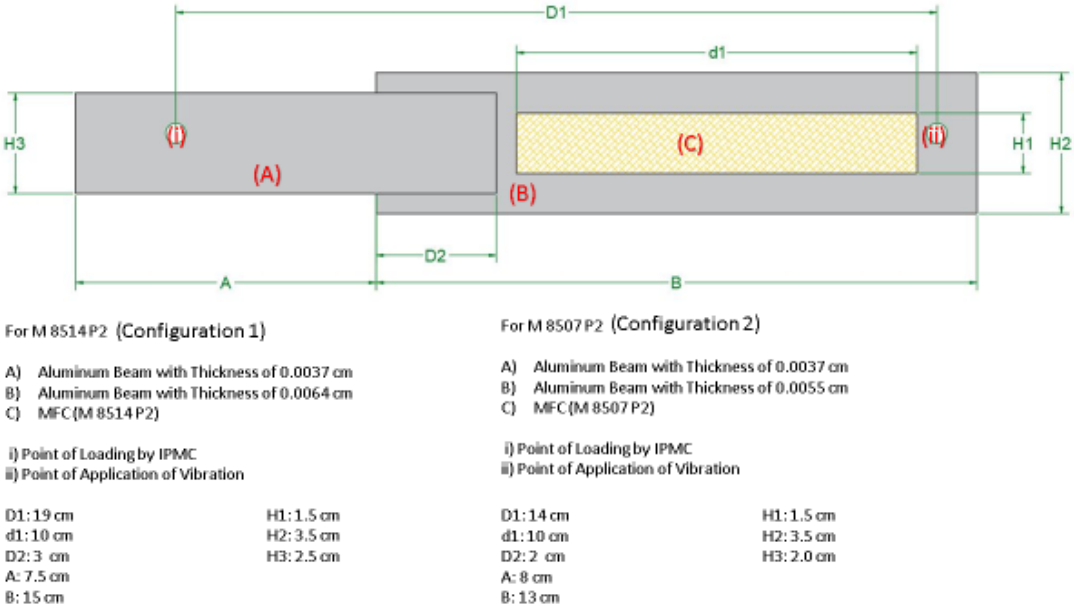

Fig. 6.1 Plan view of the device

This MFC has an active length of 85 mm, an active width of 14 mm, a free strain of 630 ppm, and a blocking force of 76N. The cantilever was subjected to vibration at point C, using an electrodynamic exciter. Electro dynamic exciter-Miniature shaker model no. K2007E01-Modal shop was used to simulate the vibrations.

6.2.2. Experimental setup

The exciter was driven by a function generator through a power amplifier. In the model used, the exciter has a built-in power amplifier. The output of the piezoelectric element was connected to a full wave rectifier and then to an oscilloscope. The full wave rectifier circuit is designed using 4 diodes in Wheatstone's bridge configuration. This is required to convert the AC output of the PVEH to DC. Diode IN 4001 and capacitor 220 µF were used in the full wave rectifier circuit. In the experimental setup a function generator model no. GW Instek GFG 8250A and Oscilloscope model no. HP 54603 B were used.

6.2.3. Conduction of experiments

The PVEH was subjected to continuously varying frequencies, and the resonant frequency was identified. Corresponding voltage and current outputs from PVEH were recorded. The current was

measured by incorporating a load resistor of 1 KΩ. The IPMC actuator was given 1.5 V input at point D of the cantilever. This load shifted the resonant frequency of the device. Now, the frequency sweep was given again, and located the new resonant frequency. This value and the corresponding voltage and current output of the PVEH were recorded. These steps were repeated for 1.9 V and 2.1 V input to IPMC. These steps of voltage input to IPMC were selected to bring out a frequency shift of around 2 Hz. In all the cases, the current drawn by the IPMC was also recorded. For all the steps, power harvested from PVEH as well as power spent on actuation of IPMC were calculated using equation (6.5).

$$P = V \times I \tag{6.5}$$

Where P is power, $V$is voltage and I is current.

6.2.4. Results and analysis: Configuration 1

The results of the tests conducted on the designed harvester are presented in Fig. 6.2.

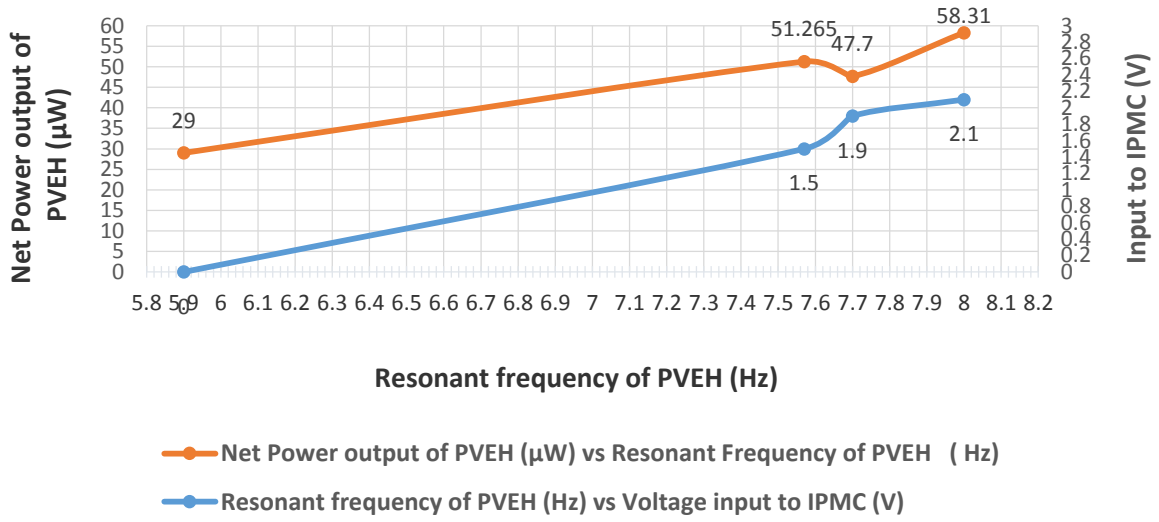

Fig. 6.2 Power output of PVEH and Voltage to IPMC vs. Resonant frequency

When the power input to IPMC is 0, the power output of the PVEH is 29 µW, and the corresponding resonant frequency is 5.9 Hz. The power output of PVEH is 52.03 µW, when the power used for the IPMC actuation is 0.765 µW, shifting the resonant frequency from 5.9 Hz to 7.57 Hz. Similarly, the power output is 49.98 µW when the power for IPMC actuation is 2.28 µW, shifting the resonant frequency to 7.7 Hz. Further, a power input of 5.88 µW to IPMC shifted the resonant frequency to 8 Hz, giving a power output of 64.19 µW from PVEH.

The net power output of PVEH is 29 μW at 5.9 Hz, 51.265 μW at 7.57 Hz, 47.7 μW at 7.7 Hz and 58.31μW at 8.0 Hz. Intervention by the IPMC results in gain of net power. It seems like the maximum net power is achieved at a resonant frequency of 8 Hz. As a first case, experiments were done till the IPMC input value of 2.1 V. It can be further increased to achieve still higher resonant frequencies, based on the characteristics of the specific IPMC specimen.

From the above graph, it is evident that by applying a low power to the IPMC, the resonant frequency of the harvester can be tuned to the ambient vibration frequency. The graphs show a near-linear trend. The force applied by the IPMC is a function of its mass also. Hence by selecting the IPMC of the required mass, the desired force application range can be achieved. For the above experiments, as stated earlier, commercially available IPMC samples were used. IPMC samples of different thicknesses can be fabricated to suit the specific requirement of force range.

It can be seen that at every stage of the shift of resonant frequency, the power output is much higher than the power spent on the actuation process. This comparison of power spent on actuation and power generated by PVEH in the process, clearly indicates that there is a substantial gain in the power harvested over a wider frequency range, applying this novel design. The design offers an effective tuning for low-frequency energy harvesters. This device can be tuned to practically many frequencies by varying the applied actuation load, whereas, many reported methods have limitations in the range of tuning.

The low power required for the IPMC actuation can be tapped from the harvested energy and hence can enable a closed-loop autonomous system in place. This can be achieved by integrating a low-power microcontroller in the device, which looks for the ambient frequency change and changes the input to IPMC. The ambient vibration frequency can be detected from the voltage output of the harvester itself. In ongoing work, a lookup table for PVEH output vs ambient frequency is being programmed in the controller, using which ambient frequency can be identified. This makes the technology of self-powered sensors a reality, since the inevitable variations in ambient frequency do not affect the energy converted and, in fact could optimize it.

6.3 Effect of distance of loading point from the IPMC actuator: Configuration 2

The results reported above were focused on using a fixed point for actuation. Further work was conducted to investigate the effect of variation in loading point on the net power gain using the same set-up described above. Configuration 2 consisted of the MFC type M8507P2. This MFC

has an active length of 85 mm, an active width of 7 mm, a free strain of 605 ppm, and a blocking force of 38N. A different MFC cantilever with different dimensions was used with a view of demonstrating the concept proof in different cases. This MFC was also bonded on an aluminum substrate (thicker root section) in unimorph configuration as shown in Figure 2. The extension beam was bonded to the root section. The electrodynamic exciter was used to give controlled frequency vibrations to the harvester at point C. The schematic setup of the device is given in Fig. 6.3. The distance of the IPMC tip from the cantilever surface (h) is a variable.

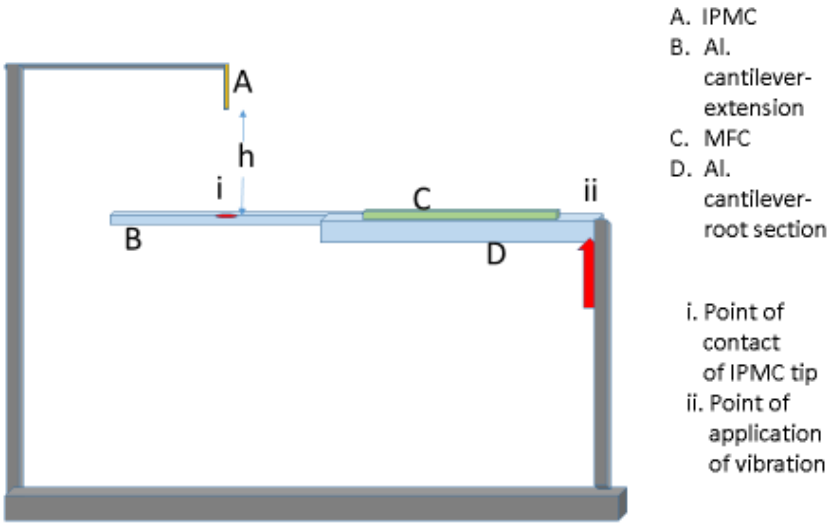

Figure 6.3 Schematic setup of the device

6.3.1. Results and Analysis: Configuration 2

The resonant frequency of the device with no input to IPMC was determined by applying varying frequencies of input to the shaker through a function generator. Then IPMC input voltage of 1.5V was given at a distance of 30 mm (h) above the cantilever. This maximum height was fixed based on the deflection of the beam, so that impact is enabled. Then it was found that the resonant frequency has shifted to a higher value. This was repeated for various values of h: 25mm, 20mm, 16 mm, and 10mm. In each case, the new resonant frequency, the power output of PVEH, and the power input to IPMC were monitored. The point of IPMC contact on the cantilever beam was at a distance of 14 cm from the fixed end. The data is given in the plots in Fig. 6.4.

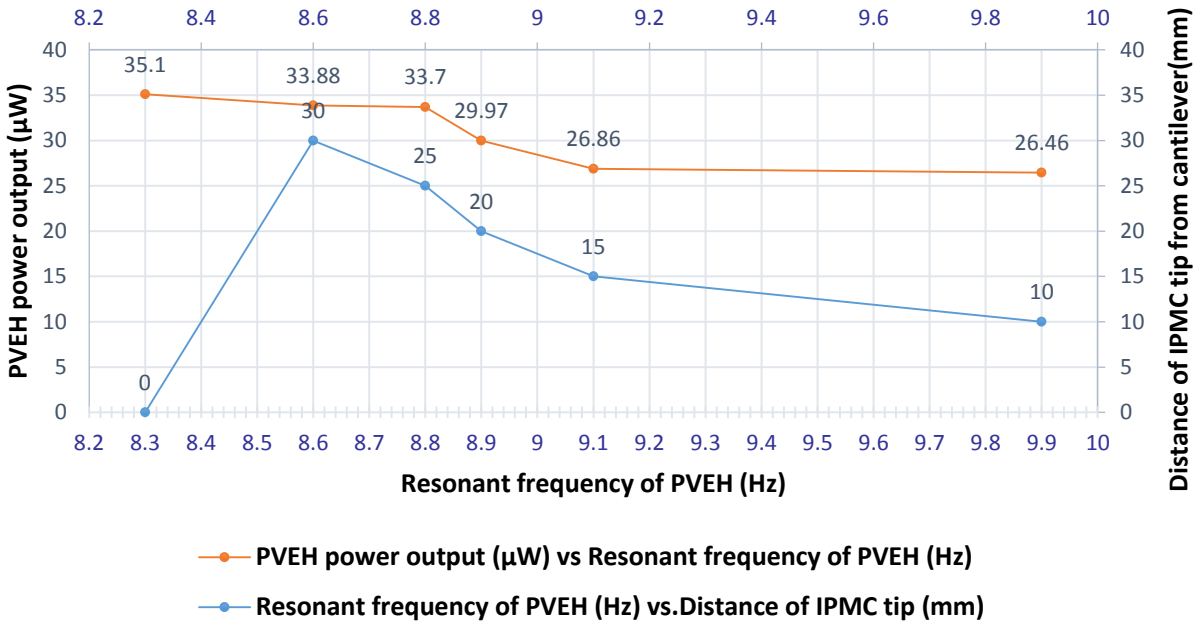

Fig. 6.4. PVEH power output vs Resonant frequency and Resonant frequency vs Distance of IPMC tip from cantilever (s)

When no power is applied to IPMC, the resonant frequency of the harvester is 8.4 Hz. The voltage output is 3.9 V and the current is 9 µA. When a voltage of 1.5 V is applied to IPMC at a distance of 30 mm above the cantilever surface, the impact load on the beam shifted the resonant frequency to 8.6 Hz. The PVEH output is 3.85 V and 8.8 µA. The IPMC drew a current of 0.51 µA. The net power output of PVEH was 33.11 µW. With the same power input to IPMC, the distance h was changed between 25 mm and 10 mm, and the resonant frequency changed further from 8.6 Hz to 9.9 Hz, with the net power output of PVEH maintained between 33.11 µW and 25.69 µW. These results show the dependence of the distance of the point of impact loading on the tuning of frequency.

The resonant frequency shifts to higher values, when the point of loading becomes closer to the cantilever. A marginal drop in the PVEH output is observed, which won't affect the total charge generated over a period of varying frequencies.

Fig. 6.4 is the plot of the frequency of vibration vs the power output of PVEH. It can be seen that power output is maintained at a high value throughout a range of input frequencies spanning from 8.3 to 9.9 Hz. Hence this data can be effectively used along with variable power input to IPMC, to increase the frequency bandwidth of the PVEH. This method is effective in tuning the resonant frequency of a PVEH in cantilever form.

The entire study was focused on making the best advantage of MFC and resolving the basic issue associated with it, the frequency dependence. MFC is suitable for this application since it is highly flexible and has a good conversion efficiency [191]. The IPMC is identified as the most suitable smart material for tuning, since the power requirement for its actuation is very low, compared to the typical PVEH output. The actuation of IPMC at different voltage inputs actually manifests as an effective change in its stiffness. The impact of the cantilever with the actuated IPMC modifies its resonant frequency. The IPMC is suitable for miniaturization and can be easily integrated with the PVEH design. Another salient feature is that the tailorable properties of IPMC [192] make it feasible to design the actuator according to the PVEH requirements.

6.4 Concluding remarks

1. The novel tunable PVEH can continuously provide power to low-power devices such as sensors and transmitters.
2. The device generates power at the adjacent frequencies to the basic resonant frequency also, due to the stopper action of IPMC.
3. The MEMS version of the novel device can be easily integrated with sensor arrays.

Chapter: 7

The Device details

This chapter gives the device details and the possible different configurations as described in the patent application.

https://image-ppubs.uspto.gov/dirsearch-public/print/downloadPdf/20210159816

SELF-TUNING PIEZOELECTRIC VIBRATION ENERGY HARVESTER

Nov 23, 2020

Piezoelectric vibrational energy harvesters (PVEHs) include a Macro Fiber Composite (MFC)) piezoelectric transducer coupled to a cantilever to harvest vibrational energy. One or more Ionic Polymer Metal Composite (IPMC) strips are situated to provide device tuning over a wide frequency range by applying variable contact force to the cantilever. Power consumption for tuning is sufficiently low that the tuning actuator (IPMCs) can be powered using harvested energy.

Description

CROSS REFERENCE TO RELATED APPLICATION

This application claims the benefit of U.S. Provisional Application No. 62/939,511, filed Nov. 22, 2019, which is hereby incorporated by reference in its entirety.

FIELD

The disclosure pertains to energy harvesting.

BACKGROUND

Harvesting electrical energy from mechanical vibrations has been attracting attention of researchers from various interdisciplinary fields, because of its wide range of applicability in various fields of science and technology, including providing autonomous power supply for health monitoring of critical structures. Many materials have been studied towards for this application and piezoelectric materials have been proven to be a good option. Piezoelectric Vibration Energy Harvesters (PVEH) are being developed with the goal of achieving a wider effective band width to improve harvesting efficiency. Some use However, none of the proposed PVEHs are satisfactory, and alternative approaches are needed.

SUMMARY

The disclosure pertains to PVEH devices that can use tuning of a resonant frequency of a novel design of PVEH at different amplitude values of input signals. In examples, the resonant frequency

of the PVEH is electrically tuned using Ionic Polymer Metal Composites (IPMC). Actuation force associated with an IPMC is utilized for applying a required load on the cantilever of the energy harvester. A stacked IPMC can be used instead of a single unit. The stacked IPMC consists of two IPMCs, attached only at the ends and powered by a single supply.

Devices can comprise a cantilever and a piezoelectric transducer coupled to the cantilever to produce an electrical output signal in response to a vibration of the cantilever. An actuator is situated to variably contact the cantilever to establish a resonant frequency of the cantilever. The actuator can be one or more Ionic Polymer Metal Composite (IPMC) strips. In examples, the actuator is coupled to the cantilever to establish the resonant frequency based on a stiffness of the cantilever and an actuator driver coupled to the actuator to apply an electrical signal to the actuator to establish the resonant frequency of the cantilever. The cantilever can be a cantilever beam or a cantilever plate formed of, for example, stainless steel or aluminum. In some examples, a sensor circuit is coupled to the piezoelectric transducer to determine an electrical signal to be applied by an actuator driver to provide a predetermined output power from the piezoelectric transducer. In some examples, the sensor circuit is coupled to determine an available vibrational frequency. The actuator can be configured to adjust at least one of a cantilever stiffness or cantilever resonant frequency based on the available vibrational frequency. The cantilever can comprise a first cantilever section and a second cantilever section, wherein the first cantilever section is a base section and the second cantilever section is an extension section. The base section can be thicker than the extension section, and the base section and the extension section are secured at respective major surfaces or minor surfaces. The actuator can contact the base section or the extension section. In an example, the base section has a thickness of 0.64 mm and the extension section has a thickness of 0.37 mm, and the base section and the extension section are bonded to each other with an adhesive layer or welding at respective major surfaces. The piezoelectric transducer can be a macro fiber composite (MFC) transducer and can be bonded to a major surface of the cantilever over substantially an entire length and width of the major surface. The actuator can be situated to variably contact the cantilever in a central 80% of a cantilever length or area. A memory can store a plurality of actuator drive values and associated cantilever resonance frequencies or stiffnesses and a digital to analogy convertor coupled to the memory to apply a selected drive value to the actuator. In some examples, the actuator has a diamond shape and includes first and second actuators that are stacked.

In some examples, the actuator is a single layer ionic polymer metal fiber composite (MFCs) or a pair of such MFCs.

Methods comprise subjecting a cantilever to vibrations and contacting the cantilever at one or more locations or with one or more contact forces using an actuator. A resonant frequency of the cantilever is identified based on the vibrations for each of the one or more locations and/or each of the one or more contact force and an actuator drive value associated with the resonant frequency is stored for each of the one or more locations and/or each of the one or more contact forces. The vibrations can be applied as a series of single frequency vibrations. The resonant frequency for each of the one or more locations and/or each of the one or more contact forces can be determined based on an output of a piezoelectric transducer coupled to the cantilever.

Methods comprise subjecting a cantilever to vibrations and contacting the cantilever at one or more locations using an actuator. Based on coupling of the vibrations by the cantilever to a piezoelectric transducer, an actuator drive for one or more vibrational frequencies and associated with a selected piezoelectric transducer output power is determined.

Methods comprise contacting a cantilever using a actuator and adjusting the contact based on an output power from a transducer coupled to receive mechanical vibrations from the cantilever. In further examples, an electrical device is powered or charging an electrical storage device is charged based on a transducer output.

The foregoing and other features and advantages will become more apparent from the following detailed description, which proceeds with reference to the accompanying figures.

BRIEF DESCRIPTION OF THE DRAWINGS

FIG. 1 is a plan view of a representative piezoelectric vibration energy harvester (PVEH) device.

FIG. 1A is a sectional view of the PVEH device of FIG. 1.

FIG. 2 is a plan view of another representative PVEH device.

FIG. 3 illustrates a PVEH-based energy harvesting and calibration system.

FIG. 3A illustrates a representative configuration of two IPMC devices for use in frequency tuning a PVEH device.

FIG. 3B illustrates a representative rectifier circuit.

FIG. 3C illustrates a representative IPMC.

FIG. 3D illustrates the IPMC of FIG. 3C with an applied voltage.

FIGS. 4A-4C are plan views of a representative PVEH devices with dimensions.

FIG. 5 illustrates resonance frequency of PVEH devices as a function of drive voltage to one or more IPMC devices.

FIG. 6 illustrates a representative PVEH-based method.

DETAILED DESCRIPTION

Introduction

The disclosure pertains to piezoelectric vibration energy harvesters (PVEHs) and associated methods and devices. In typical examples, the disclosed devices are responsive at low frequencies such as less than 1 kHz, 500 Hz, 250 Hz, 100 Hz, 50 Hz, 25 Hz, 10 Hz, 5 Hz, 2.5 Hz, 1 Hz, or lower. The devices can be frequency tuned using power harvested by the devices. In examples, a representative PVEH integrates two smart materials, a piezoelectric material (such as a Macro Fiber Composite (MFC)) situated to harvest energy and an Ionic Polymer Metal Composite (IPMC) situated to provide device tuning over a wide frequency range.

MFCs consist of a piezoelectric sheet formed of piezoelectric fibers of square cross section which are bonded together. This piezoelectric sheet is placed between layers of adhesive, electrodes and a polyimide film. The electrodes are typically made in an interdigitated pattern to enable better contact with the fibers and in-plane poling/actuation. This pattern also helps in achieving low voltage drop at the interface. MFCs can be environmentally sealed and hence be non-porous. MFCs have advantages over other piezoelectric elements. MFCs are flexible and are thus suitable for PVEHs having high deflections. MFCs can be bonded to surfaces effectively and can provide energy conversion at their resonant frequencies when used in cantilever mode. However, output power drops at other vibration frequencies. In he disclosed examples, active tuning can be provided using IPMCs, which can be compact, have low mass, and required little power. IPMCs consist of a per fluorinated ion exchange membrane such as a Nafion membrane situated between two electrodes, typically metals or other conductors coated with a noble metal, gold or platinum. When subjected to low voltages (typically 1 to 4 V), positively charged hydrated cations in the Nafion membrane network are repelled by the anode and hence move to the negative electrode. The water molecules that are tagged to cations also move within the membrane. The resulting osmotic pressure gradient causes bending of IPMC strips with the direction of bending dependent on the polarity of the applied voltage. In addition to bending an IPMC, an applied voltage also increases IPMC stiffness. Both bending and stiffness changes in response to an applied voltage can be used vary a load supplied by an IPMC,

In the examples, specific configurations of cantilevers are used for purposes of illustration but other cantilever configurations can be used. Cantilevers can have one fixed end and one free end only, or other combinations such as cantilevers in multiple directions, or cantilevers supported within the cantilever span, etc.

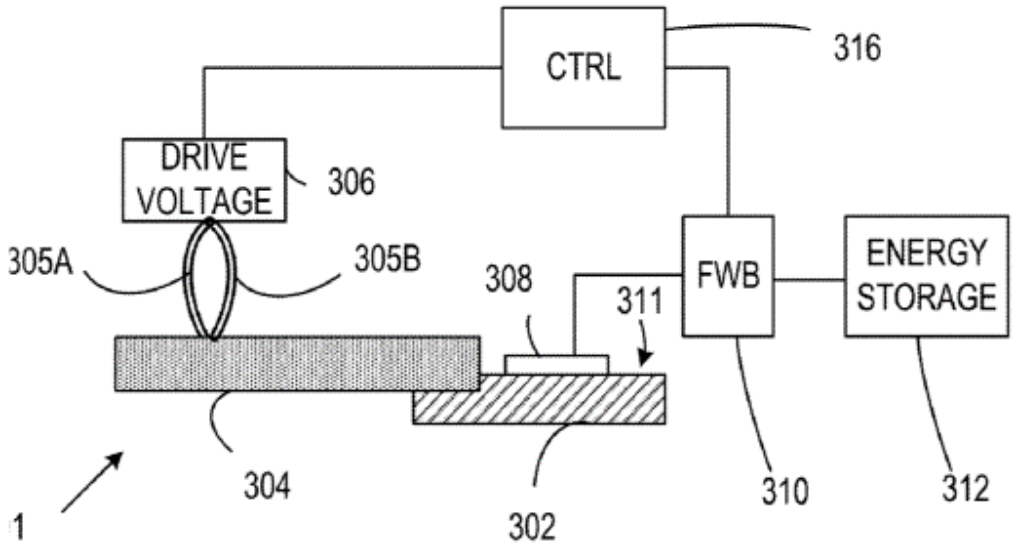

Example 1

Referring to FIGS. 1-1A, a PVEH device **100** includes a cantilever base **102** to which a cantilever **104** is secured. The cantilever **104** extends from the cantilever **102** and is generally thinner than the cantilever **104**. An MFC **106** or other flexible piezoelectric transducer is secured to the cantilever **104**. A location **110** on the cantilever **104** is designated for frequency response tuning based on loading applied to the location **110**. For evaluation purposes, a location **112** is designed for the application of vibrational forces whose energy is to be harvested. In the sectional view of FIG. 1A, a tuning member **114** is coupled to a support member **116** and is situated to contact the cantilever **104** at the location **110** to tune a cantilever resonance frequency. In typical examples, the tuning member **114** includes one or more IPMCs that are coupled to electrical power source (a voltage source) such as an energy storage device to which the PVEH **100** delivers energy. In this way, harvested energy can be used for PVEH tuning.

In one example, the cantilever **102** is 1 mm thick aluminum and the cantilever **104** is 0.5 mm thick stainless steel. Complete dimensions of such a device are shown in FIG. 4B. As shown, the

MFC **106** is bonded to the thinner cantilever **104**. The thicker cantilever base **104** generates higher strain.

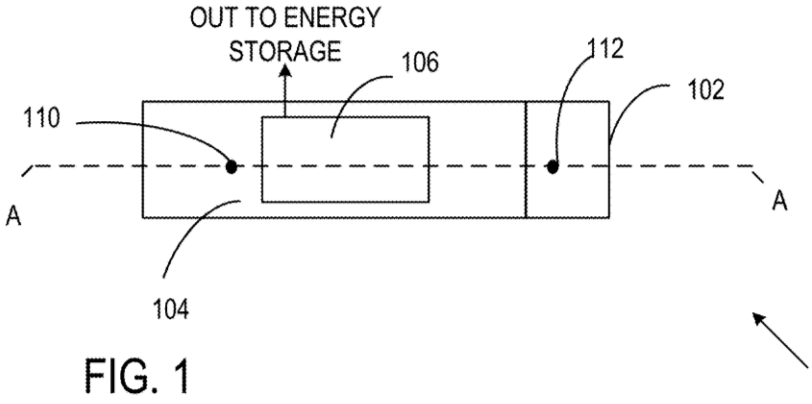

FIG. 1

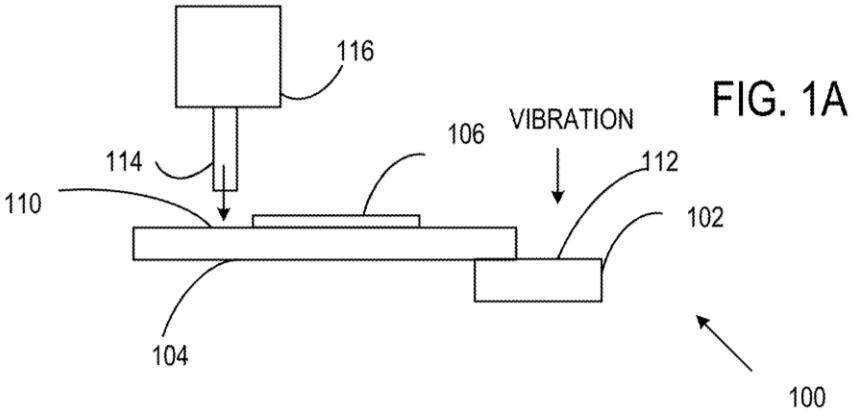

FIG. 1A

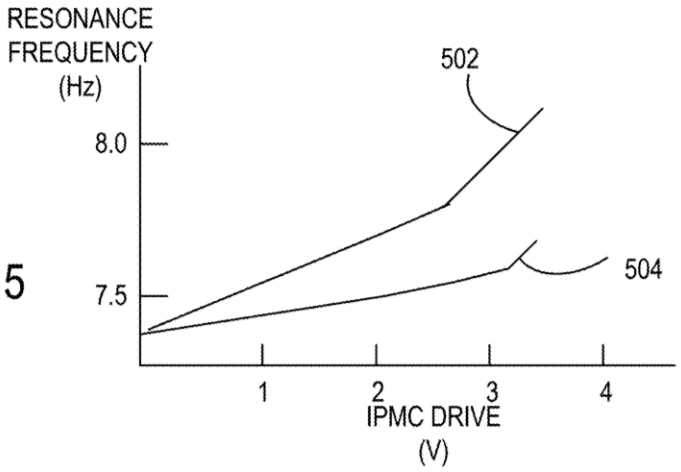

FIG. 5

FIG. 2

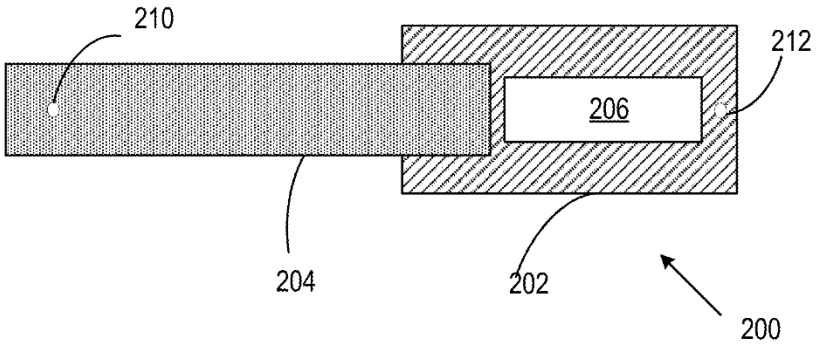
210
212
206
204
202
200

FIG. 3

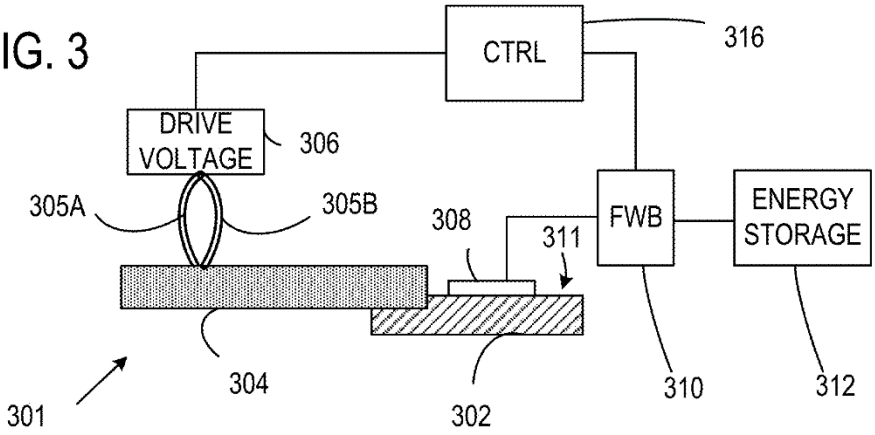
CTRL
316
DRIVE VOLTAGE
306
305A
305B
308
311
FWB
ENERGY STORAGE
304
301
302
310
312

FIG. 4A

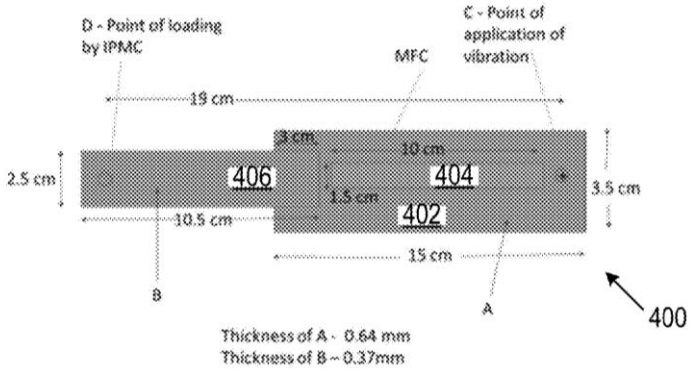

FIG. 4B

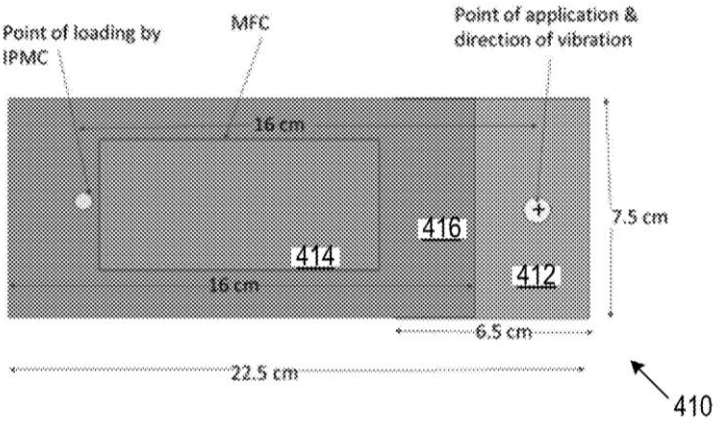

FIG. 4C

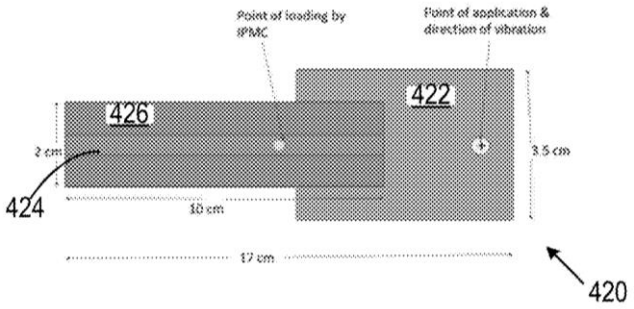

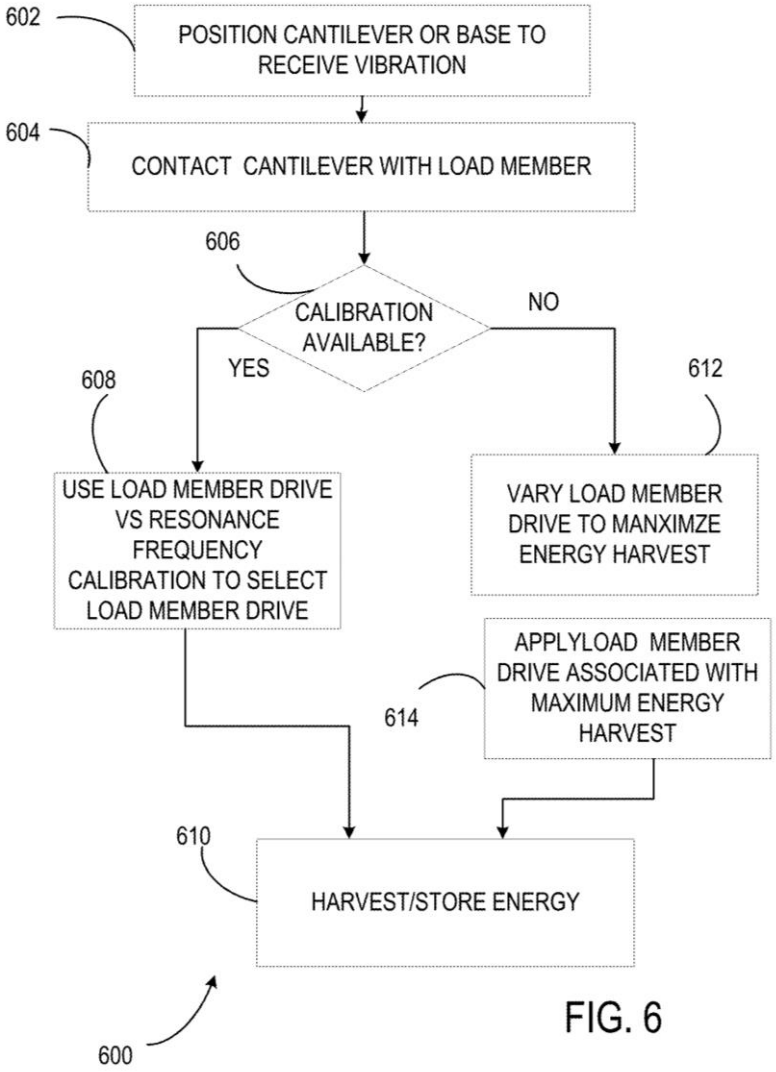

FIG. 6

Example 2

Referring to FIG. 2, a representative PVEH device **200** includes a cantilever base **202** to which a cantilever **202** is bonded. An MFH **206** or other piezoelectric device is secured to the cantilever base **202**. Preferred locations **210**, **212** for loading for tuning and application of vibrations, respectively, are indicated, but other locations can be used. Dimensions of such a PVEH device are shown in FIG. 4A.

Example 3

Referring to FIG. 3, an energy harvesting system **300** includes a PVEH device **301** having a cantilever base **302** to which a cantilever **304** is secured. In this example, an MFH **308** is secured

to the cantilever base **302** but in other examples, an MFH is secured to a cantilever instead of or in addition to a cantilever base. A tuning member **305** includes one or more IPMC devices such as IPMC devices **305**A, **305**B that are secured to each other at their ends. The tuning member **305** is coupled to a support **306** and is situated to contact the cantilever **304**. Loading of the cantilever **304** can be varied based on a voltage or other electrical signal applied to the IPMC devices **305**A, **305**B and supplied by a control circuit **316**. The MFH **308** is coupled to a full wave bridge (FWB) circuit **310** and rectified output from the MFH **308** is delivered to energy storage **312** such as a battery or capacitor. During setup or calibration, the control circuit **316** can be externally powered to vary loading provided by the IPMC devices **305**A, **305**B to the cantilever **304** while vibration is applied to the cantilever **302** at, for example, location **311**. During energy harvesting the tuning load can be selected based on a voltage or other drive supplied by the FWB circuit **310** or the energy storage **312**. In this case, the control circuit **316** can be a passive circuit. [resistive divider w voltage regulation). Typically, one or more rectifiers (such as the FWB circuit) are used to provide single polarity output for charging a capacitor or a battery, but energy storage can be based on bipolar output. A FWB is particularly useful for efficiency, but other arrangements of one or more rectifiers can be used.

FIG. 3A illustrates a representative tunable load member **305** that includes IPMCs **352**, **354** that are coupled at a tip **356**. A support member **360** secures ends **358**, **359** of the IPMCs **352**, **354**, respectively, for application of a drive voltage that causes the IMPCs **352**, **354** to bend so as to extend or contract.

FIG. 3B illustrates a circuit **370** that includes a full wave bridge (FWB) rectifier formed of diodes such as diode **372**. The FWB is coupled to charge a capacitor **374** and to receive inputs voltages from a piezoelectric device **376**.

FIG. 3C-3D illustrate a representative IPMC strip **380** having noble metal conductor layers **381**, **382** that sandwich an ionic polymer membrane **384**. If desired, additional electrical contacts can be formed on the conductor layer **381**, **382** for electrical connection to a voltage source that provides a voltage V_{DRIVE} that causes the IPMC strip **380** to deform as shown in FIG. 3D.

Example 4

FIGS. 4A-4B illustrate representative examples of PVEH devices and shown typical dimensions. In FIG. 4A, a PVEH device **400** includes a cantilever base **402** to which a cantilever **406** is

secured. An MFH **404** is bonded to the cantilever base **402**. In FIG. 4B, a PVEH device **410** includes a cantilever base **412** to which a cantilever **416** is secured. An MFH **414** is bonded to the cantilever **412**. In FIG. 4C, a PVEH device **420** includes a cantilever base **422** to which a cantilever **426** is secured. An MFH **424** is bonded to the cantilever **422**. In FIGS. 4A-4C, preferred locations for loading for tuning and application of vibration are also shown.

Example 5

FIG. 5 illustrates PVEH resonance frequency tuning by application of a voltage to IPMC devices that are situated to contact a PVEH cantilever. Curves **502**, **504** illustrate tuning of two different device configurations and show that increased loading (i.e., larger voltages in this example) can increase resonance frequency. Such calibration curves can be used to select an operating load for a PVEH device and a control circuit can be configured to provide a suitable voltage using harvested energy if external energy sources are to be avoided. An external source can be used for tuning during harvesting. However, energy usage for tuning is preferably less than (or very much less than) energy harvested.

Example 6

With reference to FIG. 6, a representative method **600** includes positioning a cantilever or cantilever base to receive vibrations such as ambient vibrations at **602**. At **604**, the cantilever is contacted with a tunable load member. At **606**, it is determined if load calibration is available. If so, at **606**, calibration data of resonance frequency versus load member drive is used to select a load member drive, and at **610**, the PVEH device is situated for harvesting energy. If calibration is unavailable at **606**, load member drive is varied at **602** to determined preference values for energy harvesting. At **614**, the load member drive associated with maximum or other preferred values of energy harvesting is applied and at **610**, energy is harvested.

General Considerations

As used in this application and in the claims, the singular forms “a,” “an,” and “the” include the plural forms unless the context clearly dictates otherwise. Additionally, the term “includes” means “comprises.” Further, the term “coupled” does not exclude the presence of intermediate elements between the coupled items. The systems, apparatus, and methods described herein should not be construed as limiting in any way. Instead, the present disclosure is directed toward all novel and non-obvious features and aspects of the various disclosed embodiments, alone and in various combinations and sub-combinations with one another. The disclosed systems, methods, and

apparatus are not limited to any specific aspect or feature or combinations thereof, nor do the disclosed systems, methods, and apparatus require that any one or more specific advantages be present or problems be solved. Any theories of operation are to facilitate explanation, but the disclosed systems, are not limited not limited to such theories of operation.

The examples above are described with reference to particular piezoelectric devices, cantilever materials, circuit configurations, and material dimensions for convenience but the disclosure is not to be limited to the explanatory configurations. Loading of cantilevers is illustrated using IPMCs but other actuators can be used. The terms "major surface" and "minor surface" refer to surfaces having larges and smaller surface areas, respectively, and are intended to distinguish the edge surfaces of substrates from larger surfaces. Tuning members can include IPMCs or other devices, and actuator mechanisms such as IPMCs can contact cantilever elements directly or use additional components for contact.

In view of the many possible embodiments to which the principles of the disclosure may be applied, it should be recognized that the illustrated embodiments are only preferred example and should not be taken as limiting. We therefore claim as our invention all that comes within the scope and spirit of these claims.

Claims

1. A device, comprising:

a cantilever;

a piezoelectric transducer coupled to the cantilever to produce an electrical output signal in response to a vibration of the cantilever; and

an actuator situated to variably contact the cantilever to establish a resonant frequency of the cantilever.

2. The device of claim 1, wherein the actuator is an Ionic Polymer Metal Composite (IPMC).

3. The device of claim 1, wherein the actuator is coupled to the cantilever to establish the resonant frequency based on a stiffness of the cantilever.

4. The device of claim 1, further comprising an actuator driver coupled to the actuator to apply an electrical signal to the actuator to establish the resonant frequency of the cantilever.

5. The device of claim 1, wherein the cantilever is a cantilever beam or a cantilever plate.

6. The device of claim 1, wherein the cantilever is stainless steel or aluminum.

7. The device of claim 1, further comprising a sensor circuit coupled to the piezoelectric transducer to determine an electrical signal to be applied by an actuator driver to provide a predetermined output power from the piezoelectric transducer.

8. The device of claim 7, wherein the sensor circuit is coupled to determine an available vibrational frequency.

9. The device of claim 8, wherein the actuator driver is configured to adjust at least one of a cantilever stiffness or cantilever resonant frequency based on the available vibrational frequency.

10. The device of claim 4, wherein the actuator driver is coupled to vary a cantilever resonance frequency or stiffness or both and select a resonance frequency or stiffness or both associated with a preferred output of the piezoelectric transducer.

11. The device of claim 1, wherein the cantilever comprises a first cantilever section and a second cantilever section.

12. The device of claim 11, where the first cantilever section is a base section and the second cantilever section is an extension section.

13. The device of claim 12, wherein the base section is thicker than the extension section, and the base section and the extension section are secured at respective major surfaces.

14. The device of claim 12, wherein the base section is thicker than the extension section, and the base section and the extension section are secured at respective minor surfaces.

15. The device of claim 12, wherein the actuator contacts the base section or the extension section.

16. The device of claim 12, wherein the base section has a thickness of 0.64 mm and the extension section has a thickness of 0.37 mm, and then base section and the extension section are bonded to each other with an adhesive layer or welding at respective major surfaces.

17. The device of claim 1, wherein the piezoelectric transducer is a macro fiber composite (MFC) transducer.

18. The device of claim 17, wherein the MFC transducer is bonded to a major surface of the cantilever over substantially an entire length and width of the major surface.

19. The device of claim 1, wherein the actuator is situated to variably contact the cantilever in a central 80% of a cantilever length or area.

20. The device of claim 1, further comprising:

a memory storing a plurality of actuator drive values and associated cantilever resonance frequencies or stiffnesses; and

a digital to analogy convertor coupled to the memory to apply a selected drive value to the actuator.

21. The device of claim 1, wherein the actuator has a diamond shape and includes first and second actuators that are stacked.

22. The device of claim 1, wherein the actuator contacts the cantilever a distance of 16 cm from a point of application of a vibration.

23. The device of claim 1, wherein the actuator is a single layer ionic polymer metal fiber composite.

24. The device of claim 1, wherein the cantilever has one fixed end, one free, end, two fixed ends, two free ends, extends in two or more directions, or is supported within a cantilever span.

25. A method, comprising:

subjecting a cantilever to vibrations;

contacting the cantilever at one or more locations or with one or more contact forces using an actuator;

identifying a resonant frequency of the cantilever based on the vibrations for each of the one or more locations and/or each of the one or more contact forces; and

storing an actuator drive value associated with the resonant frequency for each of the one or more locations and/or each of the one or more contact forces.

26. The method of claim 25, wherein the vibrations are applied as a series of single frequency vibrations.

27. The method of claim 25, wherein the resonant frequency for each of the one or more locations and/or each of the one or more contact forces is determined based on an output of a piezoelectric transducer coupled to the cantilever.

28. A method, comprising:

subjecting a cantilever to vibrations;

contacting the cantilever at one or more locations using an actuator; and

based on coupling of the vibrations by the cantilever to a piezoelectric transducer, determining an actuator drive for one or more vibrational frequencies and associated with a selected piezoelectric transducer output power.

29. A method, comprising:

contacting a cantilever using a actuator; and

adjusting the contact based on an output power from a transducer coupled to receive mechanical vibrations from the cantilever.

30. The method of claim 29, further comprising powering an electrical device or charging an electrical storage device based on a transducer output.

Patent History

Publication number: 20210159816

Type: Application

Filed: Nov 23, 2020

Publication Date: May 27, 2021

Inventors: Rishi Gupta (Victoria), Sreekumari Raghavan (Victoria)

Application Number: 17/102,285

Classifications

International Classification: H02N 2/18 (20060101); H01L 41/04 (20060101); H01L 41/08 (20060101); H01L 41/113 (20060101); H01L 41/18 (20060101);

Chapter 8

Conclusions and Scope for Future Research

The aim of this research was to arrive at a novel method to tune the resonant frequency of a cantilever -type PVEH, using an active element. This was done in four phases. The first phase was to identify the low power smart actuator and to identify the key characteristics required for this application. The second phase was to modify and design the PVEH, such that the actuator could generate the desired impact on the cantilever beam. The third phase was to integrate the actuator with the PVEH and prove the functionality of the device to alter the resonant frequency of the device. The fourth phase was to conduct a comprehensive range of functional tests on the device and to estimate the net power gain at various conditions by experiments. The results were found to be consistent when repeated. In the fifth phase, the results were analyzed and found to be in conformance with theoretical analysis. Further, the novel device was used in powering a triaxial MEMS accelerometer, a strain gauge bridge, and a Bluetooth sensor and transmitter device.

8.1 Key findings

- IPMC can be used as a stopper in a cantilever-type PVEH configuration.
- Different configurations of IPMC can be used to achieve the desired stopper effect.
- The shift in the resonant frequency is a function of the blocking force developed in the IPMC actuator. The blocking force of IPMC is a function of the input voltage to IPMC, the cation concentration in IPMC, and the hydration level of the membrane. Within the selected range of blocking force, the value can be tuned by changing the low voltage input to IPMC.
- Since IPMC actuation can be controlled by changing its input voltage, it acts as a tunable stopper.
- IPMC provides a desired low-power actuation for the device, which is crucial in the harvester application.
- A net positive power gain was achieved, sufficient to power the IPMC and an external device connected to the system.
- The range of impact force depends on the blocking force of the IPMC.
- PVEH integrated with IPMC is amenable to MEMS fabrication. In MEMS design, various other configurations can also be realized, that will enable better performance.
- IPMC as a stopper leads to a broadening of the frequency response of the harvester.

8.2 Recommendations for Future Research

8.2.1 Limitations of the research presented here and scope for Future Research

- The IPMC used in the study was Nafion-based, since other types of IPMC were not available. Experiments can be done with other IPMCs when they are available.
- The IPMC used in the investigation has water as the solvent. It may be noted that the literature indicates that water-based IPMC has been proven to be working at very low temperatures also [193]. However, it has the drawback of getting dehydrated during extended operation. Experiments can be done with IPMC having solvents other than water, when available.
- Further experimental studies can be done to establish the robustness of the system.

8.2.2 Feasibility of MEMS design of the novel PVEH

The novel design is amenable to MEMS fabrication since cantilever configuration and IPMC can be miniaturized using MEMS technology. Fig. 1 depicts a typical MEMS scheme.

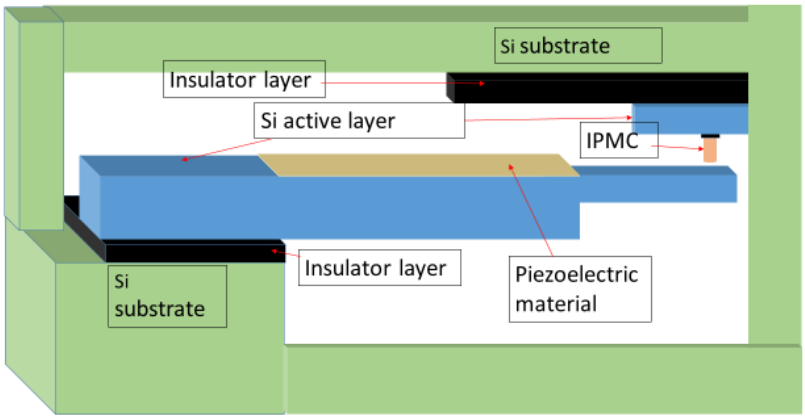

Fig. 8.1 A typical MEMS scheme of the novel PVEH

The Silicon On Insulator (SOI) process can be adopted here, considering the various advantages [20]. Most importantly, in SOI-based MEMS process, it is possible to combine bulk and micromachining methods as required. The insulating layer is typically Silicon oxide and the top active Silicon layer will be crystalline Silicon. In Fig. 8, the active layer is the cantilever beam with the required step configuration on which the piezoelectric material is deposited. The substrate Silicon layer will be of the order of a few hundreds of microns. The insulating layer will be of

thickness of one micron or less and the device layer (active layer) of tens of microns. The interdigitated electrode pattern that will be used in the device will enable maximum power transfer. The PVEH can be integrated with IPMC which functions as a stopper. The literature indicates that IPMC is highly suitable for MEMS scale fabrication [21-24]. The above-mentioned Si based process works well for IPMC also. It can be formed in a microscale and with different orientation of actuation. IPMC MEMS can be integrated with other electronics easily, which will be useful in this present device scheme. Distributed microactuators can also be fabricated using IPMC.

8.2.3 Other configurations that can be explored for MEMS device

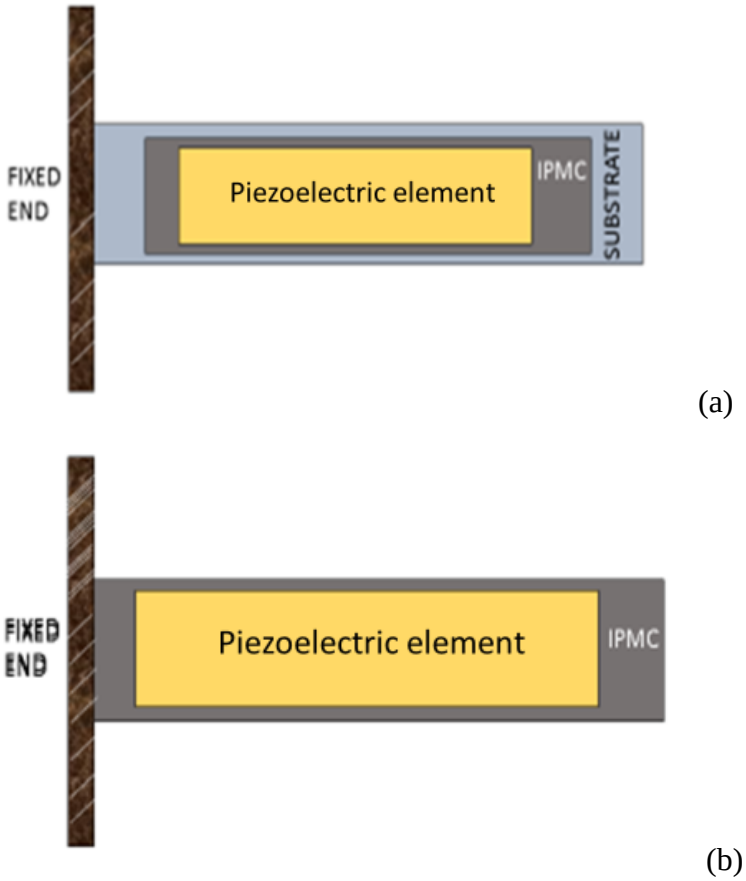

Fig. 8.2(a) and (b) Other configurations of MEMS device as perceived

This dissertation demonstrated how the IPMC actuator can be used as a stopper for the cantilever beam and how that configuration can shift the resonant frequency of the PVEH. Fig. 8.2 depicts two other new configurations of the PVEH, which can be explored. Fig. 8.2 (a) shows the

configuration in which, the piezoelectric element is bonded on an IPMC strip and that unit is bonded on a substrate material. Here, when the IPMC is given a power input, it bends, which will result in bending the whole cantilever beam or PVEH. This leads to a change in the resonant frequency of the cantilever beam. Fig. 8.2 (b) shows another configuration in which the IPMC strip itself functions as the substrate for the piezoelectric element. Here the actuation of the IPMC substrate introduces a change in the resonant frequency of PVEH. These two configurations can be realized in MEMS design.

In the MEMS configuration, other electronics such as low-power accelerometers and microcontrollers can be integrated. This will enable continuous monitoring of the ambient vibration frequency and powering the IPMC with the appropriate input values. For efficient extraction of the power generated by the harvester, low power electronic circuits are available which can be integrated in the MEMS configuration, the details of which are available in the literature [194, 195,196].

8.2.4 Development of IPMC having higher blocking force

IPMC can be tailored to various characteristics during its fabrication by changing its anion/cation concentration and by maintaining the hydration level. The properties can also be changed by changing the thickness of Nafion film, during fabrication. This makes it highly suitable for applications where variable loading is required. stack actuator can be designed with more number of elements. The integration of IPMC into a MEMS harvester is easy to achieve, due to its tailorable characteristics. An additional advantage is that it can be designed with multiple electrodes to enable the desired loading.

Researchers have worked on porous Nafion membranes by applying a silica sol-gel process and an etching process using hydrofluoric acid [50]. An IPMC was fabricated using this porous Nafion. The IPMC thus prepared, with the smallest pore size exhibited higher electrical conductivity and higher blocking force by around 1.4 times of the conventional Nafion-based IPMC on application of direct power input. Another current field of research reported by other researchers is in the fabrication of Casted IPMC [69]. To realize the desired high thickness of Nafion film, a casting method with Nafion dispersion is being applied. The IPMC was fabricated using the casted Nafion, which was 420 μm thick. The input voltage given to actuate the IPMC was 0 to 4.5 V DC. The performance was compared with the IPMC fabricated from the

commercially available Nafion. It was found that the blocking force was higher for the casted Nafion-based IPMC. Another interesting research is in using a corrosive material as the electrodes of IPMC, to improve its displacement and the blocking force [51]. Normally a noble metal is used as the electrodes to achieve perfect electrical conductivity, avoiding corrosion. However, it was observed that when a corrosive metal, silver, is used as electrodes, the electrodes bring out a reversible redox reaction when it is subjected to external voltage. This reaction changed the material characteristics of IPMC, generating higher displacement and blocking force. It is also reported in the literature that nano-thorn electrodes instead of flat ones can improve the blocking force by 3 to 5 times more for low voltage in the range of 1 to 3 V [70]. Hence it is highly feasible to realize a tunable PVEH of even better performance using these IPMCs of higher blocking force that are newly getting developed. There are also reports of research on various actuation control methods that lead to still lower power consumption of the IPMC [52, 49].

Bibliography

[1] Dewan, A., Ay, S. U., Karim, M. N., & Beyenal, H. (2014). Alternative power sources for remote sensors: A review. *Journal of power sources*, *245*, 129-143.

[2] Khaligh, A., & Onar, O. C. (2017). *Energy harvesting: solar, wind, and ocean energy conversion systems*. CRC press.

[3] Nishimoto, H., Kawahara, Y., & Asami, T. (2010, November). Prototype implementation of ambient RF energy harvesting wireless sensor networks. In *SENSORS, 2010 IEEE* (pp. 1282-1287). IEEE.

[4] https://www.intechopen.com/chapters/65239

[5] Basset, P., Galayko, D., Cottone, F., Guillemet, R., Blokhina, E., Marty, F., & Bourouina, T. (2014). Electrostatic vibration energy harvester with combined effect of electrical nonlinearities and mechanical impact. *Journal of Micromechanics and Microengineering*, *24*(3), 035001.

[6] Spreemann, D., & Manoli, Y. (2012). Electromagnetic vibration energy harvesting devices: Architectures, design, modeling and optimization (Vol. 35). Berlin/Heidelberg, Germany: Springer.

[7] Wang, L. and F. Yuan, *Vibration energy harvesting by magnetostrictive material.* Smart Materials and Structures, 2008. 17(4): p. 045009.

[8] Ikeda, T., *Fundamentals of piezoelectricity*. 1996: Oxford university press

[9] Li, L., Xu, J., Liu, J., & Gao, F. (2018). Recent progress on piezoelectric energy harvesting: structures and materials. *Advanced Composites and Hybrid Materials*, *1*(3), 478-505.

[10] Punning, A., Anton, M., Kruusmaa, M., & Aabloo, A. (2005). An engineering approach to reduced power consumption of IPMC (Ion-Polymer Metal Composite) actuators. *2005 International Conference on Advanced Robotics, ICAR '05, Proceedings*, *2005*(August), 856–863. https://doi.org/10.1109/ICAR.2005.1507507

[11] Yu, C. Y., Zhang, Y. W., & Su, G. D. J. (2015). Reliability tests of ionic polymer metallic composites in dry air for actuator applications. *Sensors and Actuators, A: Physical*, *232*, 183–189. https://doi.org/10.1016/j.sna.2015.06.002

[12] Wang, H. S., Cho, J., Song, D. S., Jang, J. H., Jho, J. Y., & Park, J. H. (2017). High-Performance Electroactive Polymer Actuators Based on Ultrathick Ionic Polymer-Metal

Composites with Nanodispersed Metal Electrodes. *ACS Applied Materials and Interfaces*, *9*(26), 21998–22005. https://doi.org/10.1021/acsami.7b04779

[13] Shahinpoor, M., Bar-Cohen, Y., Simpson, J. O., & Smith, J. (1998). Ionic polymer-metal composites (IPMCs) as biomimetic sensors, actuators and artificial muscles - A review. *Smart Materials and Structures*, *7*(6), 1–27. https://doi.org/10.1088/0964-1726/7/6/001

[14] Nemat-nasser, S., & Thomas, C. W. (n.d.). C HAPTER 6 Ionomeric Polymer-Metal Composites. *Electroactive Polymers Actuators As*, 171–230

[15] Paquette, J. W., Kim, K. J., Nam, J. D., & Tak, Y. S. (2003). An equivalent circuit model for ionic polymer-metal composites and their performance improvement by a clay-based polymer nano-composite technique. *Journal of Intelligent Material Systems and Structures*, *14*(10), 633-642.

[16] Shoji, E., & Hirayama, D. (2007). Effects of humidity on the performance of ionic polymer-metal composite actuators: Experimental study of the back-relaxation of actuators. *Journal of Physical Chemistry B*, *111*(41), 11915–11920. https://doi.org/10.1021/jp074611q

[17] Ansaf, B., Duong, T. H., Jaksic, N. I., Depalma, J. L., Al-Allaq, A. H., Deherrera, B. M., & Li, B. (2018). Influence of Humidity and Actuation time on Electromechanical Characteristics of Ionic Polymer-Metal Composite Actuators. *Procedia Manufacturing*, *17*(July), 960–967. https://doi.org/10.1016/j.promfg.2018.10.148

[18] Caponetto, R., Graziani, S., Pappalardo, F. L., & Sapuppo, F. (2013). Experimental characterization of ionic polymer metal composite as a novel fractional order element. *Advances in Mathematical Physics*, *2013*. https://doi.org/10.1155/2013/953695

[19] Saccardo, M. C., Zuquello, A. G., Tozzi, K. A., Gonçalves, R., Hirano, L. A., & Scuracchio, C. H. (2020). Counter-ion and humidity effects on electromechanical properties of Nafion®/Pt composites. *Materials Chemistry and Physics*, *244*(November 2019), 122674. https://doi.org/10.1016/j.matchemphys.2020.122674

[20] Zamani, S., & Nemat-Nasser, S. (2005). Experimental study of Nafion-based ionic polymer-metal composites (IPMCs) with glycerol as solvent. *Smart Structures and Materials 2005: Electroactive Polymer Actuators and Devices (EAPAD)*, *5759*(January), 165. https://doi.org/10.1117/12.599956

[21] Sasaki, M., Lin, W., Tamagawa, H., Ito, S., & Kikuchi, K. (2013). Self-sensing control of Nafion-based Ionic Polymer-Metal Composite (IPMC) actuator in the extremely low humidity environment. *Actuators*, *2*(4), 74–85. https://doi.org/10.3390/act2040074

[22] Chen, Z., Tan, X., & Shahinpoor, M. (2005). Quasi-static positioning of ionic Polymer-metal composite (IPMC) actuators. *IEEE/ASME International Conference on Advanced Intelligent Mechatronics, AIM*, *1*(November), 60–65. https://doi.org/10.1109/aim.2005.1500966

[23] Branco, P. J. C. (2007). *Evaluation of dielectric gel coating for encapsulation of ionic polymer metal composite (IPMC) actuators*. *140*, 232–238. https://doi.org/10.1016/j.sna.2007.06.035

[24] Aw, K., Fu, L., & McDaid, A. (2013). An IPMC actuated robotic surgery end effector with force sensing. *International Journal of Smart and Nano Materials*, *4*(4), 246–256. https://doi.org/10.1080/19475411.2013.862579

[25] Olsen, Z. J., Kim, K. J., & Oh, I. K. (2021). Developing next generation ionic polymer–metal composite materials: perspectives for enabling robotics and biomimetics. *Polymer International*, *70*(1), 7–9. https://doi.org/10.1002/pi.6128

[26] Tiwari, R., & Kim, K. J. (2013). IPMC as a mechanoelectric energy harvester: Tailored properties. *Smart Materials and Structures*, *22*(1). https://doi.org/10.1088/0964-1726/22/1/015017

[27] Pugal, D. (2017). *Physics Based Model of Ionic Polymer-Metal Composite Electromechanical and Mechanoelectrical Transduction*. (August 2012). https://doi.org/10.13140/RG.2.2.18421.58089

[28] Bennett, M. D., & Leo, D. J. (2004). Ionic liquids as stable solvents for ionic polymer transducers. *Sensors and Actuators, A: Physical*, *115*(1), 79–90. https://doi.org/10.1016/j.sna.2004.03.043

[29] Aabloo, A., & Belikov, J. (2020). *Challenges and Perspectives in Control of Ionic Polymer-Metal Composite (IPMC) Actuators : A Survey*. *8*. https://doi.org/10.1109/ACCESS.2020.3007020

[30] Jung, K., Nam, J., & Choi, H. (2003). Investigations on actuation characteristics of IPMC artificial muscle actuator. *Sensors and Actuators, A: Physical*, *107*(2), 183–192. https://doi.org/10.1016/S0924-4247(03)00346-7

[31] Kim, B., Kim, B. M., Ryu, J., Oh, I.-H., Lee, S.-K., Cha, S.-E., & Pak, J. (2003). Analysis of mechanical characteristics of the ionic polymer metal composite (IPMC) actuator using cast

ion-exchange film. *Smart Structures and Materials 2003: Electroactive Polymer Actuators and Devices (EAPAD), 5051*(May 2014), 486. https://doi.org/10.1117/12.484296

[32] Tamagawa, H., Okada, K., Mulembo, T., Sasaki, M., Naito, K., Nagai, G., … Ikeda, K. (2019). Simultaneous enhancement of bending and blocking force of an ionic polymer-metal composite (IPMC) by the active use of its material characteristics change. *Actuators*, *8*(1). https://doi.org/10.3390/act8010029

[33] Ma, S., Zhang, Y., Liang, Y., Ren, L., Tian, W., & Ren, L. (2020). *High-Performance Ionic-Polymer – Metal Composite : Toward Large-Deformation Fast-Response Artificial Muscles*. *1908508*, 1–9. https://doi.org/10.1002/adfm.201908508

[34] Tabatabaie, S. E. (2019). *Novel Configurations of Ionic Polymer-Metal Composites (IPMCs) As Sensors, Actuators, and Energy Harvesters*. The University of Maine.

[35] https://application.wiley-vch.de/books/sample/3527345124_c01.pdf

[36] Siang, J.; Lim, M. h.; Salman Leong, M. Review of Vibration-Based Energy Harvesting Technology: Mechanism and Architectural Approach. *Int. J. Energy Res.* 2018, *42*, 1866–1893, doi:10.1002/er.3986.

[37] Elvin, N.; Erturk, A. *Advances in Energy Harvesting Methods*; Springer Science & Business Media, 2013; ISBN 978-1-4614-5705-3.

[38] Roundy, S.; Zhang, Y. Toward Self-Tuning Adaptive Vibration-Based Microgenerators. In Proceedings of the Smart Structures, Devices, and Systems II; SPIE, February 28 2005; Vol. 5649, pp. 373–384.

[39] Beeby, S.P.; Tudor, M.J.; White, N.M. Energy Harvesting Vibration Sources for Microsystems Applications. *Meas. Sci. Technol.* 2006, *17*, R175–R195, doi:10.1088/0957-0233/17/12/R01.

[40] Priya, S., & Inman, D. J. (Eds.). (2009). *Energy harvesting technologies* (Vol. 21, p. 2). New York: Springer.

[41] Phillips, M. R., & Carman, G. P. (2020). Numerical analysis of an active thermomagnetic device for thermal energy harvesting. *Journal of Energy Resources Technology*, *142*(8), 082102.

[42] Wang, L.; Zhao, L.; Luo, G.; Zhao, Y.; Yang, P.; Jiang, Z.; Maeda, R. System Level Design of Wireless Sensor Node Powered by Piezoelectric Vibration Energy Harvesting. *Sens. Actuators Phys.* 2020, *310*, 112039.

[43] Kundu, S.; Nemade, H.B. Piezoelectric Vibration Energy Harvester with Tapered Substrate

Thickness for Uniform Stress. *Microsyst. Technol.* 2021, *27*, 105–113.

[44] Yoon, H.; Kim, M.; Park, C.-S.; Youn, B.D. Time-Varying Output Performances of Piezoelectric Vibration Energy Harvesting under Nonstationary Random Vibrations. *Smart Mater. Struct.* 2017, *27*, 015004.

[45] Chen, R.; Ren, L.; Xia, H.; Yuan, X.; Liu, X. Energy Harvesting Performance of a Dandelion-like Multi-Directional Piezoelectric Vibration Energy Harvester. *Sens. Actuators Phys.* 2015, *230*, 1–8.

[46] Vibration Energy Harvesting of Multifunctional Carbon Fiber Composite Laminate Structures - ScienceDirect Available online: https://www.sciencedirect.com/science/article/pii/S0266353819302751?casa_token=EwXeXdWtsQ4AAAAA:t6sDGVGH4wp1wlpUU0zVSd9xUKfi35S114RAsac0oCJajZNIE3uQ-tAzSSxTnKCsjMz0Hjk2UCg (accessed on 16 November 2021).

[47] Semi-Flexible Bimetal-Based Thermal Energy Harvesters - IOPscience Available online: https://iopscience.iop.org/article/10.1088/0964-1726/22/2/025021/meta (accessed on 19 November 2021).

[48] A Review of Commercial Energy Harvesters for Autonomous Sensors | IEEE Conference Publication | IEEE Xplore Available online: https://ieeexplore.ieee.org/abstract/document/4258183 (accessed on 19 November 2021).

[49] Wang, J.; Geng, L.; Ding, L.; Zhu, H.; Yurchenko, D. The State-of-the-Art Review on Energy Harvesting from Flow-Induced Vibrations. *Appl. Energy* 2020, *267*, 114902, doi:10.1016/j.apenergy.2020.114902.

[50] Wei, C.; Jing, X. A Comprehensive Review on Vibration Energy Harvesting: Modelling and Realization. *Renew. Sustain. Energy Rev.* 2017, *74*, 1–18, doi:10.1016/j.rser.2017.01.073.

[51] Mohanty, A.; Parida, S.; Behera, R.K.; Roy, T. Vibration Energy Harvesting: A Review. *J. Adv. Dielectr.* 2019, *09*, 1930001, doi: 10.1142/S2010135X19300019.

[52] Tran, N.; Ghayesh, M.H.; Arjomandi, M. Ambient Vibration Energy Harvesters: A Review on Nonlinear Techniques for Performance Enhancement. *Int. J. Eng. Sci.* 2018, *127*, 162–185, doi:10.1016/j.ijengsci.2018.02.003.

[53] Maamer, B.; Boughamoura, A.; Fath El-Bab, A.M.R.; Francis, L.A.; Tounsi, F. A Review on Design Improvements and Techniques for Mechanical Energy Harvesting Using Piezoelectric and Electromagnetic Schemes. *Energy Convers. Manag.* 2019, *199*, 111973,

doi:10.1016/j.enconman.2019.111973.

[54] Modern Piezoelectric Energy-Harvesting Materials | SpringerLink Available online: https://link.springer.com/book/10.1007/978-3-319-29143-7 (accessed on 16 November 2021).

[55] Mechanical Design of Piezoelectric Energy Harvesters - 1st Edition Available online: https://www.elsevier.com/books/mechanical-design-of-piezoelectric-energy-harvesters/xu/978-0-12-823364-1 (accessed on 16 November 2021).

[56] Energy Harvesting Technologies | SpringerLink Available online: https://link.springer.com/book/10.1007/978-0-387-76464-1 (accessed on 16 November 2021).

[57] Batra, A.; Bohara, B.; Currie, J. Design, Fabrication, and Testing of Piezoelectric Energy Harvesters. *Des. Fabr. Test. Piezoelectric Energy Harvest.* 2018, *SL41*, 1–58, doi:10.1117/3.2504734.ch1.

[58] Crovetto, A.; Wang, F.; Hansen, O. Modeling and Optimization of an Electrostatic Energy Harvesting Device. *J. Microelectromechanical Syst.* 2014, *23*, 1141–1155, doi:10.1109/JMEMS.2014.2306963.

[59] Khaligh, A.; Zeng, P.; Zheng, C. Kinetic Energy Harvesting Using Piezoelectric and Electromagnetic Technologies—State of the Art. *IEEE Trans. Ind. Electron.* 2010, *57*, 850–860, doi:10.1109/TIE.2009.2024652.

[60] Narita, F.; Fox, M. A Review on Piezoelectric, Magnetostrictive, and Magnetoelectric Materials and Device Technologies for Energy Harvesting Applications. *Adv. Eng. Mater.* 2018, *20*, 1700743, doi:10.1002/adem.201700743.

[61] Farinholt, K. M., Pedrazas, N. A., Schluneker, D. M., Burt, D. W., & Farrar, C. R. (2009). An energy harvesting comparison of piezoelectric and ionically conductive polymers. *Journal of Intelligent Material Systems and Structures*, *20*(5), 633-642.

[62] Jamshidi, S., Dardel, M., Pashaei, M. H., & Alashti, R. A. (2015). Energy harvesting from limit cycle oscillation of a cantilever plate in low subsonic flow by ionic polymer metal composite. *Proceedings of the Institution of Mechanical Engineers, Part G: Journal of Aerospace Engineering*, *229*(5), 814-836.

[63] Martin, B. R. (2005). *Energy harvesting applications of ionic polymers* (Doctoral dissertation, Virginia Tech).

[64] Soh, C. K., Yang, Y., & Bhalla, S. (Eds.). (2012). *Smart materials in structural health monitoring, control and biomechanics*. Springer Science & Business Media.

[65] Song, M.; Zhang, Y.; Peng, M.; Zhai, J. Low Frequency Wideband Nano Generators for Energy Harvesting from Natural Environment. *Nano Energy* 2014, *6*, 66–72, doi:10.1016/j.nanoen.2014.02.009.

[66] Li, Z.; Saadatnia, Z.; Yang, Z.; Naguib, H. A Hybrid Piezoelectric-Triboelectric Generator for Low-Frequency and Broad-Bandwidth Energy Harvesting. *Energy Convers. Manag.* 2018, *174*, 188–197, doi:10.1016/j.enconman.2018.08.018.

[67] Microsystems for Energy Harvesting | IEEE Conference Publication | IEEE Xplore Available online: https://ieeexplore.ieee.org/abstract/document/5969888 (accessed on 19 November 2021).

[68] Dhote, S.; Zu, J.; Zhu, Y. A Nonlinear Multi-Mode Wideband Piezoelectric Vibration-Based Energy Harvester Using Compliant Orthoplanar Spring. *Appl. Phys. Lett.* **2015**, *106*, 163903.

[69] Leland, E.S.; Wright, P.K. Resonance Tuning of Piezoelectric Vibration Energy Scavenging Generators Using Compressive Axial Preload. *Smart Mater. Struct.* 2006, *15*, 1413–1420, doi:10.1088/0964-1726/15/5/030.

[70] Hu, Y.; Xue, H.; Hu, H. A Piezoelectric Power Harvester with Adjustable Frequency through Axial Preloads. *Smart Mater. Struct.* 2007, *16*, 1961–1966, doi:10.1088/0964-1726/16/5/054.

[71] Eichhorn, C.; Goldschmidtboeing, F.; Woias, P. A Frequency Tunable Piezoelectric Energy Converter Based on a Cantilever Beam. *Proc. PowerMEMS* 2008, *9*, 309–312.

[72] Cao, D.; Xia, W.; Hu, W. Low-Frequency and Broadband Vibration Energy Harvester Driven by Mechanical Impact Based on Layer-Separated Piezoelectric Beam. *Appl. Math. Mech.* 2019, *40*, 1777–1790, doi:10.1007/s10483-019-2542-5.

[73] Zhao, H.; Wei, X.; Zhong, Y.; Wang, P. A Direction Self-Tuning Two-Dimensional Piezoelectric Vibration Energy Harvester. *Sensors* 2020, *20*, 77.

[74] Debnath, B.; Kumar, R. Design and Simulation Study of a New Flared-U Shaped Springs Based MEMS Piezoelectric Vibration Energy Harvester. In Proceedings of the 2020 IEEE International Conference on Computing, Power and Communication Technologies (GUCON); October 2020; pp. 101–105.

[75] Dhote, S.; Yang, Z.; Behdinan, K.; Zu, J. Enhanced Broadband Multi-Mode Compliant Orthoplanar Spring Piezoelectric Vibration Energy Harvester Using Magnetic Force. *Int. J. Mech. Sci.* 2018, *135*, 63–71, doi:10.1016/j.ijmecsci.2017.11.012.

[76] Challa, V.R.; Prasad, M.G.; Shi, Y.; Fisher, F.T. A Vibration Energy Harvesting Device with

Bidirectional Resonance Frequency Tunability. *Smart Mater. Struct.* 2008, *17*, 015035, doi:10.1088/0964-1726/17/01/015035.

[77] Ferrari, M.; Ferrari, V.; Guizzetti, M.; Marioli, D.; Taroni, A. Piezoelectric Multifrequency Energy Converter for Power Harvesting in Autonomous Microsystems. *Sens. Actuators Phys.* 2008, *142*, 329–335, doi:10.1016/j.sna.2007.07.004.

[78] Shi, C.(石纯康); Li, F.(李帆); Zhao, J.(赵建辉) An Advanced Folded Piezoelectric Vibration Energy Harvester with Low Resonant Frequency and High Power Density. *AIP Adv.* 2020, *10*, 065231, doi:10.1063/5.0002844.

[79] Kaplan, J.L.; Bonello, P.; Alalwan, M. A Simulation of the Performance of a Self-Tuning Energy Harvesting Cantilever Beam. *J. Phys. Conf. Ser.* 2016, *744*, 012083, doi:10.1088/1742-6596/744/1/012083.

[80] A frequency adjustable vibration energy harvester Available online: https://studylib.net/doc/14392284/a-frequency-adjustable-vibration-energy-harvester (accessed on 17 November 2021).

[81] Jiang, W.; Wang, L.; Zhao, L.; Luo, G.; Yang, P.; Ning, S.; Lu, D.; Lin, Q. Modeling and Design of V-Shaped Piezoelectric Vibration Energy Harvester with Stopper for Low-Frequency Broadband and Shock Excitation. *Sens. Actuators Phys.* 2021, *317*, 112458.

[82] Heit, J.; Christensen, D.; Roundy, S. A Vibration Energy Harvesting Structure, Tunable Over a Wide Frequency Range Using Minimal Actuation.; American Society of Mechanical Engineers Digital Collection, February 20 2014.

[83] Raghavan, S., & Gupta, R. (2020). A novel design and performance results of an electrically tunable piezoelectric vibration energy harvester (TPVEH). *Journal of Composites Science*, *4*(2),

[84] Aabloo, A., Belikov, J., Kaparin, V., & Kotta, Ü. (2020). Challenges and perspectives in control of ionic polymer-metal composite (IPMC) actuators: a survey. *IEEE Access*, *8*, 121059-121073

[85] Jung, S. Y., Ko, S. Y., Park, J. O., & Park, S. (2017). Enhanced ionic polymer–metal composite actuator with pore size–controlled porous Nafion membrane using silica sol–gel process. *Journal of Intelligent Material Systems and Structures*, *28*(11), 1514-1523.

[86] US Patent application no. 2021015981

[87] Energies | Free Full-Text | Tuning Techniques for Piezoelectric and Electromagnetic Vibration

Energy Harvesters Available online: https://www.mdpi.com/1996-1073/13/3/527 (accessed on 8 November 2021).

[88] An Investigation into the Performance of Macro-Fiber Composites for Sensing and Structural Vibration Applications - ScienceDirect Available online: https://www.sciencedirect.com/science/article/pii/S0888327003000815 (accessed on 2 November 2021).

[89] Zhang, S.-Q.; Li, Y.-X.; Schmidt, R. Modeling and Simulation of Macro-Fiber Composite Layered Smart Structures. *Compos. Struct.* 2015, *126*, 89–100, doi:10.1016/j.compstruct.2015.02.051.

[90] Kovalovs, A.; Barkanov, E.; Gluhihs, S. Active Control of Structures Using Macro-Fiber Composite (MFC). *J. Phys.: Conf. Ser.* 2007, *93*, 012034, doi:10.1088/1742-6596/93/1/012034.

[91] Schönecker, A.J.; Daue, T.; Brückner, B.; Freytag, C.; Hähne, L.; Rödig, T. Overview on Macrofiber Composite Applications. In Proceedings of the Smart Structures and Materials 2006: Active Materials: Behavior and Mechanics; SPIE, April 6 2006; Vol. 6170, pp. 408–415.

[92] Borowiec, M.; Bocheński, M.; Gawryluk, J.; Augustyniak, M. Analysis of the Macro Fiber Composite Characteristics for Energy Harvesting Efficiency. In Proceedings of the Dynamical Systems: Theoretical and Experimental Analysis; Awrejcewicz, J., Ed.; Springer International Publishing: Cham, 2016; pp. 27–37.

[93] Smart Material Available online: https://smart-material.com/?gclid=Cj0KCQjww4OMBhCUARIsAILndv6qddtvHWTild6JcUJNOWWWBxrs-R1B0CuwR-QXyzAmzUo0AH5yIEIaAoeBEALw_wcB (accessed on 2 November 2021).

[94] Lagosh, A.V.; Broyko, A.P.; Kalyonov, V.E.; Khmelnitskiy, I.K.; Luchinin, V.V. Modeling of IPMC Actuator. In Proceedings of the 2017 IEEE Conference of Russian Young Researchers in Electrical and Electronic Engineering (EIConRus); IEEE, 2017; pp. 916–918.

[95] Bhandari, B.; Lee, G.-Y.; Ahn, S.-H. A Review on IPMC Material as Actuators and Sensors: Fabrications, Characteristics and Applications. *Int. J. Precis. Eng. Manuf.* 2012, *13*, 141–163.

[96] Brunetto, P.; Fortuna, L.; Giannone, P.; Graziani, S.; Pagano, F. A Small Scale Viscometer Based on an IPMC Actuator and an IPMC Sensor. In Proceedings of the 2010 IEEE Instrumentation & Measurement Technology Conference Proceedings; IEEE, 2010; pp. 585–

589.

[97] Chang, X.L.; Chee, P.S.; Lim, E.H.; Tan, R.C.C. A Novel Crenellated Ionic Polymer-Metal Composite (IPMC) Actuator with Enhanced Electromechanical Performances. *Smart Mater. Struct.* 2019, *28*, 115011.

[98] S. Nemat-Nasser and J. Li, "Electromechanical response of ionic polymer– metal composites," J. Appl. Phys., vol. 87, no. 7, pp. 3321–3331, 2000

[99] Li, H., Tian, C., & Deng, Z. D. (2014). Energy harvesting from low frequency applications using piezoelectric materials. *041301*, 1–20. https://doi.org/10.1063/1.4900845

[100] Yang, L., Zhang, D., Zhang, X., Tian, A., & Wang, X. (2020). Models of displacement and blocking force of ionic - polymer metal composites based on actuation mechanism. *Applied Physics A*, *126*(5), 1–7. https://doi.org/10.1007/s00339-020-03546-x

[101] Zhao, Y., Xu, D., Sheng, J., Meng, Q., Wu, D., Wang, L., ... & Sun, D. (2018). Biomimetic beetle-inspired flapping air vehicle actuated by ionic polymer-metal composite actuator. *Applied Bionics and Biomechanics*, *2018*.

[102] Palmre, V., Pugal, D., Kim, K. J., Leang, K. K., Asaka, K., & Aabloo, A. (2014). Nanothorn electrodes for ionic polymer-metal composite artificial muscles. *Scientific reports*, *4*(1), 1-10.

[103] Shahinpoor, M. (2001, April). Potential applications of electroactive polymer sensors and actuators in MEMS technologies. In *Smart materials* (Vol. 4234, pp. 203-214). International Society for Optics and Photonics.

[104] Aladwani, A., Aldraihem, O., & Baz, A. (2014). A distributed parameter cantilevered piezoelectric energy harvester with a dynamic magnifier. *Mechanics of Advanced Materials and Structures*, *21*(7), 566-578.

[105] Raju, S. S., Umapathy, M., & Uma, G. (2020). Design and analysis of high output piezoelectric energy harvester using non uniform beam. *Mechanics of Advanced Materials and Structures*, *27*(3), 218-227.

[106] Askari, M., Brusa, E., & Delprete, C. (2021). Design and modeling of a novel multi-beam piezoelectric smart structure for vibration energy harvesting. *Mechanics of Advanced Materials and Structures*, 1-23.

[107] Panda, S. K., & Srinivas, J. (2022). Electro-structural analysis and optimization studies of laminated composite beam energy harvester. *Mechanics of Advanced Materials and Structures*, *29*(25), 4193-4205.

[108] Meng, L., Li, A., & Wei, G. (2022). Electromechanical coupling analysis of three-dimensional braided piezoelectric composites energy harvester. *Mechanics of Advanced Materials and Structures*, *29*(27), 6585-6594.

[109] Chand, R. R., & Tyagi, A. (2022). Parabolic tapering piezoelectric rotational energy harvester: Numerical analysis with experimental validation. *Mechanics of Advanced Materials and Structures*, 1-10.

[110] Fan, T. (2020). Nano porous piezoelectric energy harvester by surface effect model. *Mechanics of Advanced Materials and Structures*, *27*(9), 754-760.

[111] Liao, Y., & Cheng, H. (2020, April). An integrated design approach of piezoelectric vibration energy harvesters. In *Active and Passive Smart Structures and Integrated Systems XIV* (Vol. 11376, pp. 58-72). SPIE.

[112] DuToit, N. E., & Wardle, B. L. (2007). Experimental verification of models for micro fabricated piezoelectric vibration energy harvesters. *AIAA journal*, *45*(5), 1126-1137.

[113] Yang, Y., & Tang, L. (2009). Equivalent circuit modeling of piezoelectric energy harvesters. *Journal of intelligent material systems and structures*, *20*(18), 2223-2235.

[114] Cheng, C., Chen, Z., Shi, H., Liu, Z., & Xiong, Y. (2016). System-level coupled modeling of piezoelectric vibration energy harvesting systems by joint finite element and circuit analysis. *Shock and Vibration*, *2016*.

[115] Jiang, X. Z., Li, Y. C., Wang, J., & Li, J. C. (2014). Electromechanical modeling and experimental analysis of a compression-based piezoelectric vibration energy harvester. *International Journal of Smart and Nano Materials*, *5*(3), 152-168.

[116] Berdy, D. F., Srisungsitthisunti, P., Jung, B., Xu, X., Rhoads, J. F., & Peroulis, D. (2012). Low-frequency meandering piezoelectric vibration energy harvester. *IEEE transactions on ultrasonics, ferroelectrics, and frequency control*, *59*(5), 846-858.

[117] Zhao, Y., Qin, Y., Guo, L., & Tang, B. (2018). Modeling and experiment of a v-shaped piezoelectric energy harvester. *Shock and Vibration*, *2018*.

[118] Wang, Y., He, H., & Xu, R. (2015). An analytical model for a piezoelectric vibration energy harvester with resonance frequency tunability. Advances in Mechanical Engineering, 7(6), 168781401559029.

[119] Liu, J., Fang, H., Xu, Z., Mao, X., Shen, X., Chen, D. Cai, B. (2008). A MEMS-based piezoelectric power generator array for vibration energy harvesting. Microelectronics Journal, 39(5), 802-806.

[120] Berdy, D. F., Jung, B., Rhoads, J. F., & Peroulis, D. (2012). Wide-bandwidth, meandering vibration energy harvester with distributed circuit board inertial mass. Sensors & Actuators: A. Physical, 188, 148-157.

[121] Koven, R., Mills, M., Gale, R., & Aksak, B. (2017). Low-frequency and broadband vibration energy harvesting using base-mounted piezoelectric transducers. IEEE Transactions on Ultrasonics, Ferroelectrics, and Frequency Control, 64(11), 1735-1743.

[122] Eichhorn, C., Goldschmidtboeing, F., & Woias, P. (2009). Bidirectional frequency tuning of a piezoelectric energy converter based on a cantilever beam. Journal of Micromechanics and Microengineering, 19(9), 094006.

[123] Hajati, A., Kim, S., & (2011). Ultra-wide bandwidth piezoelectric energy harvesting. Applied Physics Letters, 99(8), 083105-083105-3.

[124] Wu, X., Lin, J., Kato, S., Zhang, K., Ren, T., & Liu, L. (2008). A frequency adjustable vibration energy harvester. *Proceedings of PowerMEMS*, 245-248.

[125] Huang, P., Tsai, T., & Yang, Y. (2013). Wide-bandwidth piezoelectric energy harvester integrated with parylene-C beam structures. Microelectronic Engineering, 111, 214-219.

[126] Ma, H. A., Liu, J. Q., Tang, G., Yang, C. S., Li, Y. G., & He, D. N. (2011). A broadband frequency piezoelectric vibration energy harvester. Key Engineering Materials, 483, 626-630.

[127] Yang, W., & Towfighian, S. (2017). A hybrid nonlinear vibration energy harvester. Mechanical Systems and Signal Processing, 90, 317-333.

[128] Zhou, S., Cao, J., Erturk, A., & Lin, J. (2013). Enhanced broadband piezoelectric energy harvesting using rotatable magnets. Applied Physics Letters, 102(17), 173901.

[129] Ibrahim, D. S., Muthalif, A. G., & Saleh, T. (2014). Piezoelectric based vibration energy harvester with tip attraction magnetic force: modeling and simulation. *Mathematics and Computers in Science and Industry*, *23*, 80-86.

[130] Geiyer, D., & Kauffman, J. L. (2015). Chaotification as a means of broadband energy harvesting with piezoelectric materials. *Journal of Vibration and Acoustics*, *137*(5).

[131] Liu, S. T., & Su, W. J. (2019). Design and analysis of a stopper-engaged two-degrees-of-freedom nonlinear piezoelectric energy harvester. *Engineering Research Express*, *1*(2), 025032.

[132] Li, P., Liu, Y., Wang, Y., Luo, C., Li, G., Hu, J. & Zhang, W. (2015). Low-frequency and wideband vibration energy harvester with flexible frame and interdigital structure. *AIP advances*, *5*(4), 047151.

[133] Ai, R., Monteiro, L. L., Monteiro Jr, P. C. C., Pacheco, P. M., & Savi, M. A. (2019, March). Piezoelectric vibration-based energy harvesting enhancement exploiting nonsmoothness. In *Actuators* (Vol. 8, No. 1, p. 25). MDPI.

[134] Meruane, V., & Pichara, K. (2016). A broadband vibration-based energy harvester using an array of piezoelectric beams connected by springs. Shock and Vibration, 2016, 1-13. doi:10.1155/2016/9614842

[135] Halim, M. A., & Park, J. Y. (2014). Theoretical modeling and analysis of mechanical impact driven and frequency up-converted piezoelectric energy harvester for low-frequency and wide-bandwidth operation. *Sensors and actuators A: physical*, *208*, 56-65.

[136] Aryanpur, R. M., & White, R. D. (2012, March). Multi-link piezoelectric structure for vibration energy harvesting. In *Active and Passive Smart Structures and Integrated Systems 2012* (Vol. 8341, p. 83411Y). International Society for Optics and Photonics.

[137] Pan, C. T., Liu, Z. H., & Chen, Y. C. (2012). Study of broad bandwidth vibrational energy harvesting system with optimum thickness of PET substrate. Current Applied Physics, 12(3), 684-696.

[138] Hasan Göksenin, ÇetinBilsaySümer, (2015), A Flexible Piezoelectric Energy Harvesting System for Broadband and Low-frequency Vibrations, Procedia Engineering, Volume 120, 2015

[139] LIU Wen HAN MengDi MENG Bo SUN XuMing HUANG XianLiang ZHANG HaiXia. (2014). Low frequency wide bandwidth MEMS energy harvester based on spiral-shaped PVDF cantilever. 57(6), 1068- 1072.

[140] Rezaeisaray, M., El Gowini, M., Sameoto, D., Raboud, D., & Moussa, W. (2014). Wide-bandwidth piezoelectric energy harvester with polymeric structure. *Journal of Micromechanics and Microengineering*, *25*(1), 015018.

[141] Huang, H., & Chen, K. (2016). Design, analysis, and experimental studies of a novel PVDF-based piezoelectric energy harvester with beating mechanisms. Sensors & Actuators: A. Physical, 238, 317-328.

[142] Friswell, M. I., Ali, S. F., Bilgen, O., Adhikari, S., Lees, A. W., & Litak, G. (2012). Non-linear piezoelectric vibration energy harvesting from a vertical cantilever beam with tip mass. Journal of Intelligent Material Systems and Structures, 23(13), 1505-1521.

[143] Li, S., Li, X., Crovetto, A., Peng, Z., Zhang, A., Hansen, O. Wang, F. (2016). Bi-resonant structure with piezoelectric PVDF films for energy harvesting from random vibration sources at low frequency. Sensors & Actuators: A. Physical, 247, 547-554.

[144] Dauksevicius, R., Gaidys, R., Ostasevicius, V., Lockhart, R., Quintero, A. V., de Rooij, N., & Briand, D. (2019). Nonlinear piezoelectric vibration energy harvester with frequency-tuned impacting resonators for improving broadband performance at low frequencies. *Smart Materials and Structures*, *28*(2), 025025.

[145] Environmental robots Inc., Products, viewed on 25th January 2022, https://www.environmental-robots.com/

[146] Raghavan, S., Sharma, A., & Gupta, R. (2023). Resonant frequency tuning of a novel piezoelectric vibration energy harvester (PVEH). *Mechanics of Advanced Materials and Structures*, 1-16.

[147] Tadokoro, S., Yamagami, S., Takamori, T., & Oguro, K. (2000, June). Modeling of Nafion-Pt composite actuators (ICPF) by ionic motion. In *Smart Structures and Materials 2000: Electroactive Polymer Actuators and Devices (EAPAD)* (Vol. 3987, pp. 92-102). SPIE.

[148] Chen, Z., Member, S., & Tan, X. (2008). A Control-Oriented and Physics-Based Model for Ionic Polymer – Metal Composite Actuators. *October*, *13*(5), 519–529.

[149] Najafi, K., Galchev, T., Aktakka, E. E., Peterson, R. L., & McCullagh, J. (2011, June). Microsystems for energy harvesting. In *2011 16th International Solid-State Sensors, Actuators and Microsystems Conference* (pp. 1845-1850). IEEE.

[150] Hunt, A. (2017). *Application-oriented performance characterization of the ionic polymer transducers (IPTs)* (Doctoral dissertation, Tallinn University of Technology).

[151] Zhao, L., & Yang, Y. (2018). An impact-based broadband aeroelastic energy harvester for concurrent wind and base vibration energy harvesting. *Applied Energy*, *212*, 233-243.

[152] Zhou, K., Dai, H. L., Abdelkefi, A., Zhou, H. Y., & Ni, Q. (2019). Impacts of stopper type and material on the broadband characteristics and performance of energy harvesters. *AIP Advances*, *9*(3), 035228.

[153] Zhao, Y., Xu, D., Sheng, J., Meng, Q., Wu, D., Wang, L., & Sun, D. (2018). Biomimetic beetle-inspired flapping air vehicle actuated by ionic polymer-metal composite actuator. *Applied Bionics and Biomechanics*, *2018*.

[154] Zhou, K., Dai, H. L., Abdelkefi, A., & Ni, Q. (2020). Theoretical modeling and nonlinear analysis of piezoelectric energy harvesters with different stoppers. *International Journal of Mechanical Sciences*, *166*, 105233

[155] Van Schaijk, R., Elfrink, R., Oudenhoven, J., Pop, V., Wang, Z., & Renaud, M. (2013). A MEMS vibration energy harvester for automotive applications. *Smart Sensors, Actuators, and MEMS VI*, Vol. 8763, p. 876305. https://doi.org/10.1117/12.2016916

[156] Hosseinkhani, A., Younesian, D., Eghbali, P., Moayedizadeh, A., & Fassih, A. (2021). Sound and vibration energy harvesting for railway applications: A review on linear and nonlinear techniques. *Energy Reports*, *7*, 852–874. https://doi.org/10.1016/j.egyr.2021.01.087

[157] Deng, L., Fang, Y., Wang, D., & Wen, Z. (2018). A MEMS based piezoelectric vibration energy harvester for fault monitoring system. *Microsystem Technologies*, *24*, 3637-3644.

[158] Goel, C., & Srinivas, G. (2021). Mechanisms and applications of vibration energy harvesting in solid rocket motors. *Microsystem Technologies*, *27*(10), 3927–3933. https://doi.org/10.1007/s00542-020-05200-1

[159] Beeby, S. P., & Zhu, D. (2015). Vibration energy harvesting: fabrication, miniaturisation and applications. *Smart Sensors, Actuators, and MEMS VII; and Cyber Physical Systems*, *9517*, 951703. https://doi.org/10.1117/12.2179783

[160] Khan, F. U., & Ahmad, I. (2016). Review of energy harvesters utilizing bridge vibrations. *Shock and Vibration*, *2016*. https://doi.org/10.1155/2016/1340402

[161] Ali, F., Raza, W., Li, X., Gul, H., & Kim, K. H. (2019). Piezoelectric energy harvesters for biomedical applications. *Nano Energy*, *57*, 879-902.

[162] Hwang, G. T., Byun, M., Jeong, C. K., & Lee, K. J. (2015). Flexible piezoelectric thin-film energy harvesters and nanosensors for biomedical applications. *Advanced healthcare materials*, *4*(5), 646-658.

[163] Panda, S., Hajra, S., Mistewicz, K., In-na, P., Sahu, M., Rajaitha, P. M., & Kim, H. J. (2022). Piezoelectric energy harvesting systems for biomedical applications. *Nano Energy*, 107514.

[164] Han, M., Wang, H., Yang, Y., Liang, C., Bai, W., Yan, Z., & Rogers, J. A. (2019). Three-dimensional piezoelectric polymer microsystems for vibrational energy harvesting, robotic interfaces and biomedical implants. *Nature Electronics*, *2*(1), 26-35.

[165] Mhetre, M. R., Nagdeo, N. S., & Abhyankar, H. K. (2011, April). Micro energy harvesting for biomedical applications: A review. In *2011 3rd international conference on electronics computer technology* (Vol. 3, pp. 1-5). IEEE.

[166] Zheng, Q., Shi, B., Li, Z., & Wang, Z. L. (2017). Recent progress on piezoelectric and triboelectric energy harvesters in biomedical systems. *Advanced Science*, *4*(7), 1700029.

[167] Ding, J., Challa, V. R., Prasad, M. G., & Fisher, F. T. (2013). Vibration energy harvesting and its application for nano-and microrobotics. In *Selected Topics in Micro/Nano-robotics for Biomedical Applications* (pp. 59-83). Springer, New York, NY.

[168] Townsend, S., Grigg, S., Picelli, R., Featherston, C., & Kim, H. A. (2019). Topology optimization of vibrational piezoelectric energy harvesters for structural health monitoring applications. *Journal of intelligent material systems and structures*, *30*(18-19), 2894-2907

[169] Park, G., Rosing, T., Todd, M. D., Farrar, C. R., & Hodgkiss, W. (2008). Energy harvesting for structural health monitoring sensor networks. *Journal of Infrastructure Systems*, *14*(1), 64-79.

[170] Maruccio, C., Quaranta, G., De Lorenzis, L., & Monti, G. (2016). Energy harvesting from electrospun piezoelectric nanofibers for structural health monitoring of a cable-stayed bridge. *Smart Materials and Structures*, *25*(8), 085040.

[171] Smart Material corporation Smart Material Available online: https://smart-material.com/ - viewed on 3rd January 2022

[172] Saadon, S., & Sidek, O. (2011). A review of vibration-based MEMS piezoelectric energy harvesters. *Energy conversion and management*, *52*(1), 500-504.

[173] Shahinpoor, M. (2001, April). Potential applications of electroactive polymer sensors and actuators in MEMS technologies. In *Smart materials* (Vol. 4234, pp. 203-214). International Society for Optics and Photonics.

[174] Shahinpoor, M., & Kim, K. J. (2004). Ionic polymer–metal composites: IV. Industrial and medical applications. *Smart materials and structures*, *14*(1), 197.

[175] Chang, X. L., Chee, P. S., & Lim, E. H. (2020, July). Ionic Polymer Actuator With Crenellated Structures for MEMs Application. In *2020 IEEE International Conference on Semiconductor Electronics (ICSE)* (pp. 160-163). IEEE.

[176] Chung, C. K., Fung, P. K., Hong, Y. Z., Ju, M. S., Lin, C. C. K., & Wu, T. C. (2006). A novel fabrication of ionic polymer-metal composites (IPMC) actuator with silver nano-powders. *Sensors and Actuators B: Chemical*, *117*(2), 367-375.

[177] Lei, H., Li, W., & Tan, X. (2012, April). Microfabrication of IPMC cilia for bio-inspired flow sensing. In *Electroactive Polymer Actuators and Devices (EAPAD) 2012* (Vol. 8340, pp. 331-339). SPIE.

[178] Marzencki, M., Basrour, S., Charlot, B., Spirkovich, S., & Colin, M. (2005). A MEMS piezoelectric vibration energy harvesting device. *Proceedings of PowerMEMS*, 45-48.

[179] Sahdom, A. (2019). Application of Micro Electro-Mechanical Sensors (MEMS) Devices with Wifi Connectivity and Cloud Data Solution for Industrial Noise and Vibration Measurements. *Journal Of Physics: Conference Series*, *1262*, 012025. doi: 10.1088/1742-6596/1262/1/012025

[180] Berdy, D., Srisungsitthisunti, P., Jung, B., Xu, X., Rhoads, J., & Peroulis, D. (2012). Low-frequency meandering piezoelectric vibration energy harvester. *IEEE Transactions On Ultrasonics, Ferroelectrics And Frequency Control*, *59*(5), 846-858. doi: 10.1109/tuffc.2012.2269

[181] Alameh, A., Gratuze, M., Elsayed, M., & Nabki, F. (2018). Effects of Proof Mass Geometry on Piezoelectric Vibration Energy Harvesters. *Sensors*, *18*(5), 1584. doi: 10.3390/s18051584

[182] Qi, S., Shuttleworth, R., Olutunde Oyadiji, S., & Wright, J. (2010). Design of a multiresonant beam for broadband piezoelectric energy harvesting. *Smart Materials And Structures*, *19*(9), 094009. doi: 10.1088/0964-1726/19/9/094009

[183] Leadenham, S., & Erturk, A. (2015). Nonlinear M-shaped broadband piezoelectric energy harvester for very low base accelerations: primary and secondary resonances. *Smart Materials And Structures*, *24*(5), 055021. doi: 10.1088/0964-1726/24/5/055021

[184] Huang, P., Tsai, T., & Yang, Y. (2013). Wide-bandwidth piezoelectric energy harvester integrated with parylene-C beam structures. *Microelectronic Engineering*, *111*, 214-219. doi: 10.1016/j.mee.2013.03.158

[185] Zhou, S., Yan, B., & Inman, D. (2018). A Novel Nonlinear Piezoelectric Energy Harvesting System Based on Linear-Element Coupling: Design, Modeling and Dynamic Analysis. *Sensors*, *18*(5), 1492. doi: 10.3390/s18051492

[186] Ma, H., Liu, J., Tang, G., Yang, C., Li, Y., & He, D. (2011). A Broadband Frequency Piezoelectric Vibration Energy Harvester. *Key Engineering Materials*, *483*, 626-630. doi: 10.4028/www.scientific.net/kem.483.626

[187] Lu, Q., Scarpa, F., Liu, L., Leng, J., & Liu, Y. (2018). An E-shape broadband piezoelectric energy harvester induced by magnets. *Journal Of Intelligent Material Systems And Structures*, *29*(11), 2477-2491. doi: 10.1177/1045389x18770871

[188] Fan, K., Tan, Q., Zhang, Y., Liu, S., Cai, M., & Zhu, Y. (2018). A monostable piezoelectric energy harvester for broadband low-level excitations. *Applied Physics Letters*, *112*(12), 123901. doi: 10.1063/1.5022599

[189] Jung, H., Lee, S., Jeong, S., & Yoo, H. (2018). Segmented impact-type piezoelectric energy harvester for self-start impedance matching circuit. *Smart Materials And Structures*, *27*(11), 114006. doi: 10.1088/1361-665x/aacdc6

[190] Anton, S., & Sodano, H. (2007). A review of power harvesting using piezoelectric materials (2003–2006). *Smart Materials And Structures*, *16*(3), R1-R21. doi: 10.1088/0964-1726/16/3/r01

[191] Smart Material, Energy harvester, viewed on 26th March 2020, https://www.smart-material.com/

[192] Mohsen Shahinpoor and Kwang J Kim, (2001), Ionic polymer-metal composites: I. Fundamentals, Smart Materials and Structures, Vol 10, Number 4

[193] Paquette, J. W., Kim, K. J., & Fuchs, A. (2003, July). Low-temperature operation of ionic polymer metal composite actuators. In *Smart Structures and Materials 2003: Electroactive Polymer Actuators and Devices (EAPAD)* (Vol. 5051, pp. 254-261). SPIE.

[194] Yang, Y., Chen, Z., Kuai, Q., Liang, J., Liu, J., & Zeng, X. (2022). Circuit techniques for high efficiency piezoelectric energy harvesting. *Micromachines*, *13*(7), 1044.

[195] Dicken, J., Mitcheson, P. D., Stoianov, I., & Yeatman, E. M. (2012). Power-extraction circuits for piezoelectric energy harvesters in miniature and low-power applications. *IEEE Transactions on power electronics*, *27*(11), 4514-4529

[196] Peng, Y., Choo, K. D., Oh, S., Lee, I., Jang, T., Kim, Y., & Sylvester, D. (2019). An efficient piezoelectric energy harvesting interface circuit using a sense-and-set rectifier. *IEEE Journal of Solid-State Circuits*, *54*(12), 3348-3361.

Annexures

The proposed design of the tunable PVEH was arrived at, through various pilot studies that were carried out based on the philosophy of tuning of resonant frequency of a cantilever beam. Various experiments and studies based on the basic requirement for changing the stiffness of the cantilever beam were carried out during this phase of research. The annexures detail those experimental procedures, results and the thought process towards the novel design. The exploration to find a tunable actuation system led to the studies of other smart materials such as SMA (Shape Memory Alloy), EAP (Electro Active Polymer), IPMC etc. SMA actuates based on the changes in the material property due to temperature changes. This does not provide a low power method for the PVEH design. Similarly, even though EAP actuators can provide good actuation force, it requires high power input. It was found that IPMC meets the low power requirements of a PVEH design.

Possibility of using IPMC as integral part of a substrate is also explored and the experiment conducted is given in annexure.

The subsequent annexures also give the technical specifications of the instruments used, important definitions of terms and units and detailed graphs pertaining to the experimental results of the novel design.

Annexure - 1

Initial Study

In order to develop the final design of the device, a series of preliminary experiments were conducted on PVEH with disc type piezoelectric element. This was done by using different values of mass (1.8 gms and 2.8 gms) along the cantilever beam, considering the range that is effective for the dimensions of the harvester, and the voltage output was recorded. Fig. 1 shows the set-up of the preliminary tests that included a PVEH cantilever beam fixed on one side on a stand (left side in figure 1) while the other side is fixed by an exciter. Fig. 2 shows the scheme of the clamped-clamped PVEH setup.

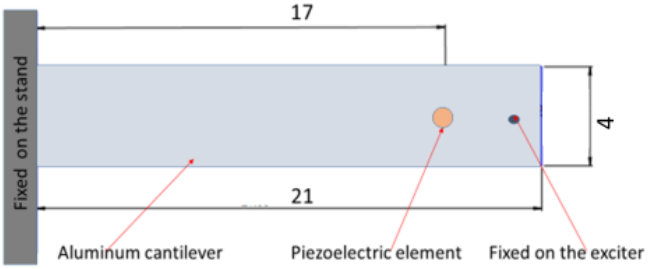

Fig. A1.1 PVEH set-up in clamped/clamped configuration (Dimensions in cm)

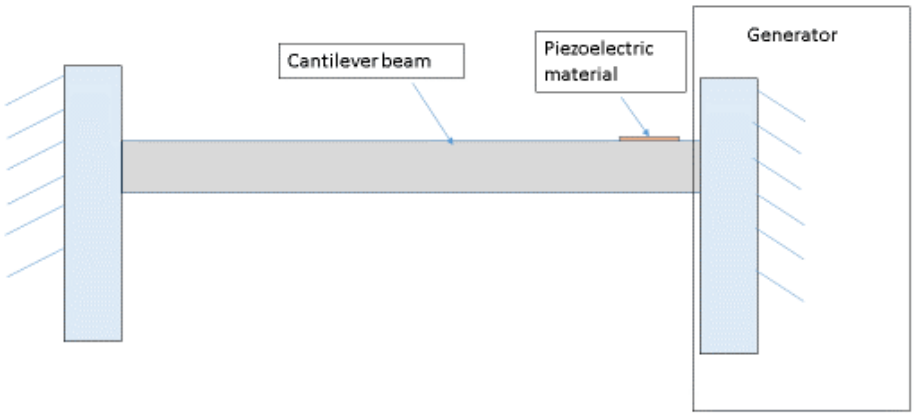

Fig. A1.2 Representation of a clamped-clamped PVEH

The experiment involved the use of two different masses placed at different locations (at 9, 12, 13, 17, 19.5 cm respectively from the end that was fixed on the stand) along the beam. The PVEH

cantilever beam was subjected to a constant frequency of 35 Hz and corresponding voltage was recorded. The experimental setup is shown in Fig. 3.

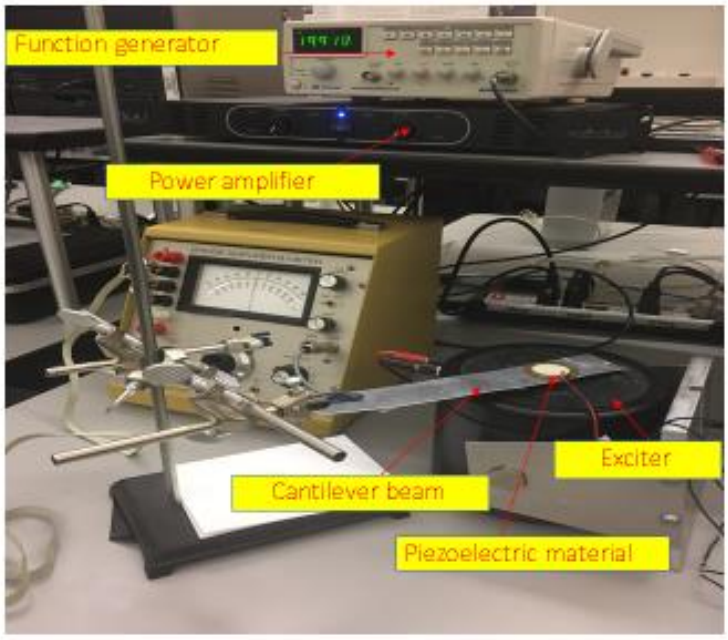

Fig. A1.3 Experimental set up for the initial study

The recorded data was plotted for the location of the mass vs the corresponding voltage output for each mass (Fig.8). When there was no mass, the recorded output voltage was 850 mV and the cantilever beam was not in resonance, At a distance of 17 cm from the fixed end of the beam, the recorded output voltage is maximum i.e., 1140 mV and 1400 mV respectively for m_1 (2.8gms) and m_2 (1.8gms). Fig. 4, 5, 6, 7 give the details in two different frequencies. This indicates that the beam could be brought into resonance by introducing a mass on the beam at a specific location. Additionally, it can also be seen that a decrease in mass enhances the recorded output voltage at the same location and same input frequency.

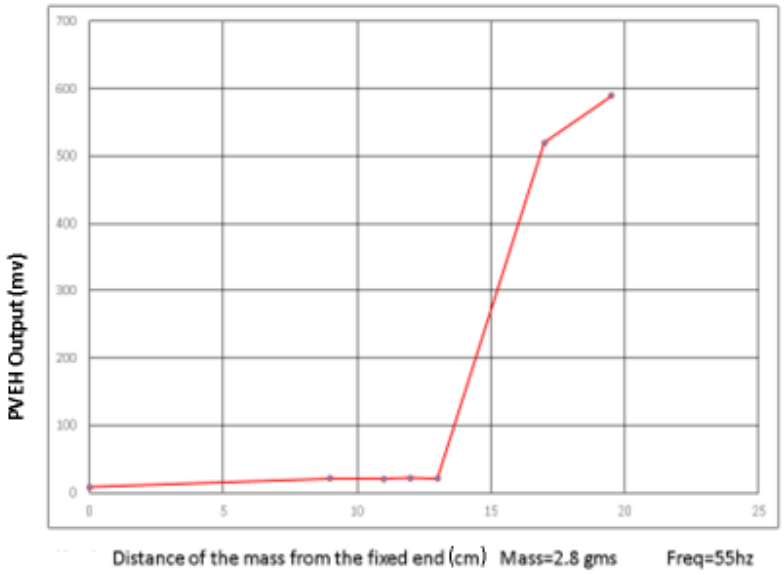

Fig. A1.4 PVEH Output for mass of 2.8 gms and frequency 55Hz

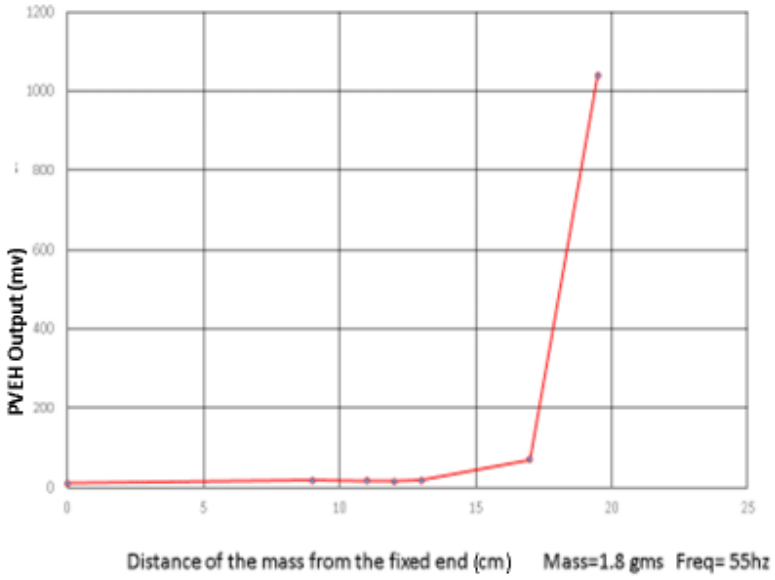

Fig. A1.5 PVEH Output for mass of 1.8 gms and frequency 55Hz

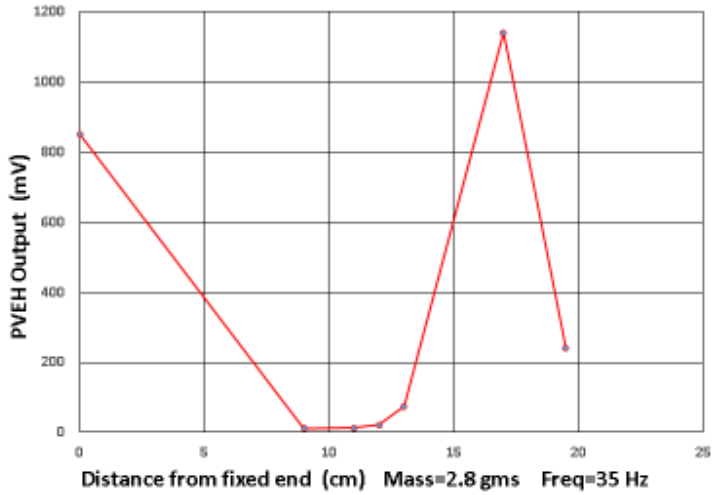

Fig. A1.6 PVEH Output for mass of 2.8 gms and frequency 35Hz

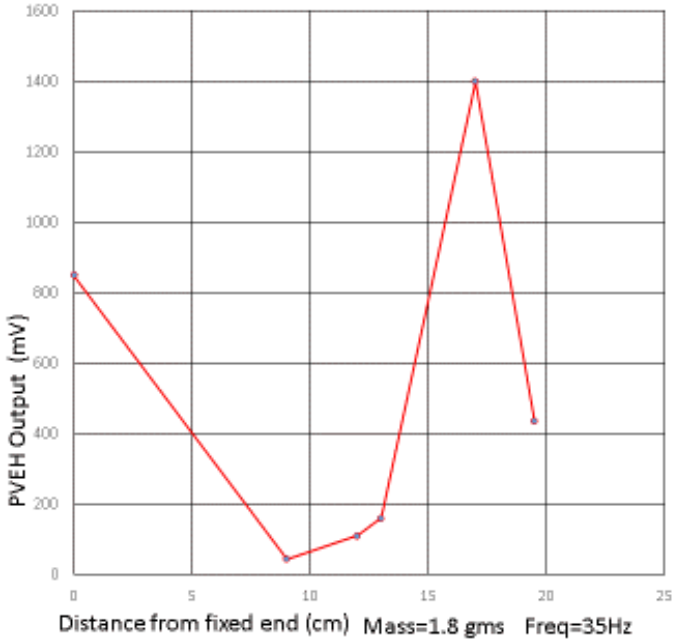

Fig. A1.7 PVEH Output for mass of 1.8 gms and frequency 35Hz

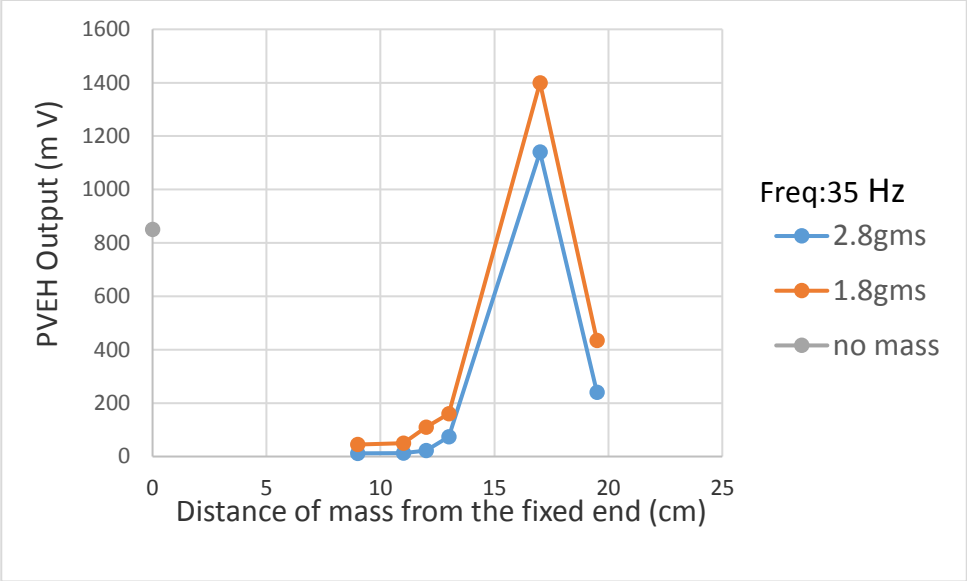

Fig. A1.8 Effect of location of mass on the resonant frequency of clamped-clamped PVEH

Representation of main passive techniques reported in literature for changing the Resonant frequency is shown in Fig. 9:

Method 1: Adding/ moving mass along the beam

Method 2: Application of an axial load

Method 3: Shifting the fixing point of the beam

Other approaches have multi beam structures with different piezoelectric materials or with springs that interconnect the beams.

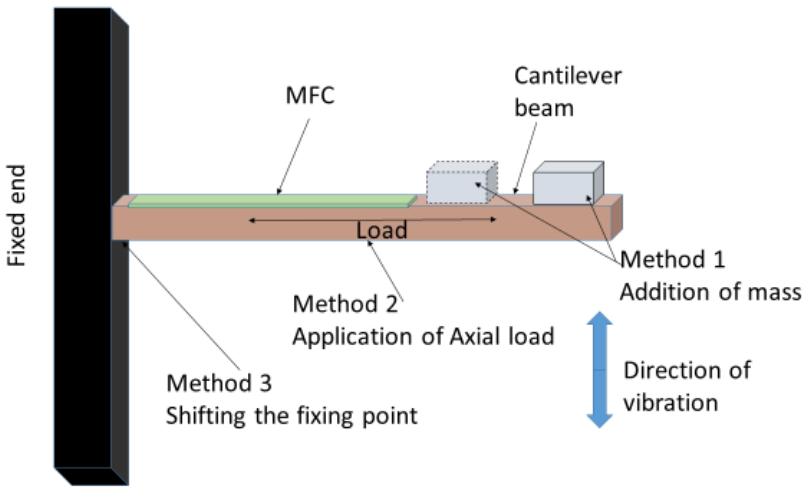

Fig. A1.9 Various methods reported to achieve a wider bandwidth

Moisture saturation tests on IPMC:

Moisture saturation test was carried out by soaking IPMC in water for 16 hours and then measuring the mass using a high precision balance. The loss of mass was noted every hour. The measurement was continued till the mass became stable.

Fig. 10 (a) shows the experimental set up used and (b) shows the mass variation with time.

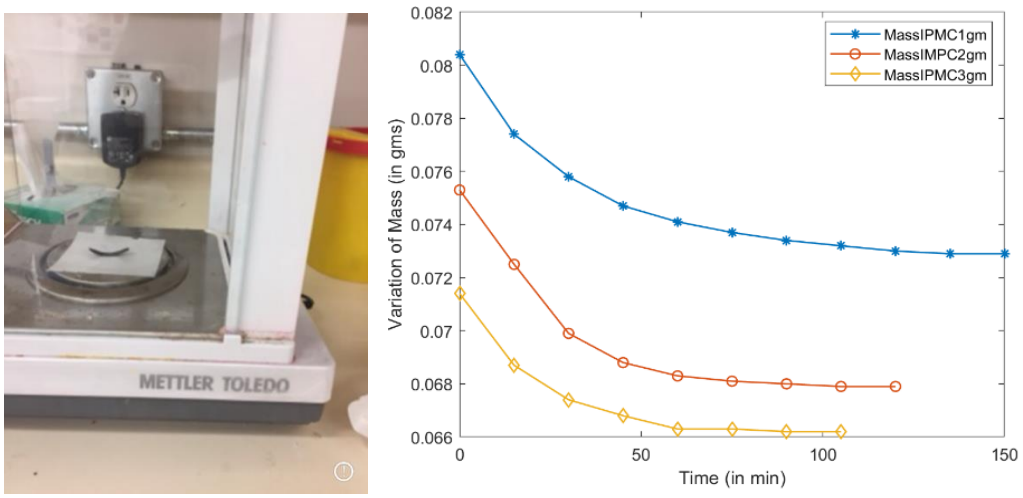

(a) (b)

Fig. A1.10 Moisture content study of IPMC (a) The setup used for measurement (b) Results

Experiments on the novel design using single IPMC actuator:

Experiments were carried out to try tuning the PVEH integrating a single IPMC as an actuator as shown in Fig. 11. The experiments were repeated on PVEH with different MFC patches.

It was observed that the IPMC did actuate giving sufficient blocking force to change the resonant frequency. Some of the results obtained are shown in Fig. 12, 13 and 14. All the cases demonstrate a fairly linear response.

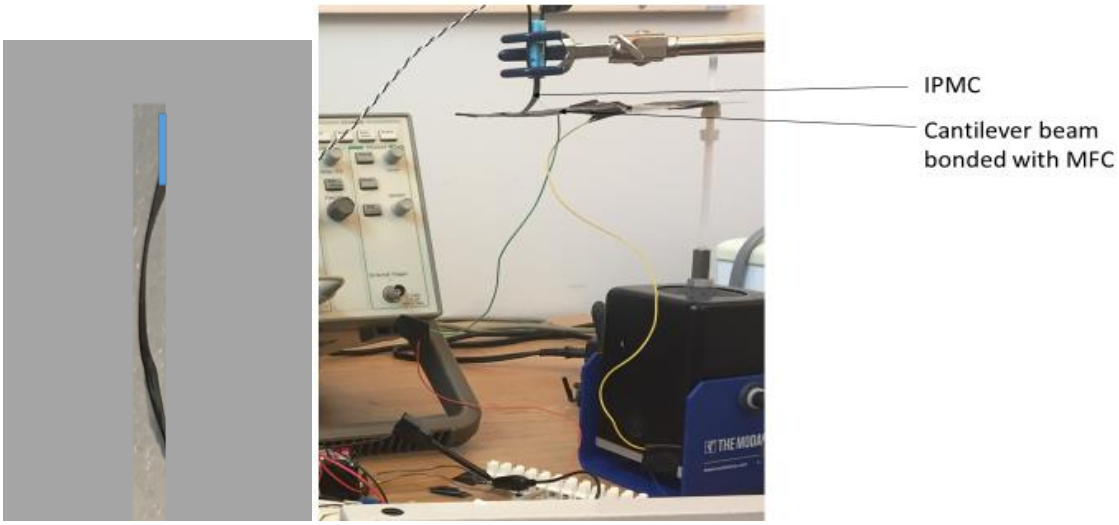

(a) **(b)**

Fig. A1.11 (a) Single IPMC (b) Experimental setup using single IPMC actuator

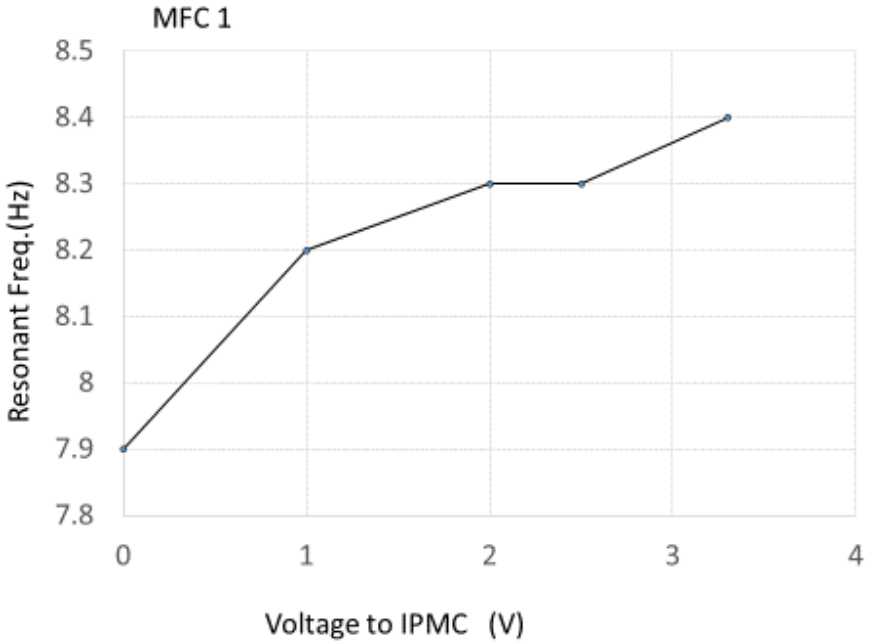

Fig. A1.12 PVEH with MFC1 and single IPMC actuator

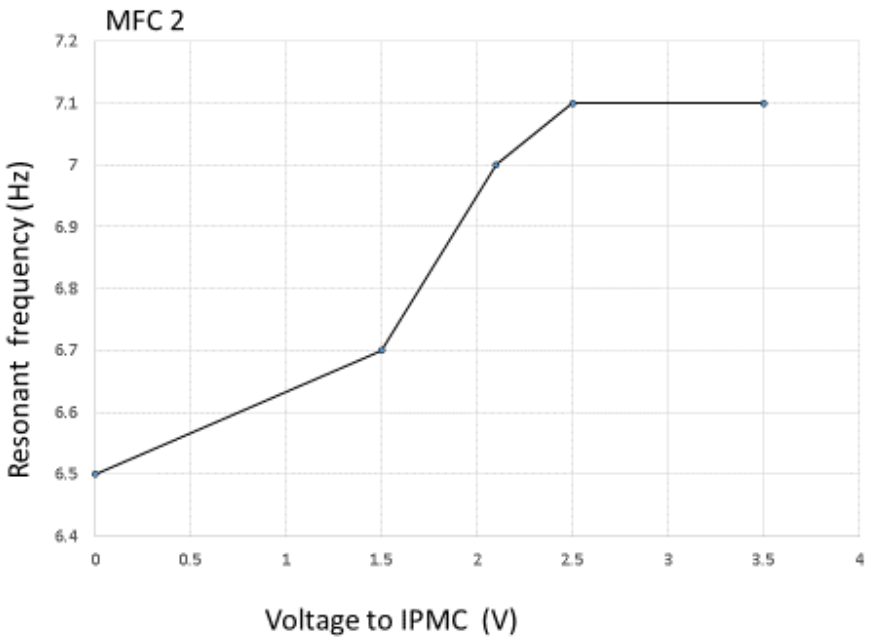

Fig. A1.13 PVEH with MFC2 and single IPMC actuator

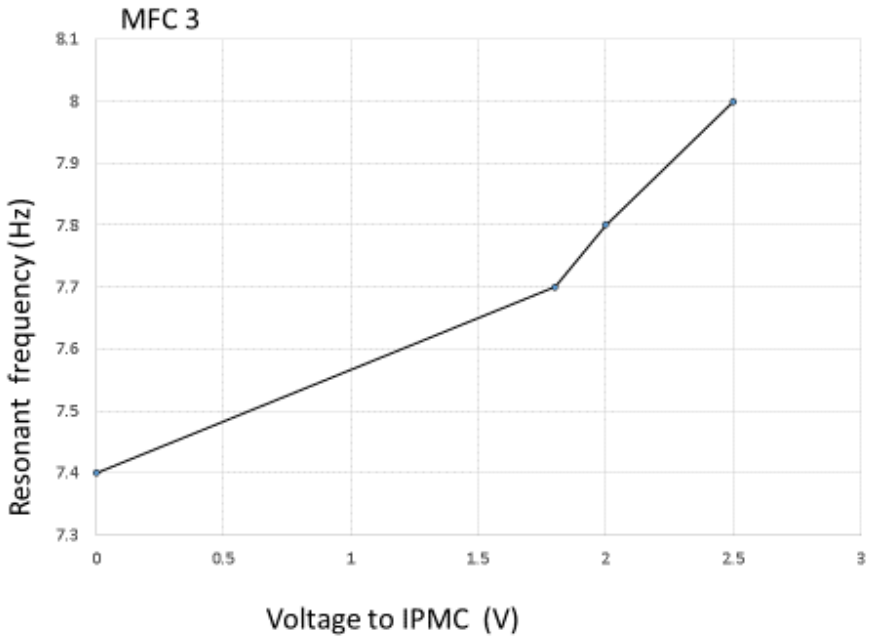

Fig. A1.14 PVEH with MFC3 and single IPMC actuator

However, the single IPMC does not provide a stable configuration for consistent contact point. Hence further design change was considered in which multiple IPMC elements are to be used. As a simpler design of such a case, it was decided to use two IPMC joined at the ends and powered

together as a single actuator. Further experiments were conducted with this dual IPMC configuration as presented in the various chapters of this dissertation.

Actuation of IPMC on a plastic substrate:

A single IPMC was bonded on to a thin plastic substrate as shown in Fig. 15 and actuated using the function generator supplied by Environmental Robots, USA.

A) IPMC
B) Circuit

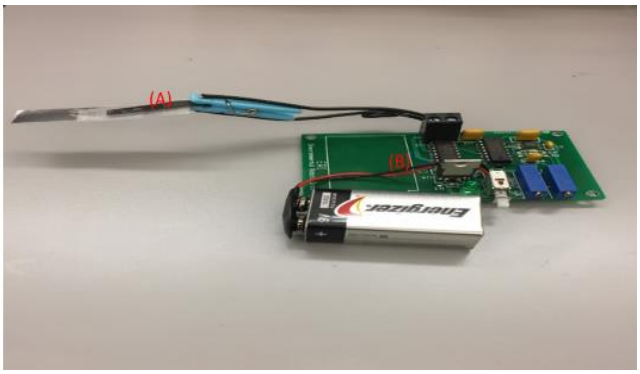

Fig. A1.15 IPMC on a plastic substrate

This experiment was carried out in order to assess the capability of the IPMC to actuate driving a substrate into an alternate position. It was observed that the IPMC could effectively actuate.

This observation leads to a possibility of a design of PVEH of cantilever design that can generate an axial load in it

Table A1.1 List of Low power MEMS devices

S. No	Device	Power requirement
1	Microphone	1.8 v 650 µA
2	Triaxial accelerometer	3 V 2 µA
3	Micro Controller Unit (MCU)	1.71 to 3.6V 100 µA
4	Humidity sensor	1.71 to 3.6V 2 µA
5	Ultra-low power wi- fi radio for IoT	28µw
6	Graphene oxide humidity sensor	15 w

Annexure 2

Further Experimental Data on the novel Tunable PVEH

Possibility of getting wider bandwidth:

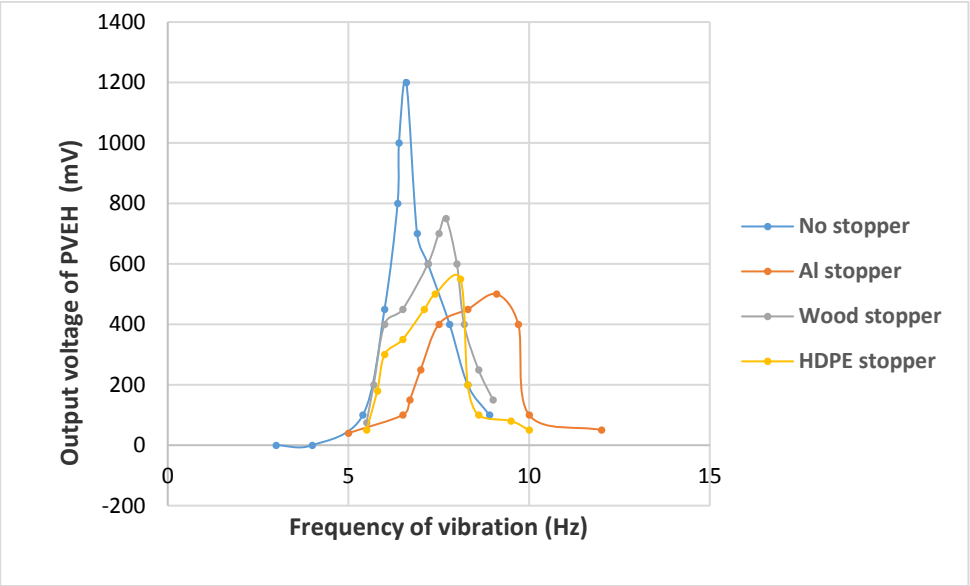

Fig. A2.1 Frequency of vibration vs Output voltage of PVEH for different stoppers

The stopper is 2.5 cm above the surface of the cantilever

Location of contact-3.5 cm from the tip of the cantilever beam

MFC: M5628P2, Acceleration: 1.5g

Fig. 1 gives the plot of frequency of vibration vs the output voltage of PVEH, when no stopper is used and when stopper of various stiffness was used. It can be seen that by introducing a stopper, resonant frequency could be shifted to a higher value. The figure shows the effect of using stoppers of different stiffness in the shifted resonant frequency.

Hence it can be inferred that if the reaction force of the stopper increases, the resonant frequency shift also will increase. This approach is made use of, in the novel design of PVEH, integrated with IPMC. A higher frequency shift can be realized by using IPMC of higher blocking force.

Literature on IPMC gives a great deal of research that is going into the field of IPMC fabrication, and many cases where higher blocking force is achieved in laboratory trials. This evolving technology is promising and can be adapted to the novel design of PVEH that is discussed here.

For example, Jung et.al. have developed a porous Nafion membrane using a silica sol–gel process, which has resulted in higher block force in the actuation mode. It was observed that blocking force of about 138% at direct current input could be generated [Jung, S. Y., Ko, S. Y., Park, J. O., & Park, S. (2017). Enhanced ionic polymer–metal composite actuator with pore size–controlled porous Nafion membrane using silica sol–gel process. *Journal of Intelligent Material Systems and Structures*, *28*(11), 1514-1523].

Zhao et.al. have studied and compared the blocking force of IPMC fabricated by the casted Nafion with IPMC fabricated by a commercial Nafion-117 [Zhao, Y., Xu, D., Sheng, J., Meng, Q., Wu, D., Wang, L., ... & Sun, D. (2018). Biomimetic beetle-inspired flapping air vehicle actuated by ionic polymer-metal composite actuator. *Applied Bionics and Biomechanics, 2018*].

Their results indicate that the blocking force of IPMC fabricated using casted Nafion is greater than IPMC fabricated using Nafion-117. It is reported that the IPMC by casted Nafion could generate 2.4 grams of force for 4V DC.

Fig. 2 shows the dual IPMC actuation unit. Fig. 3 gives the blocking force generated by the commercially available IPMC, fabricated using Nafion membrane. This data is generated by the authors in the case of dual configuration of IPMC. The blocking force generated for 4 V input was 0.265gm.

The resonant frequency shift obtained is corresponding to the blocking force of 0.265 gm. Hence a wider shift of resonant frequency can be generated by integrating the IPMCs that are getting newly developed as explained above.

Care was taken to maintain the stability of stopper arrangement, Hydration and amplitude control.

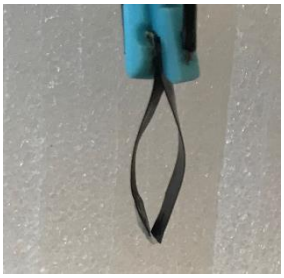

Fig. A2.2 Dual IPMC actuator unit

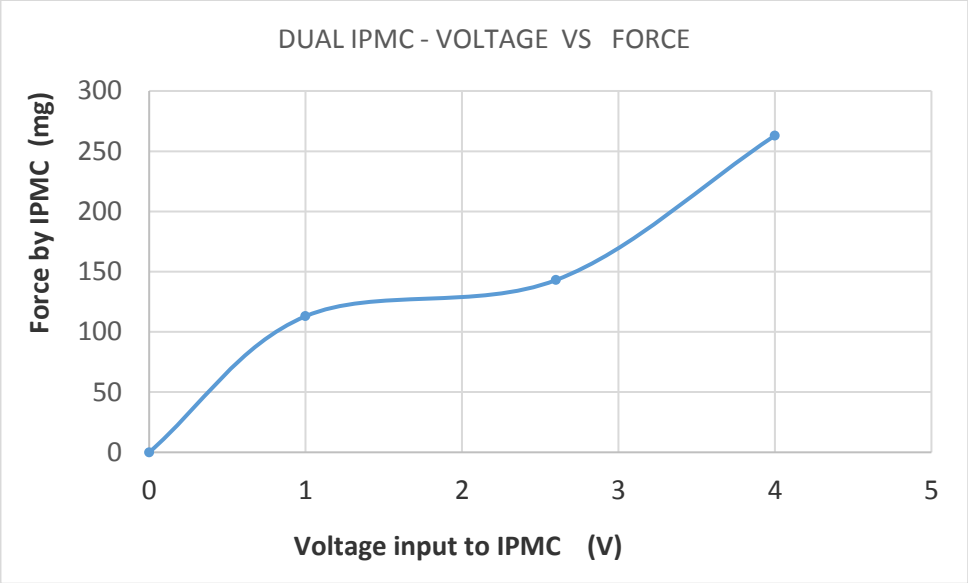

Fig. A2.3 Input voltage to IPMC vs Force generated by IPMC in dual configuration

Annexure 3

Detailed plots on the Data from the experiments

In all the graphs, frequency is in Hz, power is in µW and *g* refers to acceleration

PVEH resonant frequency increasing with increase in IPMC input voltage.

IPMC input vs Resonant frequency at different locations.

Distance from the free end of beam (Fig.2, Chapter 3)

A- 1cm, B- 2cm, C- 4cm, D- 5cm, E- 7cm, F- 8cm

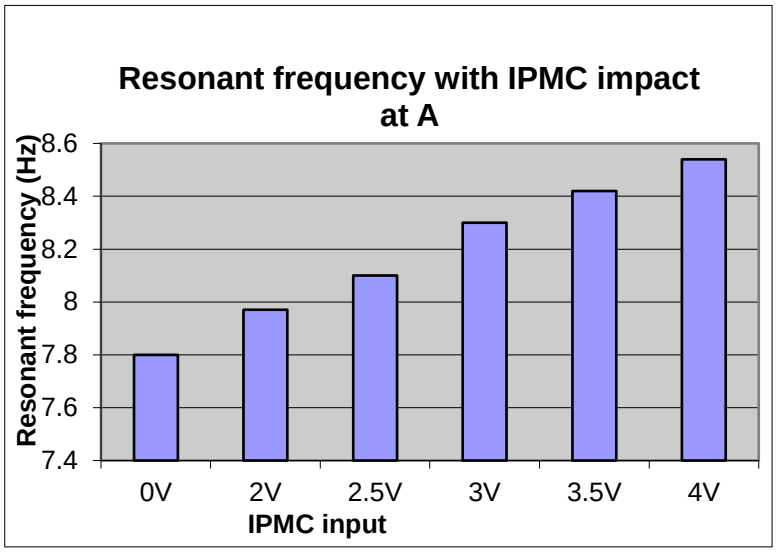

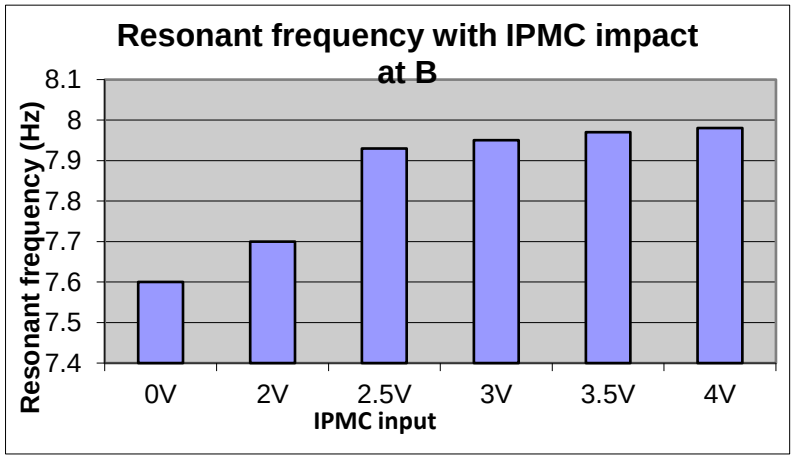

Fig A 3.1 Response when IPMC impact was at point A and at point B

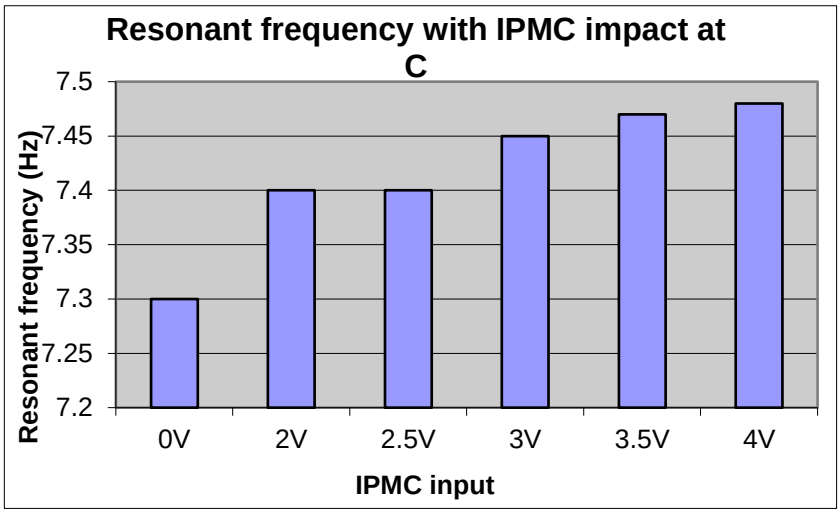

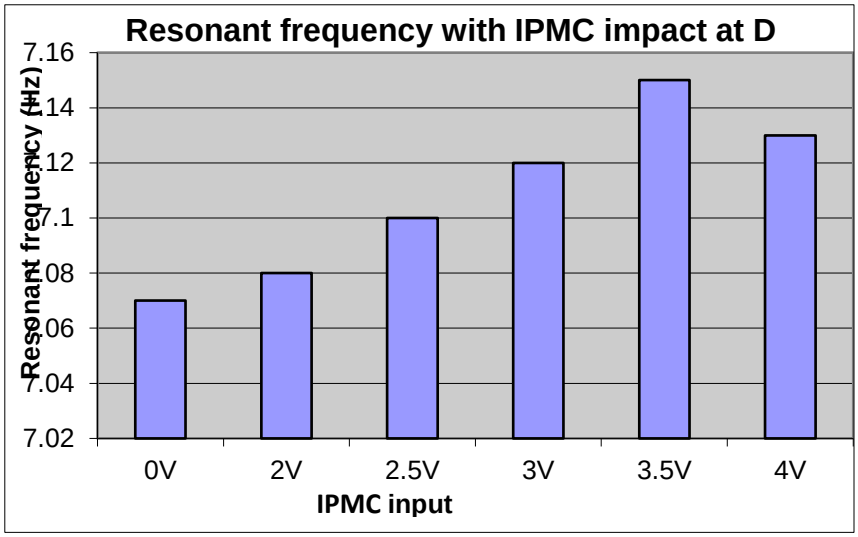

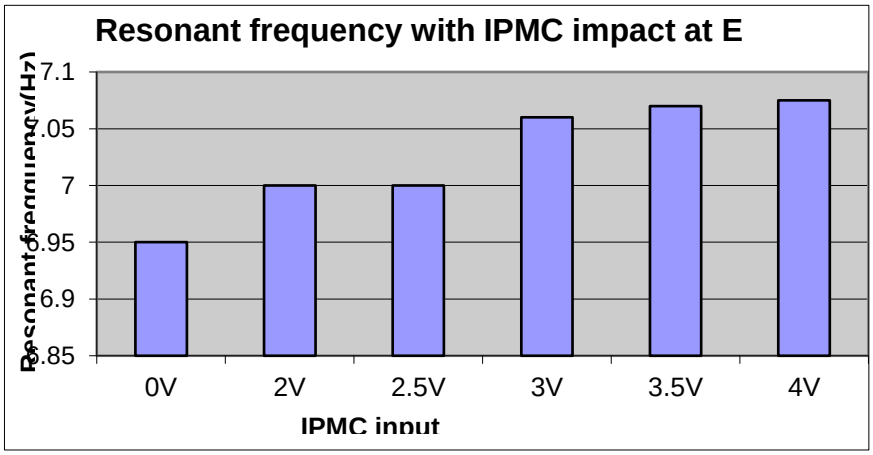

Fig A 3.2 Response when IPMC impact was at points C, D and E

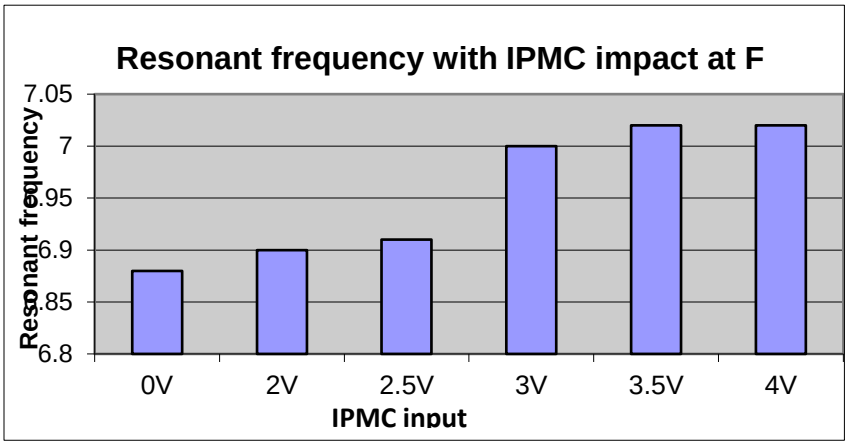

Fig A 3.3 Response when IPMC impact was at point F

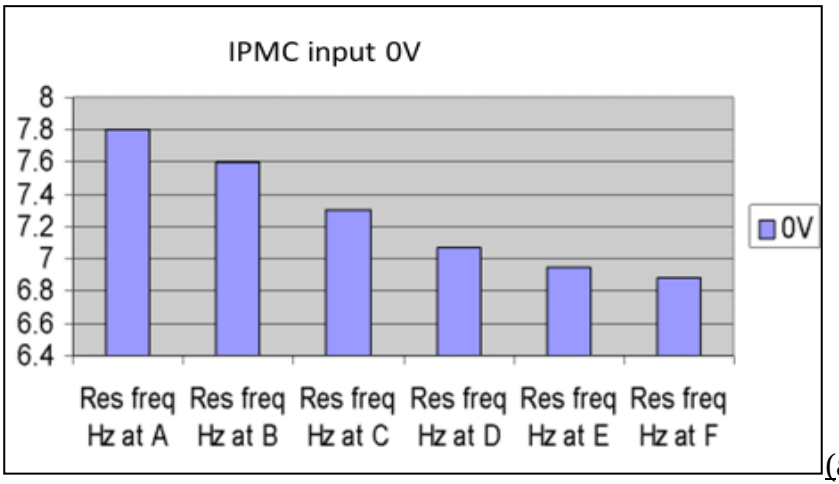

(a)

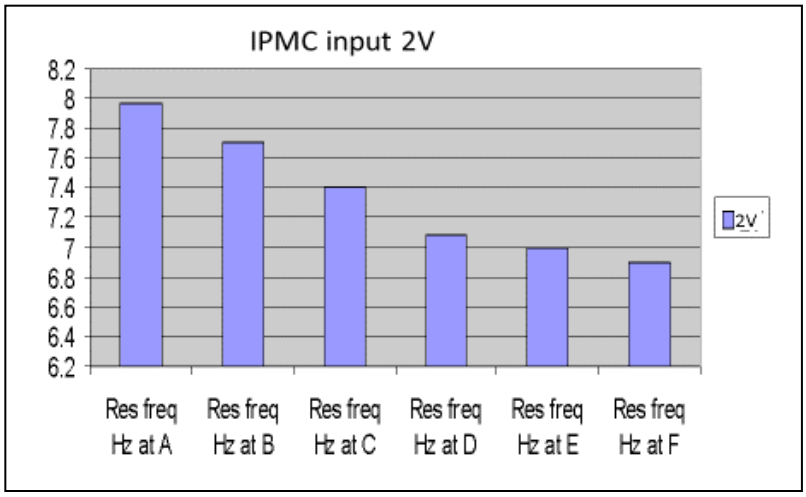

(b)

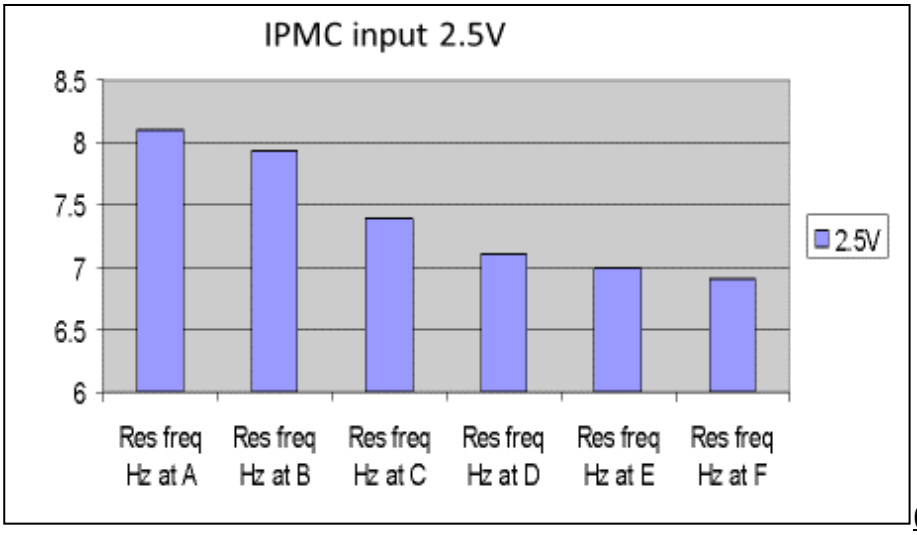
IPMC input 2.5V
8.5
8
7.5
7
6.5
6
2.5V
Res freq Hz at A
Res freq Hz at B
Res freq Hz at C
Res freq Hz at D
Res freq Hz at E
Res freq Hz at F

(c)

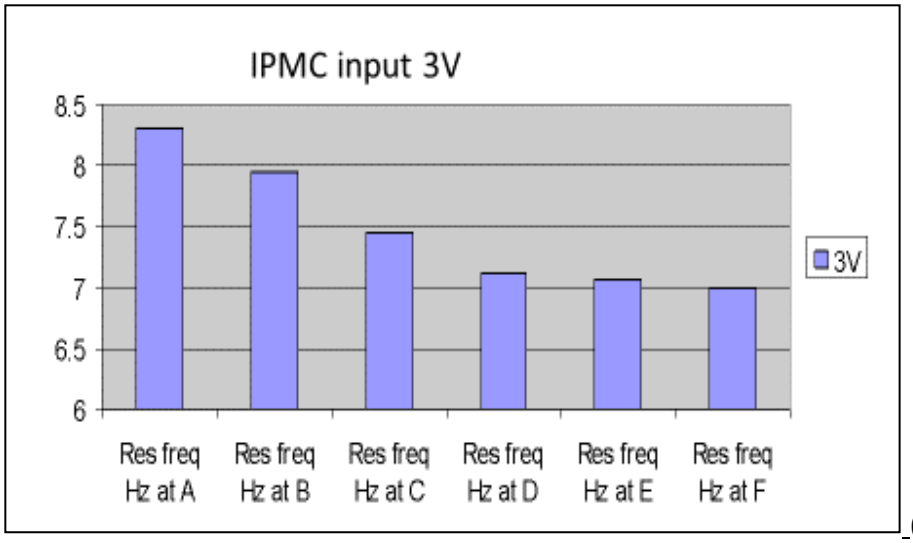
IPMC input 3V
8.5
8
7.5
7
6.5
6
3V
Res freq Hz at A
Res freq Hz at B
Res freq Hz at C
Res freq Hz at D
Res freq Hz at E
Res freq Hz at F

(d)

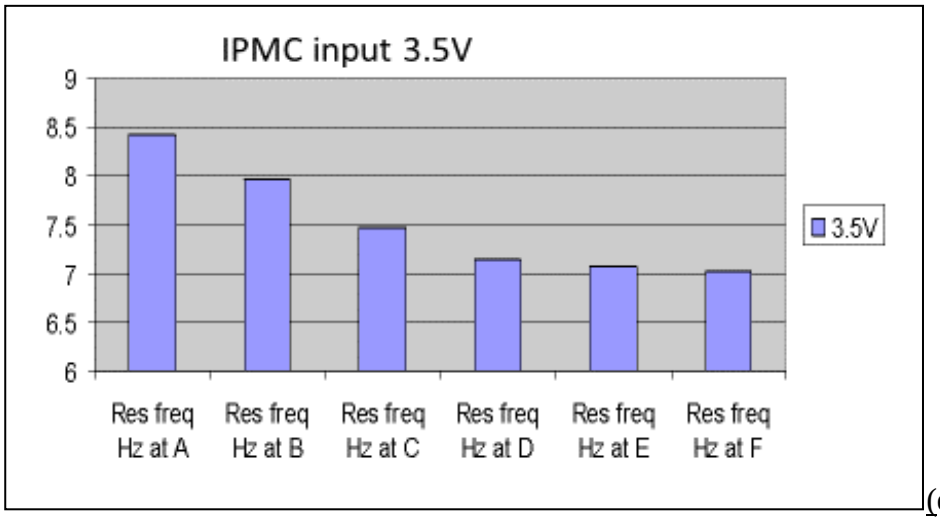
IPMC input 3.5V
9
8.5
8
7.5
7
6.5
6
3.5V
Res freq Hz at A
Res freq Hz at B
Res freq Hz at C
Res freq Hz at D
Res freq Hz at E
Res freq Hz at F

(e)

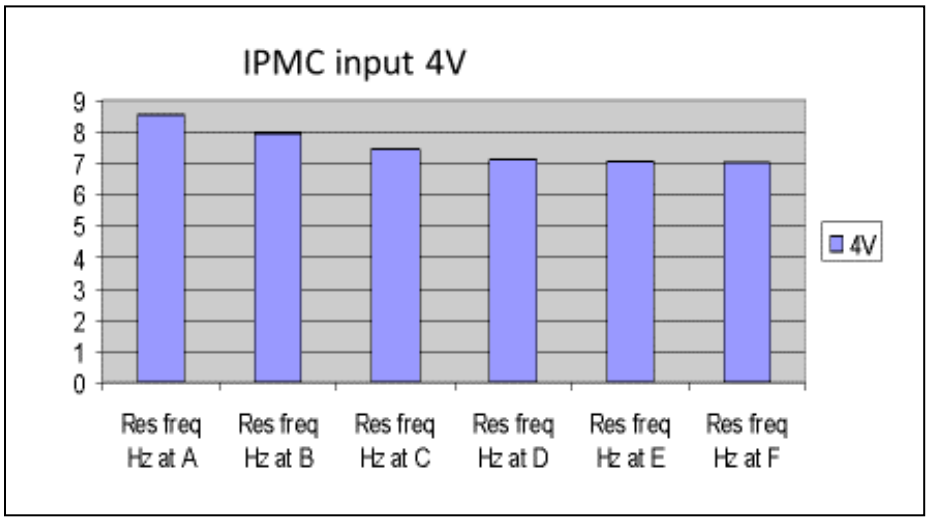

(f)

Fig A 3.4 (a), (b), (c). (d),(e) and (f) Response when IPMC input varies

Frequency response of PVEH at different g values

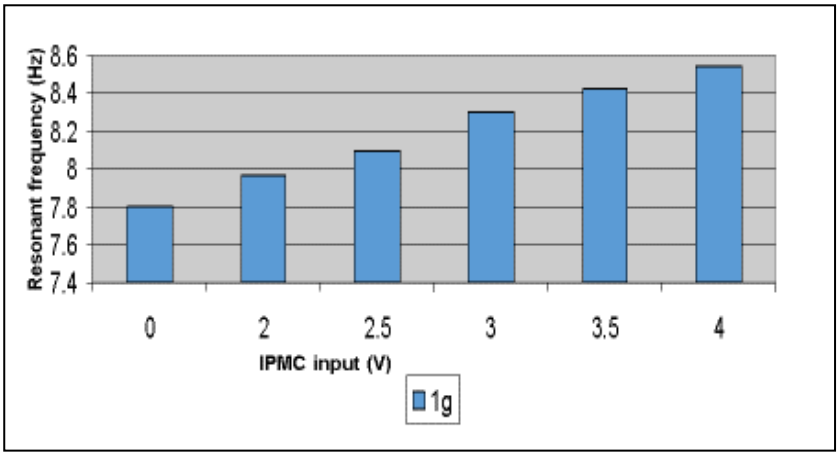

(a)

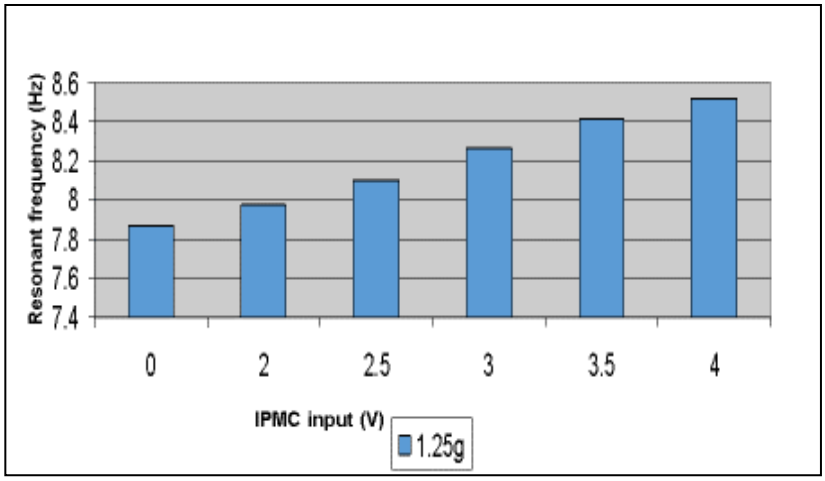

(b)

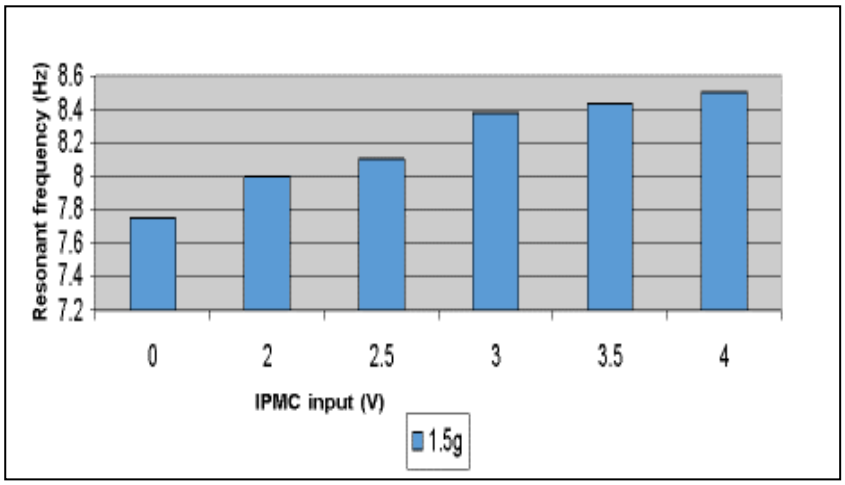

(c)

Fig. A 3.5 (a), (b) and (c) Frequency response of PVEH at different g values

Net Power Output of PVEH

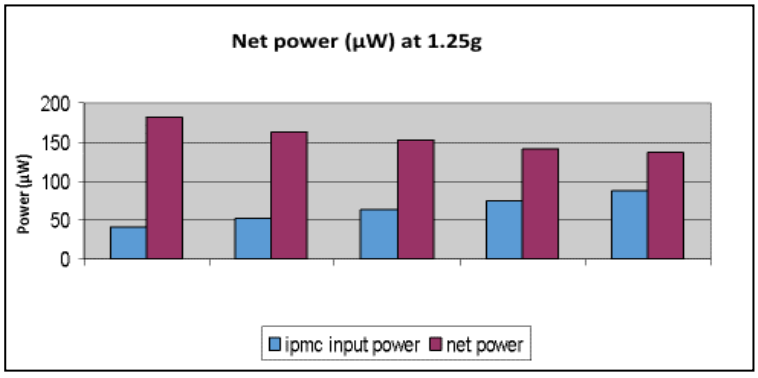

(a)

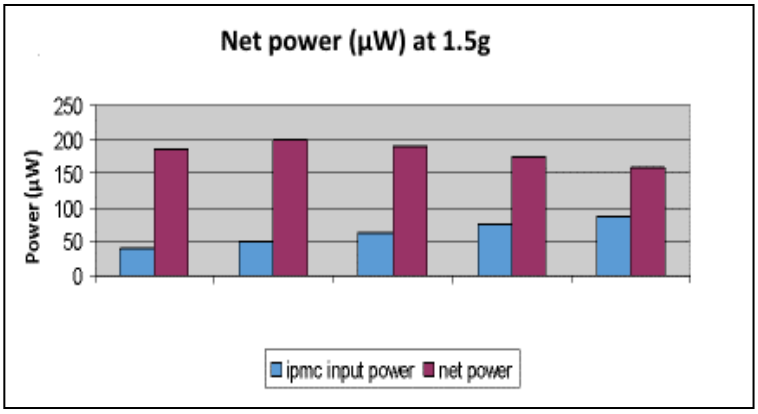

(b)

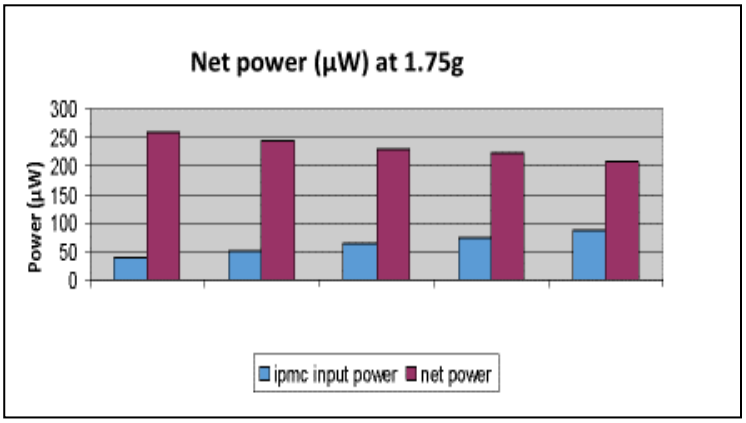

(c)

Fig. A 3.6 (a), (b) and (c) Net Power Output of PVEH

Annexure 4

Graphs indicating Broadening and associated data

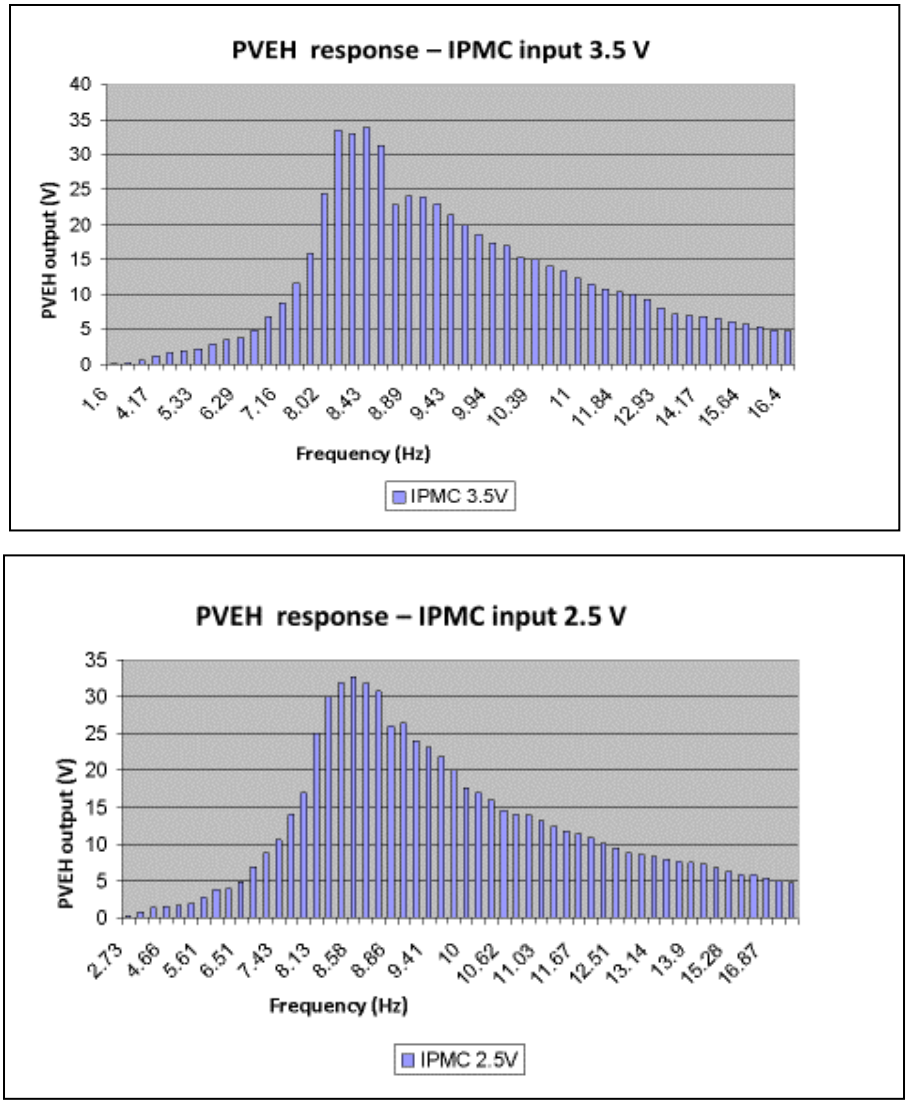

Fig. A4.1 Broadening characteristics of the novel PVEH

Annexure 5

Specifications of instruments used

1. Exciter Model : K2007E01

Output Force, sine pk (Natural Air Cooling)	31 N
Output Force, random RMS (Natural Air Cooling)	22 N
Output Force, shock pk	67 N
Stroke Length (Continuous pk-pk)	13 mm
Stroke Length (Between Stops)	14 mm
Frequency Range	9 kHz
Acceleration (No Load)	70 g pk
Acceleration (0.1 lb (0.045 kg) load)	35 g pk
Acceleration (1 lb (0.454 kg) load)	6.4 g pk
Acceleration (2 lb (0.907 kg) load)	3.3 g pk
Maximum Current	8 A
DC Resistance, armature	.37 Ohms
Amplifier Efficiency	92 %
Input Voltage, RMS (Nominal)	0-1 VAC
Input Voltage, RMS (Maximum)	1.9 VAC
Input Power	12-21 VDC
Output Power	55 W
Distortion, typical	<0.02 %
Cooling	Convection
Discrete Gain Stages	Muted,10dB,18dB,24dB
Warning Indication	Clipping and over temperature
Shutdown Protection	Over temperature and over current
Armature Weight	.045 kg
Suspension Stiffness	2.63 N/mm
Size - Height	135 mm
Size - Width	171 mm

Size - Depth	89 mm
Weight	3.1 kg
Input Connector	BNC Jack
Output Connector Type	Mini binding post
Table Mounting	

2. Agilent 34410A Multimeter

DC Voltage	**True RMS AC Voltage**
Measurement Method: **Continuously integrating multi-slope IV A/D converter** **Linearity: 0.0002% of reading (10 V range) + 0.0001% of range** **Input Resistance:** **0.1 V, 1 V, 10 V 10 MΩ or > 10 GΩ Ranges (Selectable)** **100 V, 1000 V 10 MΩ ± 1% Ranges (Fixed)** **Input Bias Current: < 50 pA at 25 °C** **Input Protection: 1000 V** **DC CMRR: 140 Db**	Measurement Method: AC-coupled True RMS measurement. Digital sampling with anti-alias filter. Crest Factor: No additional error for crest factors < 10. Limited by peak input and 300 kHz bandwidth. Peak Input: 300% of range or 1100 V Overload Ranging: Will select higher range if peak input overload is detected during auto range. Overload is reported in manual ranging. AC CMR: 70 dB2 Maximum Input: 400 Vdc, 1100 Vpk Input Impedance: 1 MΩ ± 2% in parallel with < 150 pF Input Protection: 750 Vrms all ranges

3. Oscilloscope

TBS1000 Series

Key performance specifications

150 MHz, 100 MHz, and 60 MHz bandwidth models

4-channel models

1 GS/s sample rate on all channels

2.5k point record length on all channels

Advanced triggers including pulse width trigger and line-selectable video trigger

Key features

16 automated measurements, and FFT analysis for simplified waveform analysis Built-in waveform limit testing Automated, extended data logging feature

Autoset and signal auto-ranging Built-in context-sensitive help Probe check wizard Multiple-language user interface 5.7 in. (144 mm) Active TFT Color Display Small footprint and lightweight - Only 4.9 in. (124 mm) deep and 4.4 lb. (2 kg)

4. PASCO Wireless Load Cell and Accelerometer PS3216

Load Cell Range	±50 N
Load Cell Resolution	0.03 N
Load Cell Accuracy	0.1 N
Load Cell Maximum Sample Rate	2 kHz
Acceleration Range	±16 g (three-axis)
Acceleration Maximum Sample Rate	500 Hz
Measurements	Force; Acceleration (3 axes and resultant)
Logging	Yes
Battery	Rechargeable Lithium-Polymer
Connectivity	Direct USB or via Bluetooth 4.0
Battery & Logging	
Stored Data Points Memory (Logging) [1]	>20,000
Battery - Connected (Data Collection Mode) [2]	>40 hr

Battery - Logging (Data Logging Mode) [3]	Yes
Battery Type	LiPo

5. Instek GFG-8250A Function Generator

MAIN	
Frequency Range	0.5Hz to 5 MHz (7 ranges)
Amplitude	>10Vpp (into 50Ω load)
Impedance	50Ω±10%
Attenuator	-20dB±1dB x 2
DC Offset	< -5V - >5V(into 50Ω load)
Duty Control	80% : 20% : 80% to 1MHz Continue variable
Display	6 digit LED display
SINE WAVE	
Distortion	≤1%, 0.5Hz - 100kHz
Flatness	≤0.3dB, below 500kHz; ≤1dB, below 5MHz
TRIANGLE WAVE	
Linear	≥98%, 0.5Hz - 100kHz; ≥95%, 100kHz - 5MHz
SQUARE WAVE	
Symmetry	±2%, 1Hz - 100kHz
Rise or Fall Time	≤ 50nS at maximum output (into 50Ω load)
CMOS OUTPUT	
Level	4Vpp±1Vpp - 14.5Vpp±0.5Vpp adjustable

Rise or Fall Time	≤120nS
TTL OUTPUT	
Level	≥3Vpp
Fan Out	20 TTL load
Rise/Fall Time	≤25nS
VCF	
Input Voltage	0V - 10V ±1V(100 : 1)
Input Impedance	10kΩ ±10%
FREQUENCY COUNTER	
INT./EXT.	Switch selector
Range	0.5Hz - 5MHz (5Hz - 150MHz EXT.)
Accuracy	Time base accuracy ±1 Count
Timebase	±20ppm(23°±5°) after 30 minutes warm up
Resolution	The maximum resolution is 100nHz for 1Hz and 1Hz for 100MHz
Input Impedance	1MΩ // 150pF
Sensitivity	≤35mVrms (5Hz - 100MHz) ≤45mVrms (100MHz - 150MHz)
STATS	
Power Source	AC 115V/230V±15%, 50/60Hz
Accessories	Power cord × 1, Instruction manual × 1 GTL-101 × 2
Dimensions & Weight	251(W) × 91(H) × 291(D) mm, Approx. 2.4kg

Annexure 6

Parameters and units

Symbol	Type	Size	Units	Meaning
$\mathbf{T}$	vector	6 x 1	$\frac{N}{m^2}$	stress components
$\mathbf{S}$	vector	6 x 1	$\frac{m}{m}$	strain components
$\mathbf{E}$	vector	3 x 1	$\frac{N}{C}$	electric field components
$\mathbf{D}$	vector	3 x 1	$\frac{C}{m^2}$	electric charge density displacement components
$\mathbf{s}$	matrix	6 x 6	$\frac{m^2}{N}$	compliance coefficients
$\mathbf{c}$	matrix	6 x 6	$\frac{N}{m^2}$	stiffness coefficients
$\boldsymbol{\varepsilon}$	matrix	3 x 3	$\frac{F}{m}$	electric permittivity
$\mathbf{d}$	matrix	3 x 6	$\frac{C}{N}$	piezoelectric coupling coefficients for Strain-Charge form
$\mathbf{e}$	matrix	3 x 6	$\frac{C}{m^2}$	piezoelectric coupling coefficients for Stress-Charge form
$\mathbf{g}$	matrix	3 x 6	$\frac{m^2}{C}$	piezoelectric coupling coefficients for Strain-Voltage form
$\mathbf{q}$	matrix	3 x 6	$\frac{N}{C}$	piezoelectric coupling coefficients for Stress-Voltage form

	Parameter	**Unit**
	Young's modulus	Pascal
	Stress	N/m^2, Pa
	Strain	mm
	Faraday constant	coulombs per mole (C/mol).
	Dielectric charge displacement	Coulomb per meter square ($C\ m^{-2}$)
	Electric field strength	v/m
	Resistor	ohms
	Capacitor	Farads

Annexure 7

Piezoelectricity

When the mechanical vibrations are small and the piezoelectric material is under low electric field conditions, the general constitutive equations for a piezoelectric material can be written as given below:

$$\begin{bmatrix} S \\ D \end{bmatrix} = \begin{bmatrix} s^E & d \\ d & \varepsilon^T \end{bmatrix} \begin{bmatrix} T \\ E^f \end{bmatrix} \text{ d-form} \qquad \text{(A7.1)}$$

$$\begin{bmatrix} T \\ D \end{bmatrix} = \begin{bmatrix} c^E & -e \\ e & \varepsilon^S \end{bmatrix} \begin{bmatrix} S \\ E^f \end{bmatrix} \text{ e-form} \qquad \text{(A7.2)}$$

$$\begin{bmatrix} T \\ E^f \end{bmatrix} = \begin{bmatrix} c^D & -h \\ -h & \beta^S \end{bmatrix} \begin{bmatrix} S \\ D \end{bmatrix} \text{ h-form} \qquad \text{(A7.3)}$$

$$\begin{bmatrix} S \\ E^f \end{bmatrix} = \begin{bmatrix} s^D & g \\ -g & \beta^T \end{bmatrix} \begin{bmatrix} T \\ D \end{bmatrix} \boldsymbol{g}\text{-form} \qquad \text{(A7.4)}$$

where $\boldsymbol{D}$ (C/m^2) is the electric displacement tensor; $\boldsymbol{S}$ is the strain tensor; $\boldsymbol{E^f}$ (V/m) is the applied electric field tensor; $\boldsymbol{T}$ (N/m^2) is the stress tensor; $\boldsymbol{\varepsilon}$ (F/m) is the dielectric constant tensor; $\boldsymbol{\beta}$ (m/F) is the dielectric impermeability tensor; $\boldsymbol{d}$ (m/V), $\boldsymbol{e}$ (C/m^2), $\boldsymbol{h}$ (V/m), and $\boldsymbol{g}$ (m^2/C) are the four forms of the piezoelectric coefficient tensor; $\boldsymbol{c}$ (N/m^2) is the elastic constant tensor; $\boldsymbol{s}$ (m^2/N) is the elastic compliance tensor; and the superscripts $(\,)^T$, $(\,)^S$, $(\,)^D$, and $(\,)^E$ indicate that the quantity is measured at constant stress, constant strain, constant electric displacement, and constant electric field, respectively.

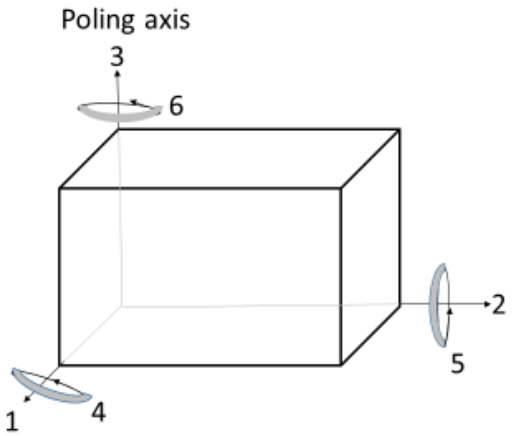

Fig. A7.1 Direction of poling on orthogonal crystallographic system

The direction of polarization is the z-axis (2) of an orthogonal crystallographic system (Fig.1). Piezoelectric material characteristics depend on the direction of the applied electric field, displacement, stress, and strain. Direction is indicated by superscripts and subscripts. Shear about one of these axes is represented by the subscript 4, 5, or 6, respectively [35].